Pt(II)-Coordinated Tricomponent Supramolecular Assemblies of Tetrapyridyl Porphyrin and Dicarboxylate Ligands: Are They 2D Bow Ties or 3D Prisms?

Paola A. Benavides,[†] Monica A. Gordillo,[†] Ashok Yadav,[†] M. Andrey Joaqui-Joaqui,[‡] and Sourav Saha*[,†]

[†]Department of Chemistry, Clemson University, Clemson, South Carolina 29634, United States

[‡]Department of Chemistry, University of Minnesota, Minneapolis, MN 55455, United States

*Email: souravs@clemson.edu

ABSTRACT

Thermodynamically favored heteroleptic coordination of one aza- and another oxo-coordinating ligand with Pt(II) ions yield tricomponent supramolecular coordination complexes (SCCs) that have much greater structural complexity and functional diversity than the traditional bicomponent SCCs containing only one of the ligands. Herein, we demonstrate that heteroleptic coordination of tetrapyridyl porphyrins (M′TPP, M′ = Zn or H_2) and various dicarboxylate ligands (XDC) having different lengths and rigidity with *cis*-$(Et_3P)_2Pt^{II}$ corners actually yields bow tie (⋈)-shaped tricomponent $[\{cis\text{-}(Et_3P)_2Pt\}_4(M'TPP)(XDC)_2]^{4+}$ complexes featuring a M′TPP core and two parallel XDC linkers held together by four heteroligated Pt^{II}(N,O) corners. Although previous reports have claimed that the self-assembly of these three components produced tetragonal prisms having two cofacial M′TPP planes connected by four XDC linkers via eight Pt^{II}(N,O) corners, our extensive ^{1}H, ^{31}P, and 2D NMR, ESI-MS, X-ray crystallographic, and computational studies unequivocally demonstrated that in reality, no such prism was formed because instead of connecting two cofacial M′TPP ligands, the XDC linkers actually bridged two adjacent pyridyl termini of an M′TPP ligand via shared Pt^{II}(N,O) corners, forming bow tie complexes. In addition to direct crystallographic evidence, the NMR spectra of these complexes revealed that the M′TPP ligands contained two distinct pyrrole protons (4 each)—those located inside the triangles were shielded by and coupled to adjacent XDC linkers, whereas the exposed ones were not—an unmistakable sign of their bow tie structures. Thus, this work not only unveiled novel bow tie-shaped coordination complexes, but also accurately defined the actual structures and compositions of M′TPP-based tricomponent SCCs.

INTRODUCTION

Owing to the dynamic, directional, and self-selecting/rectifying nature of metal–ligand coordination bonds, metal-driven self-assembly processes have emerged as one of the most attractive and versatile tools of supramolecular chemistry, yielding myriads of supramolecular coordination complexes (SCCs) ranging

from discrete metallacycles[1–10] and cages[11–23] to infinite coordination polymers and metal–organic frameworks[24–26] over the past several decades. To obtain the desired SCCs and to avoid statistical mixtures of different possibilities, typically only one rigid organic ligand is combined with a metal ion at appropriate stoichiometry to obtain bicomponent coordination complexes. Although such two-component self-assembly protocols usually afford the desired SCCs exclusively, they also restrict the structural and functional diversity of the resulting complexes that feature only one organic ligand. Expanding the scope of coordination-driven self-assembly strategies, researchers have recently discovered[26–56] that *cis*-capped Pt(II) and Pd(II) corners can simultaneously bind a carboxylate and a pyridyl ligands, preferentially yielding thermodynamically favored heteroleptic Pt(N,O) complexes instead of two different homoleptic complexes.[29–34,47–53] Furthermore, when two different homoleptic $Pt^{II}(COO^{-})_2$ and $Pt^{II}(pyridyl)_2$ complexes were mixed together at an appropriate stoichiometry, they spontaneously reorganized into thermodynamically more stable heteroleptic Pt(N,O) complexes.[30,32,33] These revelations paved the door for metal-driven self-assembly of tricomponent metallacycles and cages containing two complementary ligands that further diversified their structures, properties, and functions.

While it is fairly straightforward to assemble 2:2:4 tricomponent rectangles[30,32,41] containing two parallel dicarboxylate and two parallel dipyridyl arms held together by four heteroligated Pt^{II}(N,O) corners and 2:3:6 trigonal prisms[30,32] featuring two cofacial trigonal ligands and three ditopic linkers connected by six heteroligated Pt^{II}(N,O) corners, to promote the formation of 2:4:8 tricomponent tetragonal prisms featuring two cofacial tetratopic (tetrapyridyl or tetracarboxylate) ligands and four ditopic (dicarboxylate or dipyridyl) linkers, one must judiciously choose these ligands to ensure that the ditopic linkers can only connect the tips of two cofacial tetratopic ligands via eight heteroleptic Pt(II) corners.[30,32,35,36] This is extremely important because if a ditopic linker is able to bridge two adjacent binding sites of the tetratopic linker via shared Pt(N,O) corners, then they are likely to form 1:2:4 bow tie (⋈) complexes instead of 2:4:8 tetragonal prisms via thermodynamically favored heteroleptic coordination since the former would be entropically more favored over the latter.

Nevertheless, Stang and coworkers have recently claimed[30,33,34] that Pt(II)-driven tricomponent self-assembly of tetrapyridyl porphyrin (M′TPP, M′ = Zn- or H_2) and various aromatic and aliphatic dicarboxylate (XDC) linkers with varied length and rigidity yielded 'tetragonal prisms' $[\{cis\text{-}(Et_3P)_2Pt\}_8(M'TPP)_2(XDC)_4]^{8+}$ featuring two parallel M′TTP faces and four XDC pillars held together by eight heteroligated Pt^{II}(N,O) corners. These alleged prisms preserved the photophysical properties of M′TPP chromophores[33] and displayed promising applications in cancer photodynamic therapy[39] and guest encapsulation.[55] Encouraged by these promising literature reports,[30,33,34,39,55] we attempted to construct bi-

chromophoric tetragonal prisms composed of two M′TPP faces and four aromatic dicarboxylate linkers having complementary redox- and optically active cores, such as naphthalenediimide and perylene diimide. Surprisingly, none of our attempts to make M′TPP-based bi-chromophoric prisms was successful despite the fact that the XDC linkers were much longer than the distances between the two adjacent pyridyl-N atoms of free M′TPP ligands ($d_{N–N/free}$ = 10.9 Å), which should have led to the prism formation by eliminating the possibility of intramolecular bridging of two adjacent pyridyl groups via heteroligated Pt^{II}(N,O) corners. Prompted by these unexpected outcomes, we took a closer look at the ^{1}H NMR spectra of M′TPP-based purported tetragonal prisms that were previously reported in the literature.[30,33,34,55] Interestingly, all these so-called prisms actually displayed[30,33,34,55] two distinct singlets (1:1 ratio) for the pyrrole protons—one set of four pyrrole protons were significantly more shielded than the other four pyrrole protons (in contrast, all eight pyrrole protons of free M′TPP ligands are chemically equivalent and show one singlet)—indicating that in tricomponent SCCs, the pyrrole rings of M′TPP were no longer chemically equivalent, i.e., they were located in two different environments. These observed ^{1}H NMR signals appeared to be at odds with the proposed tetragonal prism formation because all four pyrrole rings (8Hs) of M′TPP in symmetrical tetragonal prisms should have been located in the same chemical environment and therefore should have displayed the same NMR chemical shift.[47–49,53,54] On the other hand, the observed NMR signals of two distinct pyrrole protons would actually make sense if two adjacent pyridyl groups of a M′TPP ligand were intramolecularly bridged by two parallel XDC linkers via two shared Pt(II) corners forming 2D bow tie (⋈) complexes instead of the proposed 3D prisms. In this scenario, which was previously overlooked, the two opposite pyrrole rings of M′TPP core would be located inside two isosceles triangles formed by two parallel XDC linkers and therefore shielded proportionately by their electron cloud, while the other two opposite pyrrole rings would remain exposed and not shielded directly by the XDC linkers. These inconsistencies prompted us to carefully examine whether or not the Pt(II)-driven self-assembly processes of M′TPP and XDC ligands do actually produce tricomponent prisms or yield an entirely different supramolecular architecture, such as tricomponent bow ties having the same ratio (4:1:2) of the three components.

Herein, we report the self-assembly and in-depth characterization of eight novel bow tie complexes [{*cis*-$(Et_3P)_2Pt$}$_4$(M′TPP)$(XDC)_2$]·4(TfO) composed of M′TPP ligands (M′ = Zn and H_2) and four different XDC linkers (Scheme 1). The ^{1}H, ^{31}P, and 2D (COSY and ROESY) NMR spectra and ESI-MS data of the M′TPP-based tricomponent SCCs presented the telltale signs of 2D bow tie complexes and ruled out prism formation. These compelling, albeit indirect, results suggesting the formation of bow tie complexes were further corroborated by their single-crystal structures, which revealed that each bow tie complex was composed of an M′TPP core and two parallel XDC linkers, which were connected by four heteroligated

$(Et_3P)_2Pt^{II}(N,O)$ corners. Notably, this was the first time, single crystal structures of such M′TPP-based tricomponent SCCs could be determined. In addition, the energy-minimized structures of these bow tie complexes were in good agreement with the experimental results, which collectively shined light on why the M′TPP ligands actually formed bow tie complexes instead of tetragonal prisms.

Scheme 1. Pt(II)-driven self-assembly of M′TPP ligands (M′ = Zn or H_2) and four different XDC linkers (i.e., 1,6-hexane-, 4,4′-biphenyl-, 1,4-benzene-, and 2,6-naphthalene- dicarboxylates: HDC, BPDC, BDC, and NDC) exclusively yielded novel bow tie-shaped [{*cis*-$(Et_3P)_2Pt$}$_4$(M′TPP)$(XDC)_2$]·4(TfO) complexes (BT1–BT4 and BT1′–BT4′), each featuring a M′TPP core and two parallel XDC linkers held together by four heteroleptic Pt(II) corners. No tetragonal prism was formed irrespective of the length and rigidity of the XDC linkers.

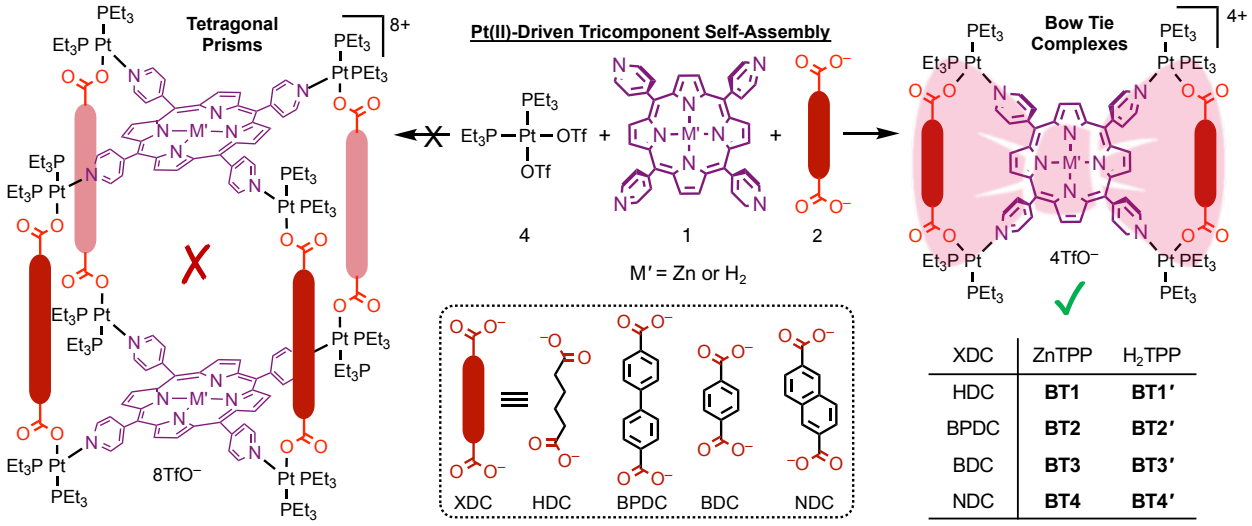

XDC	ZnTPP	H_2TPP
HDC	**BT1**	**BT1′**
BPDC	**BT2**	**BT2′**
BDC	**BT3**	**BT3′**
NDC	**BT4**	**BT4′**

RESULTS AND DISCUSSION

Heteroleptic Coordination-Driven Self-Assembly of M′TPP-Based Tricomponent Bow Ties (⋈). Since the heteroleptic coordination of tetratopic M′TPP ligands and ditopic XDC linkers with *cis*-$(Et_3P)_2Pt^{II}$ corners could lead to the formation of either (i) tetragonal 3D prisms containing two cofacial M′TPP ligands and four XDC linkers held together by eight Pt(II) corners,[30,33,34] or (ii) 2D bow ties containing a M′TPP core and two parallel XDC linkers connected by four shared Pt(II) corners, herein, we decided to determine the actual structures and compositions of the resulting SCCs through extensive multinuclear (^{1}H and ^{31}P) and 2D (COSY and ROESY) NMR, single-crystal X-ray diffraction, and ESI-MS analyses. To this end, we have employed four different XDC ligands, namely hexanedioate (HDC), 1,4-benzene dicarboxylate (BDC), 2,6-naphthalene dicarboxylate (NDC), and 4,4′-biphenyl dicarboxylate (BPDC) having different

lengths, rigidity, and π-electron density in order to determine how they would affect the structures and compositions of the resulting tricomponent SCCs. For consistency, we have adopted the exact same reaction conditions, i.e., a constant 4:1:2 (or 8:2:4) stoichiometry of *cis*-$(Et_3P)_2Pt^{II}$ corners, M′TPP, and XDC ligands, solvent mixtures (1:1:1 CH_2Cl_2/MeCN/$MeNO_2$ or 4:1 Me_2CO/H_2O) that adequately solubilized all components, temperature (~60 °C), and reaction time (~18 h) that were also applied by Stang et al.[30,33,34] in their attempts to assemble 3D prisms. Although previous reports have claimed that tricomponent self-assembly of HDC and BDC linkers with M′TPP ligand and $(Et_3P)_2Pt^{II}$ corners yielded 3D prisms,[30,33,34,39] our comprehensive 1D and 2D NMR, ESI-MS, SXRD, and computational studies unequivocally demonstrated that regardless of their length and rigidity, all four XDC linkers employed here, including HDC and BDC, exclusively afforded bow tie architectures, namely ZnTPP-based **BT1–BT4** and H_2TPP-based **BT1′–BT4′** (Scheme 1, Figure 1) instead of any 3D prisms.

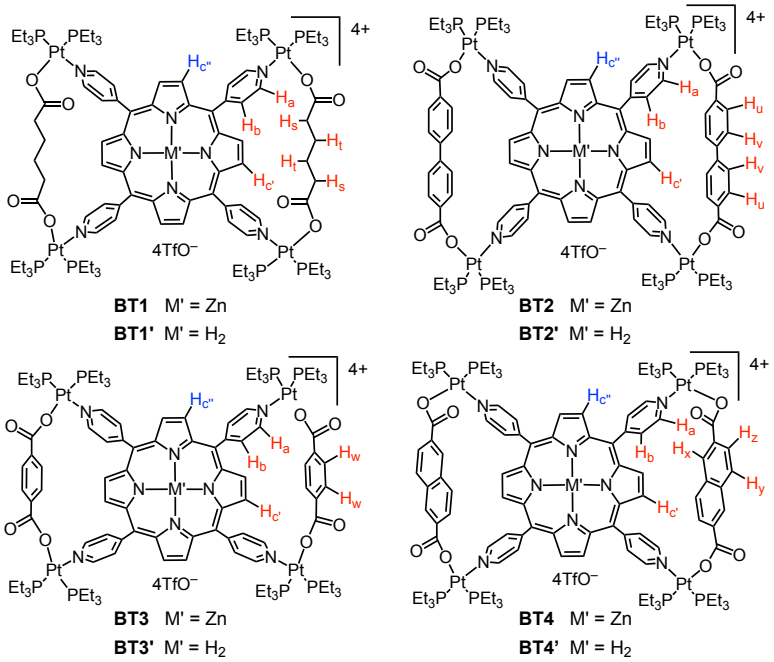

Figure 1. The chemical structures of bow tie complexes.

^{31}P NMR Spectroscopy. Simultaneous heteroleptic coordination of a pyridyl group of M′TPP ligand and a carboxylate group of XDC with two *cis*-Et_3P-capped Pt^{II} corner was evident from the ^{31}P NMR spectra of all ensuing SCCs (Figures 2 and S1). While the *cis*-$(Et_3P)_2Pt(TfO)_2$ precursor displayed a characteristic singlet at 11.14 ppm with two Pt(II) satellite peaks showing that two Pt(II)-coordinated P atoms were chemically equivalent, the resulting M′TPP-based SCCs (**BT1–BT4** and **BT1′–BT4′**) displayed two distinct doublets, one at ca. 0–2 ppm and another at 6–7 ppm ($^2J_{P-P} \approx 20–21$ Hz) indicating that the P-atoms

of two ancillary Et_3P ligands attached to the square-planar Pt(II) corners were no longer chemically equivalent.[30,33,34] The up-field doublets corresponded to the P-nucleus *trans*- to the pyridyl-N atom of M′TPP, whereas the downfield doublets were attributed to the P-nucleus *trans*- to the carboxylate O-atom of XDC, which indicated the formation of heteroleptic *cis*-$(Et_3P)_2Pt^{II}$(N,O) corners.[30,33,34] The fact that no other ^{31}P NMR signal was observed in any of these cases further confirmed that the tricomponent SCCs were formed exclusively via thermodynamically favored heteroleptic coordination of two different ligands with the Pt(II) corners and no bicomponent complex was formed via homoleptic coordination of two same ligands. Although the ^{31}P NMR data clearly demonstrated simultaneous coordination of carboxylate and pyridyl groups with the Pt(II) corners, these spectra shed little light on the actual structures and compositions of the resulting tricomponent SCCs, i.e., whether they were actually 3D prisms or 2D bow ties, as both structures would technically feature the same heteroleptic *cis*-$(Et_3P)_2Pt^{II}$(N,O) corners.

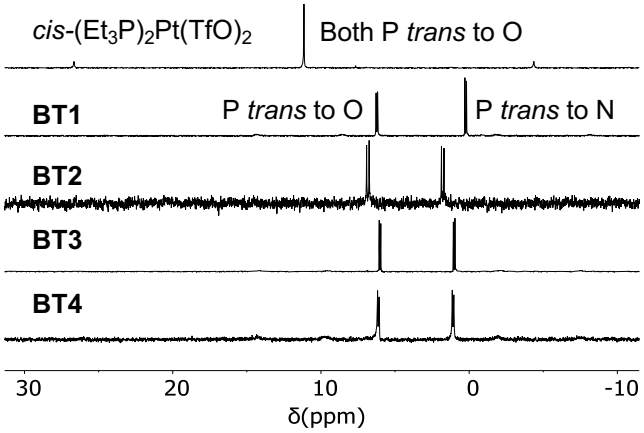

Figure 2. Partial ^{31}P NMR spectra (122 MHz, acetone-d_6) of *cis*-$(Et_3P)_2Pt(TfO)$, **BT1**, **BT2**, **BT3**, and **BT4** complexes reveal simultaneous coordination of carboxylate and pyridyl groups with heteroligated Pt(N,O) corners in the bow tie complexes.

^{1}H NMR Spectroscopy. The first telltale signs of the formation of 2D bow tie structures instead of 3D tetragonal prisms came from the ^{1}H NMR spectra of the resulting SCCs (Figures 3, S2, and S3). Not only did all M′TPP-based tricomponent SCCs, i.e., the ZnTPP-based **BT1–BT4** and H_2TPP-based **BT1′–BT4′**, display downfield shift of the α- and β-pyridyl protons (H_a and H_b) of M′TPP ligand due to Pt(II)-coordination, but most tellingly, they also displayed two distinct singlets (1:1 intensity) representing two different pyrrole protons, i.e., $H_{c'}$ and $H_{c''}$ that were no longer chemically equivalent. The splitting and different NMR chemical shifts of two distinct pyrrole protons of M′TPP ligand in the resulting SCCs were the unmistakable signs of bow tie structures, not of tetragonal prisms, as explained below.

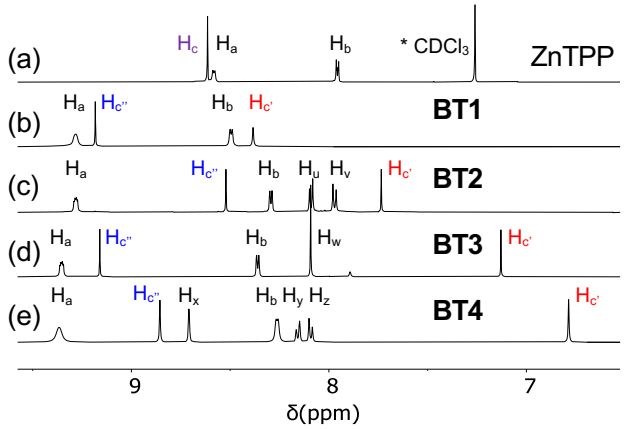

Figure 3. Partial ^{1}H NMR spectra (500 MHz) of (a) free ZnTPP ligand in $CDCl_3$, (b) **BT1**, (c) **BT2**, (d) **BT3**, and (e) **BT4** complexes (in acetone-d_6) show that the enclosed $H_{c'}$ pyrrole protons (highlighted in red) of bow tie complexes are shifted up-field commensurately with the shielding effect of the adjacent XDC linkers, whereas the chemical shifts of exposed $H_{c''}$ pyrrole protons (highlighted in blue) vary depending on the length of XDC linkers that dictate their distances from the adjacent pyridyl rings.

The D_{4h}-symmetric free ZnTPP ligand displayed two doublets at 8.58 and 7.95 ppm corresponding to its H_a and H_b pyridyl protons (8 each) and a sharp singlet at 8.61 ppm for all eight chemically equivalent H_c pyrrole protons (Figure 3). In the resulting tricomponent SCCs, the H_a and H_b peaks shifted noticeably downfield to ca. 9.3 and 8.4 ppm, respectively, due to Pt(II)-coordination. More importantly, while all eight H_c pyrrole protons of free ZnTPP were chemically equivalent (s, 8.61 ppm), **BT1–BT4** complexes displayed two distinct singlets (1:1 intensity) for $H_{c'}$ and $H_{c''}$ pyrrole protons that were no longer chemically equivalent. The chemical shifts of $H_{c'}$ and $H_{c''}$ pyrrole protons varied depending on the length and π-electron density, or lack thereof, of the XDC linkers, confirming that they were located in completely different chemical environments that were controlled by the XDC ligands. The singlet peaks corresponding to four $H_{c'}$ pyrrole protons of **BT1–BT4** complexes appeared at 8.38, 7.73, 7.13, and 6.79 ppm, respectively, which were significantly up-field shifted from the H_c signal of free ZnTPP, while the singlets corresponding to the other four $H_{c''}$ pyrrole protons appeared at 9.18, 8.52, 9.16, and 8.86 ppm, respectively. The up-field shifts of $H_{c'}$ signals of **BT1–BT4** was directly correlated to the increasing π-electron cloud and shielding effect of XDC linkers (HDC < BPDC < BDC < NDC), suggesting that these pyrrole protons were located inside the triangles of the bow tie structures (⋈) formed by two parallel XDC linkers while the less shielded and down-field $H_{c''}$ pyrrole protons were not. Naturally, the aliphatic HDC linkers in **BT1** exerted the least shielding effect on the enclosed $H_{c'}$ pyrrole protons located across the bay, causing the smallest up-field shift, followed by the BPDC linkers of **BT2** having two twisted phenyl rings that were not properly aligned

with the enclosed $H_{c'}$ pyrrole protons according to its single-crystal structure (*vide infra*). On the other hand, the enclosed $H_{c'}$ pyrrole protons of **BT3** and **BT4** experienced much greater up-field NMR chemical shifts because they were projected toward the aromatic cores of BDC and NDC linkers, as seen from their crystal structures (*vide infra*), which exerted much greater shielding effects. Thus, having the largest π-cloud and maximum shielding effect among all four XDC linkers employed here, the NDC linkers caused the largest up-field shift of the $H_{c'}$ signal in **BT4**, followed by the BDC linkers in **BT3**.

With respect to the enclosed $H_{c'}$ pyrrole protons located inside the triangles of bow tie complexes, which displayed up-field shift commensurate with the shielding effect of XDC linkers, the four exposed $H_{c''}$ pyrrole protons of **BT1–BT4** complexes appeared at downfield positions (9.18, 8.52, 9.16, and 8.86 ppm, respectively), indicating that they were not shielded by XDC linkers (Figure 3). However, the chemical shifts of exposed $H_{c''}$ pyrrole protons were still affected by the length of the XDC linkers, which controlled their distances from the adjacent pyridyl rings of ZnTPP and thus their variable shielding effects. This was further evident from their crystal structures presented below and certain structural parameters summarized in Table 1. For instance, in order to form the triangles of bow tie structures (⋈), the shorter HDC and BDC linkers (l_{BDC} = 6.9 Å) of **BT1** and **BT3** complexes, respectively, pulled the two XDC-bridged Pt(II) corners closer to each other (Table 1), which in turn, pulled the pyridyl rings of ZnTPP ligand away from the exposed $H_{c''}$ pyrrole protons. This reduced the shielding effect of pyridyl rings on $H_{c''}$ pyrrole protons in **BT1** and **BT3**, causing them to appear at more downfield positions (ca. 9.2 ppm) than the H_c protons of free ZnTPP ligand. Having a medium length (l_{NDC} = 9.2 Å), the NDC linkers of **BT4** also pulled the pyridyl rings slightly away from the exposed $H_{c''}$ pyrrole protons, causing a slight downfield shift from the H_c signal of free ZnTPP. On the other hand, the longest BPDC linkers (l_{BPDC} = 11.2 Å) of **BT2** pushed the two bridged Pt(II) corners away from each other, which in turn, pushed the pyridyl rings of ZnTPP closer to the exposed $H_{c''}$ pyrrole protons making them more shielded and up-field shifted than the H_c protons of free ZnTPP.

Similarly, the H_2TPP-based **BT1′–BT4′** complexes also displayed ^{1}H NMR spectra (Figure S2) that were fully consistent with bow tie structures, but not with tetragonal prisms. Just as in ZnTPP-based **BT1–BT4**, in these complexes, the H_a and H_b pyridyl protons of H_2TPP ligand shifted downfield due to Pt(II) coordination, whereas chemically non-equivalent $H_{c'}$ and $H_{c''}$ pyrrole protons (4 each) displayed two distinct singlets. Again, the up-field chemical shifts of $H_{c'}$ pyrrole protons—8.35 ppm in HDC-based **BT1′**, 7.74 ppm BPDC-based **BT2′**, 7.08 ppm in BDC-based **BT2′**, and 6.78 ppm in NDC-based **BT4′**—were dictated by the shielding effect of the XDC linkers, indicating that these H_2TPP protons were located inside the triangles formed by two parallel XDC linkers. On the other hand, the NMR chemical shifts of $H_{c''}$

pyrrole protons varied based on the length of the XDC linkers (not their π-clouds), which in turn defined the distance between these protons and the adjacent pyridyl rings and thereby controlled their shielding effect. The short HDC and BDC linkers in **BT1′** and **BT3′** pulled two adjacent pyridyl rings coordinated to the bridged Pt(II) corners closer to each other and away from the exposed $H_{c''}$ pyrrole protons, causing downfield shift (9.38 and 9.31 ppm, respectively). On the other hand, the long BPDC linkers in **BT2′** pushed two adjacent pyridyl rings coordinated to the bridged Pt(II) corners away from each other and closer to the exposed $H_{c''}$ pyrrole protons, which caused an up-field shift (8.58 ppm). The medium length NDC linkers in **BT4′** caused the least deviation of the pyridyl rings from their original positions, allowing the exposed $H_{c''}$ pyrrole protons to appear (8.85 ppm) close to the original position of H_c protons of free H_2TPP.

Thus, the splitting of pyrrole protons of M′TPP ligands into two sets of chemically non-equivalent $H_{c'}$ and $H_{c''}$ protons (4 each) in the tricomponent SCCs and the up-field shift of the $H_{c'}$ signal depending on the electron cloud and shielding effect of XDC linkers clearly indicated the formation of 2D bow tie structures **BT1–BT4** and **BT1′–BT4′** where two opposite pyrrole rings of M′TPP ligand bearing the $H_{c'}$ protons were located inside the triangles formed by two parallel XDC linkers while the other two pyrrole rings bearing the $H_{c''}$ protons remained exposed. It is worth noting that tricomponent SCCs have been assembled previously[33] under the same conditions using the same *cis*-$(Et_3P)_2Pt^{II}$ corner, M′TPP, and HDC and BDC ligands, which displayed the same ^{1}H NMR spectra as those displayed by **BT1**, **BT1′**, **BT2**, and **BT2′** featuring two distinct singlets for $H_{c'}$ and $H_{c''}$ pyrrole protons along with the doublets for H_a and H_b pyridyl protons and the characteristic signals of XDC protons.[33] However, these telltale signs of 2D bow tie structures were overlooked previously, which led to a mischaracterization of these four 2D bow tie complexes as 3D prisms. If tricomponent self-assembly of $(Et_3P)_2Pt^{II}$, M′TPP, and XDC linkers had indeed formed tetragonal prisms having two cofacial M′TPP planes connected by four XDC linkers via heteroleptic $(Et_3P)_2Pt^{II}$(N,O) corners, as previously claimed with HDC, BDC, and few other dicarboxylate linkers,[30,33,34,55] then all sixteen pyrrole protons of two parallel M′TPP faces should have remained chemically equivalent and displayed one singlet peak[47–49,53,54] instead of splitting into two chemically non-equivalent $H_{c'}$ and $H_{c''}$ protons that showed two distinct singlets. However, that was not observed for any of the Pt(II)/M′TPP/XDC-based tricomponent SCCs presented either here or in the literature,[30,33,34,55] which ruled out the prism formation.

2D ^{1}H–^{1}H COSY NMR Spectroscopy. The 2D COSY NMR spectra of these TTP-based tricomponent SCCs (Figure S4) provided further insights into their actual structures by revealing the coupling between the adjacent α- and β-protons. In addition to showing COSY couplings between H_a and H_b pyridyl protons

of M′TPP ligands, **BT1**, **BT2**, and **BT4** (and **BT1′**, **BT2′**, and **BT4′**) complexes also displayed couplings between H_s and H_t protons of HDC, H_u and H_v protons of BPDC, and H_x, H_y and H_z protons of NDC linkers, respectively. Conspicuously missing from the COSY NMR spectra of all these SCCs were any such α/β-proton coupling between the $H_{c'}$ and $H_{c''}$ pyrrole protons of M′TPP ligand, which further indicated that these two chemically non-equivalent protons did not belong to the same pyrrole ring but to two distinct pyrrole rings located in different environments. This scenario would be possible only in bow tie structures where two opposite pyrrole rings carrying the $H_{c'}$ protons resided inside the triangles formed by two parallel XDC linkers, whereas the other two pyrrole rings bearing $H_{c''}$ protons remained exposed, eliminating the possibility of any α/β-coupling between these two remote protons. If in fact these tricomponent SCCs were 3D prisms containing two cofacial M′TPP panels linked by four XDC linkers, then not only should all the pyrrole protons of M′TPP have remained chemically equivalent instead of splitting into distinct $H_{c'}$ and $H_{c''}$ protons, but at the very least, each pyrrole ring would have carried one $H_{c'}$ and one $H_{c''}$ protons, which would have shown α/β-coupling. The absence of such couplings ruled out the prism formation.

2D ROESY NMR Spectroscopy. Further corroborating evidence of the formation of bow tie complexes instead of 3D prisms stemmed from the ROESY NMR spectra of M′TPP-based tricomponent SCCs (Figures 4 and S5), which revealed the through-space long-range ^1H–^1H coupling between the enclosed $H_{c'}$ pyrrole protons of M′TPP located inside the triangles and the XDC protons located across the bay. No such coupling between the exposed $H_{c''}$ pyrrole protons of M′TPP and the remote XDC protons were observed (the $H_{c''}$ protons were only coupled to H_b protons of the adjacent pyridyl ring in some cases), further verifying that the enclosed $H_{c'}$ and exposed $H_{c''}$ pyrrole protons were located in two completely different chemical environments, which would be only possible in bow tie structures, not in prisms.

In **BT1** and **BT1′**, the enclosed $H_{c'}$ pyrrole protons of M′TPP were ROE-coupled with the H_t protons of HDC linker and the H_b protons of the adjacent pyridyl ring (Figures 4a and S5a), whereas the $H_{c''}$ protons were coupled to only H_b protons of the adjacent pyridyl ring, not with any HDC protons. These observations further confirmed that the $H_{c'}$ protons were located inside the triangles formed by two parallel HDC linkers, which enabled their coupling, while the exposed $H_{c''}$ protons were located far away from the HDC linkers. These couplings were also fully consistent with a bow tie structure, not with a 3D prism architecture containing two ZnTPP faces and four HDC linkers, which was proposed previously.[33] If the purported prism had been really formed, then $H_{c'}$ and $H_{c''}$ protons would have remained chemically equivalent, and both should have been coupled to the HDC protons in a similar fashion. The absence of these signs further ruled out the prism formation.

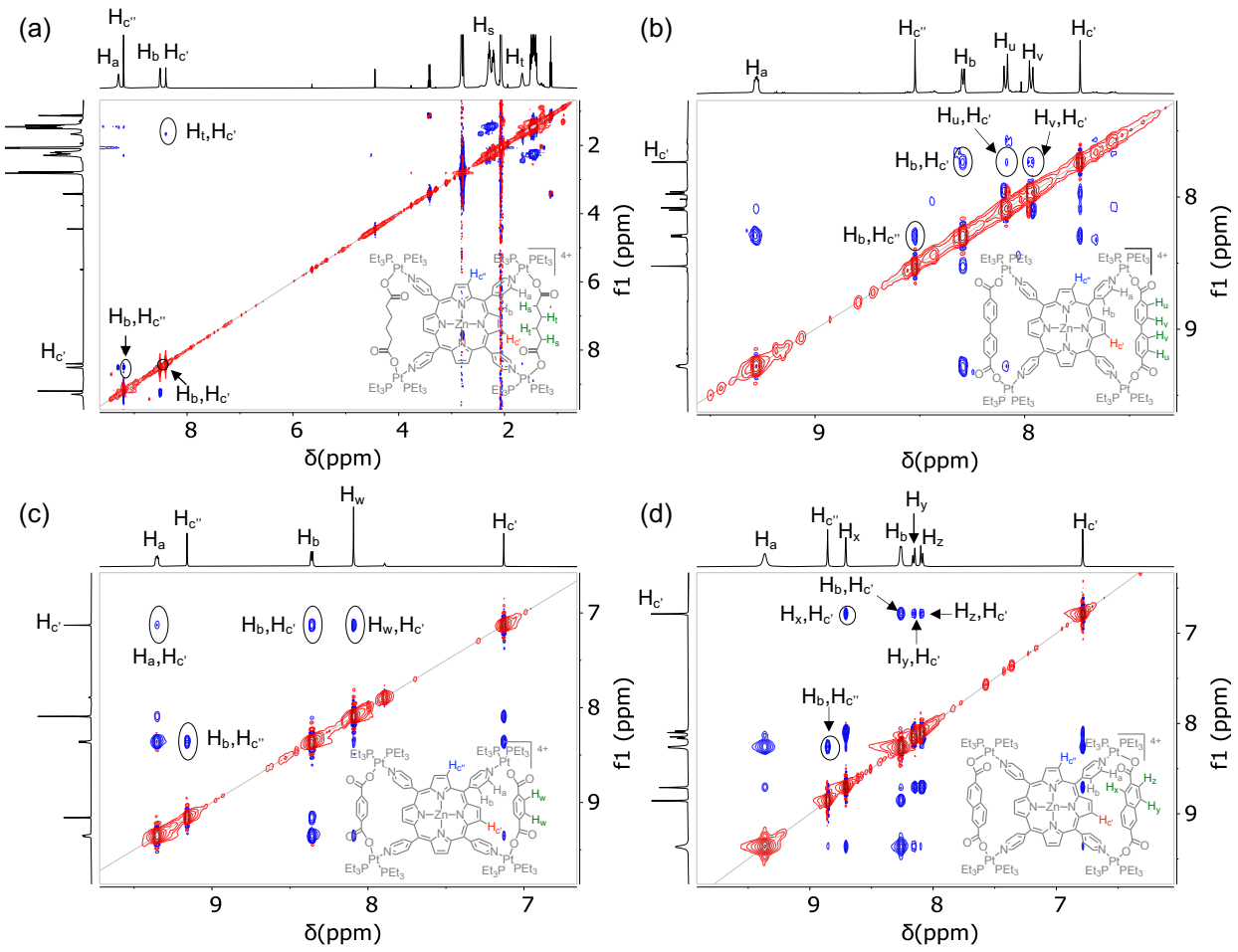

Figure 4. Partial ^{1}H–^{1}H ROESY NMR spectra (500 MHz, acetone-d_6) of (a) **BT1**, (b) **BT2**, (c) **BT3**, and (d) **BT4** show that the enclosed $H_{c'}$ pyrrole protons of these bow tie complexes located inside the isosceles triangles are through-space NOE-correlated with the protons of adjacent XDC linkers but the exposed $H_{c''}$ pyrrole protons are not coupled with the distant XDC protons.

Similarly, in **BT2** and **BT2′**, the enclosed $H_{c'}$ pyrrole protons of M′TPP were coupled with the H_u and H_v protons of BPDC linkers located across the bay (Figures 4b and S5b) as well as with the H_b protons of the adjacent pyridyl ring, whereas the exposed $H_{c''}$ protons were coupled to only adjacent H_b protons, not with any BPDC protons. These correlations further confirmed that the $H_{c'}$ pyrrole protons were located inside the triangles formed by two parallel BPDC ligands, while the exposed $H_{c''}$ protons were located far away from these linkers, a scenario that was possible only in bow tie structures.

In **BT3** and **BT3′**, the enclosed $H_{c'}$ pyrrole protons of M′TPP were coupled with the H_w protons of BDC linkers (Figures 4c and S5c), indicating that they were located inside the triangles formed by the BDC

linkers, and also with the H_b protons of the adjacent pyridyl rings because the shorter BDC linkers pulled the bridged Pt(II) corners closer to each other and consequently brought the pyridyl rings closer to enclosed $H_{c'}$ pyrrole protons. In contrast, the exposed $H_{c''}$ pyrrole protons were not coupled with any BDC protons, which were located far away. These coupling patterns were also consistent with bow tie structures, not with the previously proposed 3D prism architectures containing two M′TPP faces and four BDC linkers held together by eight heteroligated Pt(II) corners. If the purported prism had been formed, then the $H_{c'}$ and $H_{c''}$ protons should have remained chemically equivalent, and both should also have been coupled with the BDC protons (H_w) in a similar fashion. In the absence of such signals, the prism formation can be ruled out. Notably, not only did the ^{1}H NMR spectra of previously reported M′TPP-based SCCs containing BDC and HDC linkers not reconcile with the purported prism structures (*vide supra*), but also no 2D NMR and/or x-ray crystallographic evidence was presented that could have supported that claim.[30,33,34,39,55,56]

Finally, in **BT4** and **BT4′**, the enclosed $H_{c'}$ pyrrole protons of M′TPP were coupled with the H_x, H_y, and H_z protons of NDC linkers (Figures 4d and S5d), indicating that they were part of the same triangle. The $H_{c'}$ pyrrole protons were also coupled with the H_b protons of the adjacent pyridyl rings, as the NDC linkers pulled the bridged Pt(II) corners closer to each other and thereby brought the pyridyl rings closer to the $H_{c'}$ protons. On the other hand, the exposed $H_{c''}$ pyrrole protons were not coupled with any NDC protons, indicating that they were located far away from each other. In addition, the H_a protons of ZnTPP and H_x and H_y of NDC, which were part of the same triangles, were also coupled. Once again, these NOE-correlations were fully consistent with bow tie structures, not with the prisms where all pyrrole protons should have remained chemically equivalent and coupled with the NDC protons in a similar fashion.

ESI-MS Analysis. The ESI-MS analysis revealed the characteristic *m/z* peaks of dicationic $[M–2TfO]^{2+}$ species of bow tie complexes having a general formula of $[\{(Et_3P)_2Pt\}_4(M'TPP)(XDC)_2]^{4+}\bullet\ 4(TfO^-)$. The ZnTPP-based bow ties **BT1**, **BT2**, **BT3**, and **BT4** displayed (Figures 5 and S6) the respective $[M–2TfO]^{2+}$ peaks at *m/z* = 1497.09, 1593.58, 1517.01, and 1567.05, while the H_2TPP-bow ties **BT2′**, **BT3′**, and **BT4′** displayed (Figure S6) their respective $[M – 2TfO]^{2+}$ peaks at *m/z* = 1561.50, 1485.52, and 1535.60. Although all of these M′TPP-based tricomponent bow tie complexes were assembled under exactly the same conditions as those reported in the literature, none of them displayed any ESI-MS peak that would otherwise indicate the formation of tetragonal prisms.

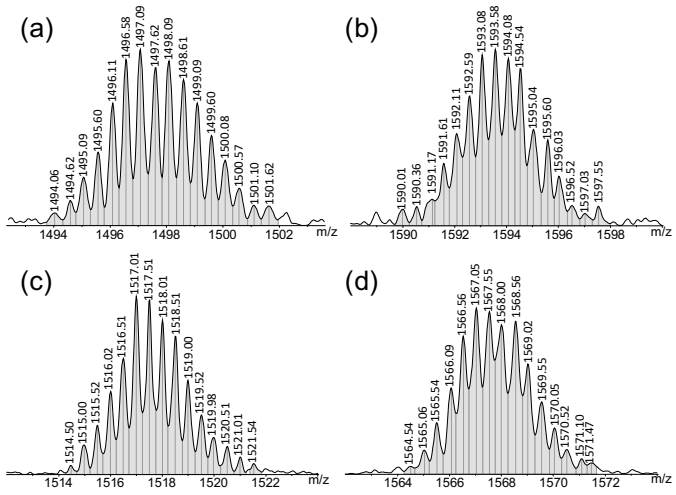

Figure 5. ESI-MS data show the $[M - 2TfO]^{2+}$ peaks of (a) **BT1**, (b) **BT2**, (c) **BT3**, and (d) **BT4** complexes.

Apparently, the *m/z* peaks of $[M - nX^{-}]^{n+}$ species (X^{-} = TfO^{-} or PF_6^{-}, n = 3 or 5) of the purported $[\{(Et_3P)_2Pt\}_8(M'TPP)_2(XDC)_4]^{8+}\bullet 8(X^{-})$ prisms containing HDC and BDC linkers were observed previously.[33] However, on a rare occasion when the entire ESI-MS profile of a tricomponent SCC assembled from $(Et_3P)_2Pt^{II}$, H_2TPP, and BDC was disclosed previously[30] (not just certain blown-up peaks), it revealed a prominent *m/z* peak at 1481.38 (~100 % relative intensity, 4–5 times higher than any other peaks in the entire panel) that actually represented the $[M - 2PF_6^{-}]^{2+}$ species of bow tie complex **BT3′**: $[\{(Et_3P)_2Pt\}_4(H_2TPP)(BDC)_2]^{4+}\bullet 4(PF_6^{-})$. Just like the diagnostic ^{1}H NMR signals of bow tie complexes ($H_{c'}$ and $H_{c''}$ signals), this characteristic ESI-MS peak of **BT3′** was also overlooked previously,[30] which unfortunately led to mischaracterization of M′TPP-based tricomponent 4:1:2 bow tie complexes as 8:2:4 prisms. Since none of the previously reported M′TPP-based tricomponent SCCs (i.e., so-called prisms) displayed the ^{1}H NMR spectra that actually supported the alleged prism formation (*vide supra*),[30,33,34,55,56] and our extensive 2D NMR and ESI-MS data discussed above as well as the single-crystal structures presented below unequivocally demonstrated the formation of bow tie complexes instead of any prisms, it is plausible that the *m/z* peaks that were previously ascribed to 8:2:4 $[\{(Et_3P)_2Pt\}_8(M'TPP)_2(XDC)_4]^{8+}\bullet 8(X^{-})$ prisms, were actually associated with the dimers of 4:1:2 $[\{(Et_3P)_2Pt\}_4(M'TPP)(XDC)_2]^{4+}\bullet 4(X^{-})$ bow tie complexes (after loss of some counterions) instead of the purported prisms. Alternatively, the self-assembled bow tie complexes may have reorganized into prisms under certain electrospray ionization conditions, giving a false impression about the alleged prisms formation that was not otherwise supported by any other experimental data. Therefore, it was risky and misleading to define the structures of M′TPP-based tricomponent SCCs primarily based on the ESI-MS analysis especially when their ^{1}H NMR spectra were not at all consistent with those assignments.

Single-Crystal X-Ray Structures of Tricomponent Bow Tie (⋈) Complexes. Finally, single-crystal X-ray diffraction analysis presented the most direct evidence of bow tie structures of M′TPP-based tricomponent SCCs. Notably, this is the first time the crystal structures of any M′TPP-based tricomponent SCCs could be determined, which together with the NMR and ESI-MS data unequivocally confirmed their bow tie structures and ruled out any prism formation. Some of these bow tie complexes crystallized directly from the NMR solutions (acetone-d_6), while others formed crystals upon vapor diffusion of CH_2Cl_2 or Et_2O into NMR solutions. Although we were able to obtain the crystals of ZnTPP-based **BT2**, **BT3**, and **BT4**, and H_2TPP-based **BT2′** and **BT3′** containing rigid aromatic BPDC, BDC, and NDC linkers, it was not possible to grow crystals of **BT1** and **BT1′** complexes containing flexible aliphatic HDC linkers. The structural features of all bow tie complexes (Table 1) were fully consistent with their respective ^{1}H and ^{31}P NMR spectra, 2D ^{1}H–^{1}H NMR (COSY and ROESY) correlations, and ESI-MS data, confirming that the same species were present both in solutions and in solid crystals.

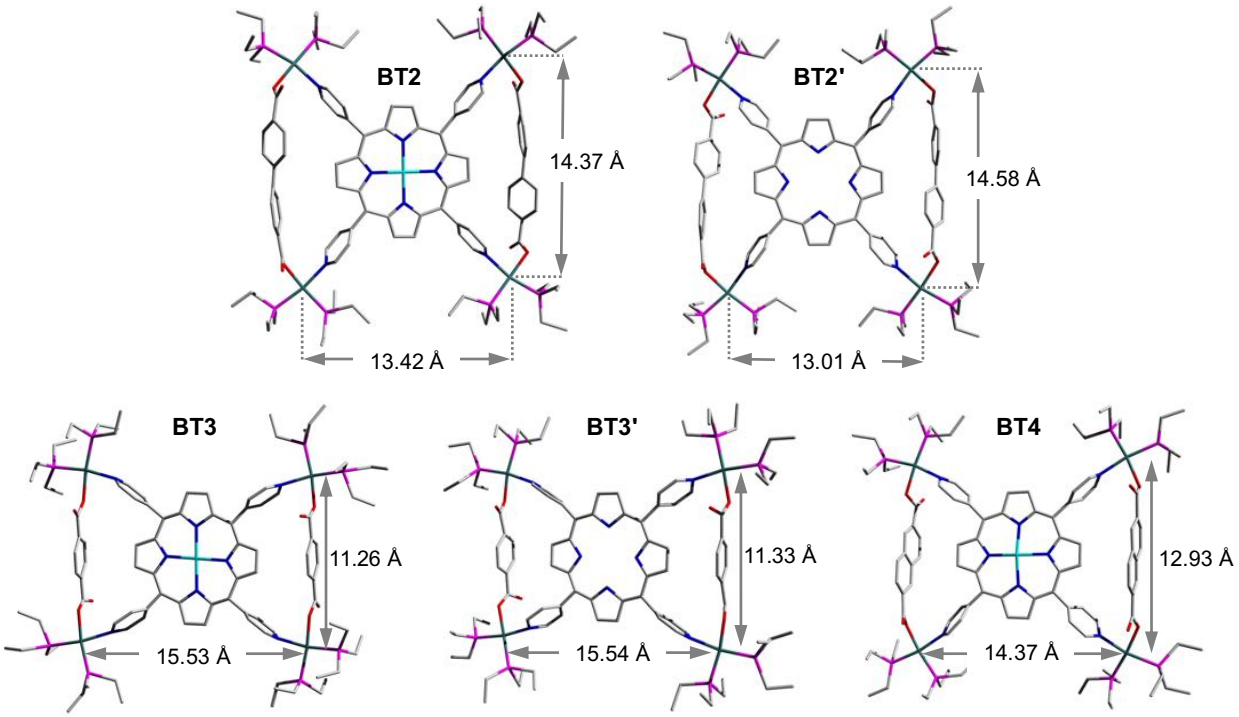

Figure 6. Single-crystal structures of **BT2**, **BT2′**, **BT3**, **BT3′** and **BT4** bow tie complexes. The distances between adjacent Pt(II) centers bridged and not bridged by XDC linkers ($d_{Pt–Pt/int}$ and $d_{Pt–Pt/ext}$) are labeled to show the differences and how that affected the shapes of the M′TPP ligands. Atom legend: green: Pt, cyan: Zn, pink: P, red: O, blue: N, grey: C. The H-atoms and TfO^- anions were omitted for clarity.

Table 1. Key structural parameters of bow tie complexes obtained from their single-crystal structures. The parameters obtained from the calculated structures are labeled with asterisks (*).

	BT1 calc.*	BT2	BT2′	BT3 (calc.*)	BT3′ (calc.*)	BT4
Space Group	—	$P\bar{1}$	$C2/c$	$C2/c$	$I4_1/a$	$P2_1/c$
$d_{Pt–Pt/int}$ (Å)	11.55*	14.37	14.58	11.26 (11.33*)	11.33 (11.33*)	12.93
$d_{Pt–Pt/ext}$ (Å)	15.41*	13.42	13.01	15.53 (15.59*)	15.54 (15.56*)	14.37
$d_{N–N/int}$ (Å)	10.19*	11.38	11.52	10.09 (10.12*)	10.07 (10.20*)	10.83
$d_{N–N/ext}$ (Å)	11.63*	10.37	10.18	11.39 (11.69*)	11.61 (11.68*)	10.80
$d_{Hc'–XDC\text{-}center}$ (Å)	2.84*	3.37	3.11	3.18 (3.50*)	3.05 (3.44*)	2.95
$d_{Hc'–Pyridine\text{-}center}$ (Å)	2.96*	3.41	3.51	3.02 (2.98*)	2.96 (3.01*)	3.19
$d_{Hc''–Pyridine\text{-}center}$ (Å)	3.37*	3.08	3.00	3.41 (3.47*)	3.47 (3.41*)	3.26
∠N–Pt–O (°)	96*, 98*	82, 85	82, 83	78, 83 (93*)	80, 83 (93*)	82, 82
$\angle(N_{Py}–Center–N_{Py})_{int}$ (°)	82*	95	97	83 (81*)	82 (82*)	88
$\angle(N_{Py}–Center–N_{Py})_{ext}$ (°)	98*	85	83	97 (99*)	98 (98*)	89
$\theta_{Porphyrin/Pyridyl\text{-}dh}$ (°)	82*, 83*	76, 77	64, 73	86, 88 (84*)	76, 80 (85*)	65, 76
$\theta_{Pyrrole/XDC\text{-}dh}$ (°)	—	—	—	80 (90*)	85 (90*)	87

The bow tie (⋈)-shaped **BT2** and **BT2′** complexes (Figure 6: $[\{(Et_3P)_2Pt\}_4(M'TPP)(BPDC)_2]^{4+}$, M′ = Zn or H_2) crystallized in $P\bar{1}$ and $C2/c$ space groups, respectively. Each complex consisted of a M′TPP core and two parallel BPDC linkers held together by four heteroleptic $(Et_3P)_2Pt(N,O)$ corners. The ∠N–Pt–O angles of slightly distorted square-planar Pt(II) corners ranged between ca. 82–85° (two diagonally opposite angles were the same), slightly less than an ideal 90° bond angle. In **BT2**, the distances between two adjacent Pt(II) corners bridged by a BPDC linker ($d_{Pt–Pt/int}$) were 14.4 Å (14.6 Å in **BT2′**), whereas the distances between two adjacent Pt(II) corners not bridged by a BPDC linker ($d_{Pt–Pt/ext}$) were 13.4 Å (13.0 Å in **BT2′**). This happened because the long BPDC linker (l_{BPDC} = 11.2 Å)[57] placed the two bridged Pt(II) corners farther away from each other, which in turn shortened the distances between the two adjacent Pt(II) corners that were not bridged by BPDC. Consequently, the distance between the two adjacent pyridyl-N atoms coordinated to two BPDC-bridged Pt(II) corners, i.e., the pyridyl-N atoms that belonged to the same triangle ($d_{N–N/int}$ = 11.4 Å in **BT2** and 11.5 Å in **BT2′**), were noticeably longer than the distance between two adjacent pyridyl-N atoms that were not part of the same triangle ($d_{N–N/ext}$ = 10.4 Å in **BT2** and 10.2 Å in **BT2′**). As a result, the N–N distances in **BT2** and **BT2′** complexes were different from the uniform distance between two adjacent pyridyl-N atoms of free M′TPP ligands ($d_{N–N/free} \approx$ 10.9 Å).[58,59] Furthermore, in **BT2**, the angle between two adjacent pyridyl rings that belonged to the same triangle ($\angle(N_{Py}–center–N_{Py})_{int}$) expanded to 95° (97° in **BT2′**), while the angle between two adjacent pyridyl rings that were not part to the same triangle ($\angle(N_{Py}–center–N_{Py})_{ext}$) contracted to 85° (83° in **BT2′**). Thus, in order to accommodate the long BPDC linker in the triangles of bow tie structures, these angles deviated by 3–5° from the ideal ~90° angle between two adjacent pyridyl rings of free M′TPP. The dihedral angles between the core porphyrin plane (pyrrole rings) and pyridyl arms were 76° in **BT2** (73° in **BT2′**) and the torsion

angle between the two phenyl rings of BPDC linker was 42° in **BT2** (37° in **BT2′**). Due to the twisted nature of the BPDC core, it was not possible to measure the dihedral angle between the pyrrole ring of M′TPP and BPDC linker located across the bay in the same triangle, but obviously they were not coplanar. The distance from the enclosed $H_{c'}$ pyrrole protons of M′TPP ligand located inside triangles to the center of the nearest phenyl ring of BPDC linker ($d_{Hc'–XDC}$) was ca. 3.4 Å in **BT2** (3.1 Å in **BT2′**), which was the longest among the bow tie complexes made of three aromatic XDC linkers employed here. In addition, the distance from the enclosed $H_{c'}$ pyrrole protons of M′TPP ligand to the center of the nearest pyridyl ring ($d_{Hc'–Pyridine\text{-}center}$) was 3.4 Å in **BT2** (3.5 Å in **BT2′**), also the longest among the bow tie complexes presented here. As a result, the enclosed $H_{c'}$ pyrrole protons of **BT2** and **BT2′** were much less shielded and less up-field shifted than those of BDC- and NDC-based bow tie complexes (Figure 6). On the other hand, the long BPDC linked pushed the pyridyl rings of M′TPP closer to the exposed $H_{c''}$ pyrrole protons ($d_{Hc''–Pyridine\text{-}center}$ ~3.1 Å) causing a modest shielding and up-field chemical shift of these protons with respect to the H_c signal of free M′TPP ligands. None of the other bow tie complexes having shorter XDC ligands displayed an up-field NMR chemical shift of the exposed $H_{c''}$ pyrrole protons; they all shifted downfield from the H_c peak of free M′TPP because the shorter linkers pulled the adjacent pyridyl rings away from the exposed $H_{c''}$ pyrrole protons and closer to the enclosed $H_{c'}$ protons (Figures 3, S2). Furthermore, the crystal structures of **BT2** and **BT2′** also explained why the enclosed $H_{c'}$ pyrrole protons located inside the triangles were ROESY-coupled with the H_u and H_v protons of the adjacent BPDC linkers located across the bay, but the exposed $H_{c''}$ pyrrole protons were not. Thus, the well-resolved structures of **BT2** and **BT2′** bow tie complexes provided a crystal-clear understanding of their NMR spectra.

Although the entire single-crystal structures of **BT2** and **BT2′** complexes, including their ancillary Et_3P ligands on the Pt(II) corners, were fully resolved, only the basic bow tie skeletons of **BT3**, **BT3′**, and **BT4** complexes consisting of the M′TPP core, two parallel BDC and NDC linkers, and four Pt(II) corners were fully resolved, but the fluxional CH_3CH_2-groups of ancillary Et_3P ligands and TfO^- anions were not, which caused large *R*-values of the latter. Nevertheless, since the ancillary Et_3P ligands and counterions were not the integral parts of bow tie structures, the poor resolution of these highly disordered components had little effect on their key structural features that were fully consistent with their respective NMR spectra.

The BDC-based bow tie complexes **BT3** and **BT3′** (Figure 6: $[\{(Et_3P)_2Pt\}_4(M'TPP)(BDC)_2]^{4+}$, M′ = Zn or H_2) also featured a M′TPP core and two parallel BDC linkers held together by four heteroleptic $(Et_3P)_2Pt(N,O)$ corners and crystallized in *C*2/c and *I*4$_1$/a space groups, respectively. While these two complexes shared the main structural parameters, the ancillary Et_3P ligands and counterions were less

disordered in **BT3′** than in **BT3**. The ∠N–Pt–O angles at distorted square-planar Pt(II) corners ranged between ca. 78–83° (two diagonally opposite angles were the same). The distances between two adjacent Pt(II) corners bridged by a short BDC linker (l_{BDC} = 6.9 Å)[57] were ca. 11.3 Å ($d_{Pt–Pt/int}$), whereas the distances between two adjacent Pt(II) corners not bridged by a BDC linker ($d_{Pt–Pt/ext}$) were ca. 15.5 Å, suggesting that the BDC linkers pulled the two bridged Pt(II) corners closer to each other, which in turn increased the distances between the two non-bridged Pt(II) corners. Consequently, the N-atoms of two adjacent pyridyl rings coordinated to two bridged Pt(II) corners, i.e., the pyridyl-N atoms that belonged to the same triangle, also came closer to each other ($d_{N–N/int} \approx$ 10.1 Å) while the distance between two pyridyl-N atoms that were not part of the same triangle increased ($d_{N–N/ext} \approx$ 11.5 Å) with respect to an almost uniform N–N distances observed in free M′TPP ($d_{N–N/free} \approx$ 10.9 Å).[58,59] Thus, even though BDC was much shorter than $d_{N–N}$ in free M′TPP, they still formed bow tie complexes instead of prisms via heteroleptic coordination with the $(Et_3P)_2Pt^{II}$ corners. To accommodate the short BDC linkers within the triangles of bow tie-shaped **BT3** and **BT3′** complexes, the angles between two adjacent pyridyl rings coordinated to the bridged Pt(II) corners ($\angle(N_{Py}–center–N_{Py})_{int}$) shrunk to ~82–83°, while the angles between two adjacent pyridyl rings not belonging to the same triangle ($\angle(N_{Py}–center–N_{Py})_{ext}$) expanded to ~97–98°, i.e., these angles deviated by 7–8° from the ideal ~90° angle in free M′TPP. The dihedral angles between the core porphyrin plane (pyrrole rings) and pyridyl arms varied between 76–88°. The dihedral angles between the enclosed pyrrole rings of M′TPP and the BDC core located across the bay of the same triangle were 80–85°, i.e., they were almost orthogonal to each other. The enclosed $H_{c'}$ pyrrole protons located inside the triangles were projected toward the center of the BDC ring ($d_{Hc'–XDC} \approx$ 3.1 Å) as well as the adjacent pyridyl rings which were pulled closer ($d_{Hc'–Pyridine\text{-}center} \approx$ 3 Å) by the short BDC linker. As a result, the $H_{c'}$ protons in **BT3** and **BT3′** complexes were highly shielded and displayed large up-field NMR chemical shifts (Figures 3, S2). On the other hand, since the pyridyl rings of M′TPP moved away from the exposed $H_{c''}$ pyrrole protons ($d_{Hc''–Pyridine\text{-}center} \approx$ 3.4 Å), they became less shielded and shifted noticeably downfield from the H_c signal of free M′TPP ligands. Furthermore, the crystal structures of these bow tie complexes provided valuable insights into why the enclosed $H_{c'}$ pyrrole protons were ROE-coupled with the H_w protons of BDC linker located across the bay, but the distant exposed $H_{c''}$ pyrrole protons were not.

The NDC-based bow tie complex **BT4** $[\{(Et_3P)_2Pt\}_4(ZnTPP)(NDC)_2]^{4+}$ (Figure 6) was composed of a ZnTPP core and two parallel NDC linkers held together by four heteroleptic $(Et_3P)_2Pt(N,O)$ corners and crystallized in $P2_1/c$ space group. All four ∠N–Pt–O angles of distorted square-planar Pt(II) corners were ca. 82°. The distances between two adjacent Pt(II) corners bridged by a NDC linker ($d_{Pt–Pt/int}$ = 12.9 Å)[57] were slightly shorter than the distances between two adjacent Pt(II) corners not bridged by a NDC

linker ($d_{Pt–Pt/ext}$ = 14.4 Å). The distance between the N-atoms of two adjacent pyridyl rings coordinated to two bridged Pt(II) corners ($d_{N–N/int}$) and the distance between two adjacent pyridyl-N atoms that were not part of the same triangle ($d_{N–N/ext}$) were almost the same (ca. 10.8 Å) and close to the uniform distances between two adjacent pyridyl-N atoms of free ZnTPP ligand ($d_{N–N/free}$ ~10.9 Å). Similarly, the angles between two adjacent pyridyl rings belonging to the same triangle ($\angle(N_{Py}–Center–N_{Py})_{int}$) and the angles between two adjacent pyridyl rings not belonging to the same triangle ($\angle(N_{Py}–Center–N_{Py})_{ext}$) were 88° and 89°, respectively, which were close to ~90° angle between adjacent pyridyl rings found in free ZnTPP. Thus, the intermediate length of NDC (l_{NDC} = 9.2 Å) caused the least distortion of the ZnTPP ligand in **BT4** than any other XDC linkers employed here. The dihedral angles between the porphyrin core and pyridyl rings were between 65–76°. The ZnTPP and the NDC planes were oriented nearly orthogonal to each other forming dihedral angles of 87°. The enclosed $H_{c'}$ pyrrole protons located inside the triangles were projected toward the NDC core ($d_{Hc'–XDC}$ ≈ 3 Å), as well as to the center of the adjacent pyridyl rings ($d_{Hc'–Pyridine\text{-}center}$ ≈ 3.2 Å). As a result, the enclosed $H_{c'}$ pyrrole protons of **BT4** experienced the maximum shielding effect and displayed a larger up-field NMR chemical shift than any other bow tie complexes presented here (*vide supra*). On the other hand, the distance between the exposed $H_{c''}$ pyrrole protons and the adjacent pyridyl rings ($d_{Hc''–Pyridine\text{-}center}$ ≈ 3.3 Å) was greater than that found in BPDC-based **BT2** and **BT2′** (ca. 3 Å) but smaller than that of BDC-based **BT3** and **BT3′** (ca. 3.4 Å). As a result, the $H_{c''}$ protons of **BT4** displayed a slight downfield chemical shift from the H_c signal of free ZnTPP (Figures 3, S2). Furthermore, the crystal structure of **BT4** also shed light on why the enclosed $H_{c'}$ pyrrole protons located inside the triangles were ROE-coupled with the H_x, H_y, and H_z protons of the adjacent NDC linker located across the bay, but the exposed $H_{c''}$ pyrrole protons were not.

Energy Optimized Structures of Bow Tie Complexes. Since the crystal structures of **BT1** or **BT1′** complexes containing flexible HDC linker could not be determined, we calculated their energy minimized structures using Gaussian 09 software (Figure 7). To verify the accuracy of the calculated **BT1** structure, we also calculated the energy minimized structures of BDC-based **BT3** and **BT3′** complexes by applying the same level of theory (PM-6), which showed excellent agreement with their actual crystal structures (Table 1). Due to similar lengths of HDC and BDC linkers, the calculated **BT1** structure displayed strong similarities with the calculated and experimental SXRD structures of **BT3**. Like other bow tie complexes, **BT1** $[\{(Et_3P)_2Pt\}_4(ZnTPP)(HDC)_2]^{4+}$ featured a ZnTPP core and two parallel HDC linkers held together by four heteroleptic $(Et_3P)_2Pt(N,O)$ corners.

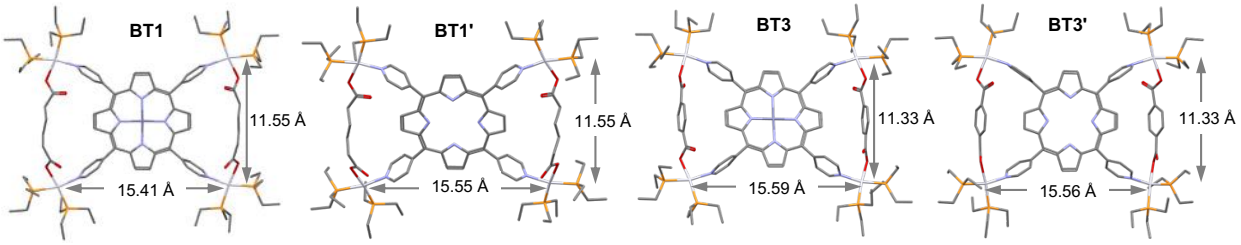

Figure 7. The optimized structures of **BT1**, **BT1′**, **BT3**, and **BT3′** complexes calculated by PM6 method. The distances between adjacent Pt(II) centers bridged and not bridged by XDC linkers ($d_{Pt–Pt/int}$ and $d_{Pt–Pt/ext}$) are labeled to show the XDC linkers affected the shapes of the M′TPP ligands.

In the calculated **BT1** structure, the ∠N–Pt–O angles at distorted square-planar Pt(II) corners were ca. 96–98°. The two adjacent HDC-bridged Pt(II) corners ($d_{Pt–Pt/int}$) were located ca. 11.6 Å apart, whereas the two adjacent Pt(II) corners not bridged by a HDC linker ($d_{Pt–Pt/ext}$) were located ca. 15.4 Å apart. The Pt–Pt distances in **BT1** were comparable to those observed in **BT3**, which suggested that the HDC and BDC linkers have similar lengths. Therefore, like BDC, the short HDC linkers also pulled the two bridged Pt(II) corners closer to each other, which in turn increased the distances between the two adjacent non-bridged Pt(II) corners. Consequently, the N-atoms of two adjacent pyridyl rings of ZnTPP coordinated to two Pt(II) corners bridged by BDC linkers, i.e., the pyridyl-N atoms that belonged to the same triangle, also came closer to each other ($d_{N–N/int} \approx 10.2$ Å) while the distance between two pyridyl-N atoms that were not part of the same triangle increased ($d_{N–N/ext} \approx 11.6$ Å) from the uniform N–N distance (ca. 10.9 Å) found in free M′TPP ligands. This happened because in order to accommodate short HDC linkers within the triangles of the bow tie structure, the angles between two adjacent pyridyl rings that belonged to the same triangle ($\angle(N_{Py}–center–N_{Py})_{int}$) shrunk to ~82°, while the angles between two adjacent pyridyl rings that were not part of the same triangle ($\angle(N_{Py}–center–N_{Py})_{ext}$) expanded to ~98°, i.e., these angles deviated by ca. 8° from the ideal ~90° angle found in free M′TPP. The distances from the enclosed $H_{c'}$ pyrrole protons to the center of nearest pyridyl ring ($d_{Hc'–Pyridine-center}$) was ca. 2.96 Å and to the nearest H_t protons of HDC linker located across the bay was ca. 2.8 Å. The enclosed $H_{c'}$ protons of HDC-based **BT1** were least up-field shifted than those of any other bow tie complexes presented here because they were mostly shielded by the adjacent pyridyl rings while the alkyl chain exerted little shielding effect. On the other hand, since the pyridyl rings of ZnTPP were pulled away from the exposed $H_{c''}$ pyrrole protons ($d_{Hc''–Pyridine-center} \approx 3.4$ Å) by short HDC linkers, they became less shielded and shifted downfield from the H_c signal of free ZnTPP ligand (*vide supra*). The exposed $H_{c''}$ pyrrole protons of **BT1** and **BT3** complexes displayed similar downfield chemical shifts because HDC and BDC linkers having similar lengths pulled the adjacent pyridyl rings away from these protons to the same extent. Furthermore, the calculated **BT1** structure provided valuable insights into

why the enclosed $H_{c'}$ pyrrole protons were ROE-coupled with the H_t protons of the adjacent HDC linker located across the bay, but the exposed $H_{c''}$ protons were not.

Thus, the single-crystal and energy-minimized structures of M′TPP-based tricomponent SCCs further corroborated that regardless of the length (within the range of 6.9–11.2 Å) and rigidity of the XDC linkers, the Pt(II)-driven self-assembly of M′TPP and XDC ligands exclusively yielded 2D bow tie complexes instead of 3D prisms. This was possible because the pyridyl arms of M′TPP core coordinated to the XDC-bridged Pt(II) corners were able to bend to some extent in order to incorporate the XDC linkers having variable lengths within the triangles of bow tie structures. In addition to our comprehensive studies that unequivocally demonstrated bow tie formation with four different XDC linkers, all previously reported M′TPP-based tricomponent SCCs based on other rigid (e.g., isophthalate and BINOL-3,3′-dicarboxylate)[33,34] and flexible (e.g., heptanedioate and octanedioate)[33] XDC linkers have also displayed the same characteristic ^{1}H NMR signals of bow tie complexes, i.e., two distinct singlets for the enclosed $H_{c'}$ and exposed $H_{c''}$ pyrrole protons of the M′TPP core, although they were thought to be tetragonal prisms. In all those cases, the lengths of the rigid linkers were within the range of XDC linkers employed here that actually formed bow tie complexes, whereas the longer flexible linkers, such as heptanedioate and octanedioate, could bulge out like an arc (i.e., quarter-circles) to form ∞-shaped complexes instead of the purported prisms. Therefore, more studies and compelling evidence beyond just ESI-MS data are needed to verify the prism formation by those XDC linkers. Since all XDC linkers employed thus far seemed to have formed M′TPP-based bow tie complexes, we envisioned that much longer and rigid 4,4′-ethyne-1,2-diyldibezoate and *N,N*-dicarboxyphenyl naphthalenediimide linkers might form tetragonal prisms by connecting the pyridyl groups of two cofacial M′TPP ligands via heteroligated Pt(II) corners because they are too long to close the triangles of bow tie complexes by intramolecularly bridging two adjacent Pt(II)-coordinated pyridyl rings of an M′TPP core. However, these extremely long and rigid linkers neither formed any prisms nor any bow tie complexes, and yielded mixtures of supramolecular assemblies without any well-defined structures. Taken together, these studies suggested that the dihedral angles between the porphyrin core and pyridyl rings of M′TPP were not suitable for the M′TPP-based 3D prism formation. As a result, M′TPP ligands could only form tricomponent bow tie complexes so long as the XDC linkers could bridge two Pt(II) corners coordinated by two adjacent pyridyl groups of M′TPP forming the bases of isosceles triangles. Beside M′TPP, another tetratopic ligand, 1,2-di(4-pyridyl)ethylene (DPE) was also used previously along with XDC linkers to construct tetragonal prisms.[35,36,40] Since the dihedral angles and the angles of projection of the pyridyl rings in DPE are different from those of M′TPP, it is plausible that the former indeed formed tetragonal prisms. However, in the light of the discovery of M′TPP-based bow tie

complexes and better understanding of why M′TPP could not form tetragonal prisms with any XDC linkers, additional 2D NMR and X-ray crystallographic studies would be beneficial to verify the structures of other supramolecular prisms.

CONCLUSION

In summary, we have demonstrated that Pt(II)-driven social self-assembly of a tetratopic M′TPP ligand and four ditopic XDC linkers having different lengths (6.9–11.2 Å) and rigidities consistently yielded novel 2D bow tie complexes $[\{(Et_3P)_2Pt\}_4(M'TPP)(XDC)_2]\cdot(4TfO)$ featuring a M′TPP core and two parallel XDC linkers that were held together by four heteroligated $Pt^{II}(N,O)$ corners. The ^{31}P NMR spectra of the resulting tricomponent SCCs confirmed the formation of heteroleptic $Pt^{II}(N,O)$ corners bearing one carboxylate and one pyridyl groups, while their ^{1}H and 2D NMR spectra presented the most compelling signs of their bow tie structures by revealing that the four pyrrole rings of M′TPP core were located in two distinct chemical environments. Two opposite pyrrole rings carrying the more shielded $H_{c'}$ protons were located inside two isosceles triangles formed by two parallel XDC linkers that bridged the Pt(II) corners coordinated to two adjacent pyridyl groups, while the other two pyrrole rings remained exposed, and their $H_{c''}$ protons were not shielded by or coupled to XDC linkers. These phenomena not only indicated the formation of bow tie complexes, but also ruled out the formation of M′TPP-based tetragonal prisms, which should have possessed all chemically equivalent pyrrole protons. The bow tie complex formation was further corroborated by ESI-MS analysis, while the most direct and compelling evidence came from single-crystal x-ray structures (and energy minimized structures when the crystal structures were not available) that revealed well-resolved bow tie skeletons consisting of a M′TPP core, two parallel XDC linkers, and four Pt(II) conners although the ancillary Et_3P groups and counterions were disordered in some cases. These results demonstrated that in order to accommodate different XDC linkers having different lengths (ca. 6.9–11.2 Å) and rigidity into isosceles triangles of bow tie structures, the pyridyl arms of M′TPP ligands moved accordingly departing from their original angles (~90°) of projections. This led to the formation of bow tie complexes exclusively, which were entropically more favored over prisms. Thus, these comprehensive studies of M′TPP-based tricomponent SCCs not only produced novel bow tie complexes, but also demonstrated that these tetratopic ligands were unable to form tetragonal prisms regardless of the length and rigidity dicarboxylate linkers. While the main focus of our fundamental studies presented here was to determine the accurate structures and compositions of M′TPP-based tricomponent SCCs, in the light of these revelations one could argue that some of the fascinating properties and functions, such as photodynamic cancer therapy that were previously attributed to alleged prisms,[30,33,34,39,55,56] actually

belonged to bow tie complexes. Further studies of potential applications of these M′TPP-based bow tie complexes as light-harvesting and energy transduction systems are underway in our laboratory.

ASSOCIATED CONTENT

Supporting Information

The Supporting Information is available free of charge on the ACS Publications website at DOI: XXXXX. Experimental details and additional data including Figures S1–S6 (PDF), and CIF files.

Accession Code

CCDC 2081606–2081610 contain crystallographic data, which can be obtained free of charge via www.ccdc.cam.ac.uk/data_request/cif, or by emailing data_request@ccdc.cam.ac.uk, or by contacting The Cambridge Crystallographic Data Centre, 12 Union Road, Cambridge CB2 1EZ, UK.

AUTHOR INFORMATION

*Corresponding Author

Email: souravs@clemson.edu

ORCID

Sourav Saha: 0000-0001-6610-4820

Paola A. Benavides: 0000-002-1701-5036

M. Andrey Joaqui-Joaqui: 0000-001-7446-6004

Note

The authors declare no competing financial interest.

ACKNOWLEDGEMENTS

This work was supported by the National Science Foundation (NSF award nos. CHE-1660329 and DMR-1809092) and Clemson University. We also acknowledge the NSF-MRI grant CHE-1725919 for the 500 MHz NMR instrument used in our studies. We thank Dr. Colin McMillen for single-crystal X-ray analysis and Dr. William T. Pennington Jr. for valuable discussions.

REFERENCES

1. Fujita, M.; Yazaki, J.; Ogura, K. Preparation of a Macrocyclic Polynuclear Complex, [(En)Pd(4,4′-Bpy)]$_4$(NO_3)$_8$ (En = Ethylenediamine, Bpy = Bipyridine), Which Recognizes an Organic Molecule in Aqueous Media. *J. Am. Chem. Soc.* **1990**, *112*, 5645–5647.

2. Stang, P. J.; Cao, D. H. Transition Metal Based Cationic Molecular Boxes. Self-Assembly of Macrocyclic Platinum(II) and Palladium(II) Tetranuclear Complexes. *J. Am. Chem. Soc.* **1994**, *116*, 4981–4982.

3. Stang, P. J.; Olenyuk, B.; Fan, J.; Arif, A. M. Combining Ferrocene and Molecular Squares: Self-Assembly of Heterobimetallic Macrocyclic Squares Incorporating Mixed Transition Metal Systems and a Main Group Element. Single-Crystal X-ray Structure of [Pt(dppf)(H_2O)$_2$][OTf]$_2$. *Organometallics* **1996**, *15*, 904–908.

4. Stang, P. J.; Olenyuk, B. Self-Assembly, Symmetry, and Molecular Architecture: Coordination as the Motif in the Rational Design of Supramolecular Metallacyclic Polygons and Polyhedra. *Acc. Chem. Res.* **1997**, *30*, 502–518.

5. Lees, A. J.; Sun, S.-S. Self-Assembly Organometallic Squares with Terpyridyl Metal Complexes as Bridging Ligands. *Inorg. Chem.* **2001**, *40*, 3154–3160.

6. Würthner, F.; You, C.-C.; Saha-Möller, C. R. Metallosupramolecular Squares: From Structure to Function. *Chem. Soc. Rev.* **2004**, *33*, 133–146.

7. Gianneschi, N. C.; Masar III, M. S.; Mirkin, C. A. Development of a Coordination Chemistry-Based Approach for Functional Supramolecular Structures, *Acc. Chem. Res.* **2005**, *38*, 825–837.

8. Northrop, B. H.; Zheng, Y.-R.; Chi, K.-W.; Stang, P. J. Self-Organization in Coordination-Driven Self-Assembly. *Acc. Chem. Res.* **2009**, *42*, 1554–1563.

9. Chifotides, H. T.; Giles, I. D.; Dunbar, K. R. Supramolecular Architectures with π-Acidic 3,6-Bis(2-Pyridyl)-1,2,4,5-Tetrazine Cavities: Role of Anion−π Interactions in the Remarkable Stability of Fe(II) Metallacycles in Solution. *J. Am. Chem. Soc.* **2013**, *135*, 3039–3055.

10. Gordillo, M. A.; Benavides, P. A.; Saha, S. Anion/Naphthalenediimide Interactions in a Pd(II)-Based Tetrameric Metallocycle. *Cryst. Growth Des.* **2019**, *19*, 6017–6022.

11. Kumazawa, K.; Biradha, K.; Kusukawa, T.; Okano, T.; Fujita, M. Multicomponent Assembly of a Pyrazine-Pillared Coordination Cage that Selectively Binds Planar Guests by Intercalation. *Angew. Chemie Int. Ed*. **2003**, *42*, 3909–3913.

12. Chakrabarty, R.; Mukherjee, P. S.; Stang, P. J. Supramolecular Coordination: Self-Assembly of Finite Two- and Three-Dimensional Ensembles. *Chem. Rev.* **2011**, *111*, 6810–6918.

13. Cook T. R.; Zheng, Y.-R.; Stang, P. J. Metal–organic frameworks and self-assembled supramolecular coordination complexes: Comparing and contrasting the design, synthesis, and functionality of metal–organic materials. *Chem. Rev.* **2013**, *112*, 734–777.

14. Cook, T. R.; Stang, P. J. Recent Developments in the Preparation and Chemistry of Metallacycles and Metallacages via Coordination. *Chem. Rev.* **2015**, *115*, 7001–7045.

15. Zarra, S.; Wood, D. M.; Roberts, D. A.; Nitschke, J. R. Molecular Containers in Complex Chemical Systems. *Chem. Soc. Rev.* **2015**, *44*, 419–432.

16. Fujii, S.; Tada, T.; Komoto, Y.; Osuga, T.; Murase, T.; Fujita, M.; Kiguchi, M., Rectifying Electron-Transport Properties through Stacks of Aromatic Molecules Inserted into a Self-Assembled Cage. *J. Am. Chem. Soc.* **2015**, *137,* 5939–5947.

17. Bloch, W. M.; Clever, G. H. Integrative Self-Sorting of Coordination Cages Based on ‘Naked’ Metal Ions. *Chem. Commun.* **2017**, *53*, 8506–8516.

18. Ronson, T. K.; Meng, W.; Nitschke, J. R. Design Principles for the Optimization of Guest Binding in Aromatic-Paneled $Fe^{II}_4L_6$ Cages. *J. Am. Chem. Soc.*, **2017**, *139,* 9698–9707.

19. Brenner, W.; Ronson, T. K.; Nitschke, J. R. Separation and Selective Formation of Fullerene Adducts within an $M^{II}_8L_6$ Cage. *J. Am. Chem. Soc.*, **2017**, *139*, 75–78.

20. Saha, S.; Regeni, I.; Clever, G. H. Structure Relationships between Bis-Monodentate Ligands and Coordination Driven Self-Assemblies. *Coord. Chem. Rev.* **2018**, *374*, 1–14.

21. Pullen, S.; Clever, G. H. Mixed-Ligand Metal–Organic Frameworks and Heteroleptic Coordination Cages as Multifunctional Scaffolds—A Comparison. *Acc. Chem. Res.* **2018**, *51*, 3052–3064.

22. Chakraborty, S.; Newkome, G. R. Terpyridine-Based Metallosupramolecular Constructs: Tailored Monomers to Precise 2D-Motifs and 3D-Metallocages. *Chem. Soc. Rev.* **2018**, *47*, 3991–4016.

23. Bardhan, D.; Chand, D. K. Palladium(II)-Based Self-Assembled Heteroleptic Coordination Architectures: A Growing Family. *Chem. Eur. J.* **2019**, *25*, 12241–12269.

24. Kitagawa, S.; Kitaura, R.; Noro, S. Functional Porous Coordination Polymers. *Angew. Chem. Int. Ed.* **2004**, *43*, 2334–2375.

25. Leong, W. L.; Vittal, J. J. One-Dimensional Coordination Polymers: Complexity and Diversity in Structures, Properties, and Applications. *Chem. Rev.* **2011**, *111*, 688–764.

26. Furukawa, H.; Cordova, K. E.; O'Keeffe, M.; Yaghi, O. M. The Chemistry and Applications of Metal-Organic Frameworks. *Science* **2013**, *341*, 974–986.

27. Chi, K. W.; Addicott, C.; Arif, A. M.; Stang, P. J. Ambidentate Pyridyl-Carboxylate Ligands in the Coordination-Driven Self-Assembly of 2D Pt Macrocycles: Self-Selection for a Single Isomer. *J. Am. Chem. Soc*. **2004**, *126*, 16569–16574.

28. Wang, M.; Zheng, Y.-R.; Ghosh, K.; Stang, P. J. Metallosupramolecular Tetragonal Prisms via Multicomponent Coordination-Driven Self-Assembly. *J. Am. Chem. Soc.* **2010**, *132*, 6282–6283.

29. Zheng, Y. R.; Lan, W. J.; Wang, M.; Cook, T. R.; Stang, P. J. Designed Post-Self-Assembly Structural and Functional Modifications of a Truncated Tetrahedron. *J. Am. Chem. Soc.* **2011**, *133*, 17045–17055.

30. Zheng, Y.-R.; Zhao, Z.; Wang, M.; Ghosh, K.; Pollock, J. B.; Cook, T. R.; Stang, P. J. A Facile Approach toward Multicomponent Supramolecular Structures: Selective Self-Assembly via Charge Separation. *J. Am. Chem. Soc.* **2010**, *132*, 16873–16882.

31. Wang, M.; Zheng, Y.-R.; Cook, T. R.; Stang, P. J. Construction of Functionalized Metallosupramolecular Tetragonal Prisms via Multicomponent Coordination-Driven Self-Assembly. *Inorg. Chem.* **2011**, *50*, 6107–6113.

32. Pollock, J. B.; Cook, T. R.; Schneider, G. L.; Stang, P. J. Multi-Component Coordination-Driven Self-Assembly: Construction of Alkyl-Based Structures and Molecular Modelling. *Chem. Asian J.* **2013**, *8*, 2423–2429.

33. Shi, Y.; Sánchez-Molina, I.; Cao, C.; Cook, T. R.; Stang, P. J. Synthesis and Photophysical Studies of Self-Assembled Multicomponent Supramolecular Coordination Prisms Bearing Porphyrin Faces. *Proc. Natl. Acad. Sci. USA* **2014**, *111*, 9390–9395.

34. Ye, Y.; Cook, T. R.; Wang, S. P.; Wu, J.; Li, S.; Stang, P. J. Self-Assembly of Chiral Metallacycles and Metallacages from a Directionally Adaptable BINOL-Derived Donor. *J. Am. Chem. Soc*. **2015**, *137*, 11896–11899.

35. Yan, X.; Cook, T. R.; Wang, P.; Huang, F.; Stang, P. J. Highly emissive platinum(II) metallacages. *Nature Chem.* **2015**, *7*, 342–348.

36. Yu, G.; Cook, T. R.; Li, Y.; Yan, X.; Wu, D.; Shao, L.; Shen, J.; Tang, G.; Huang, F.; Chen, X.; Stang, P. J. Tetraphenylethene-Based Highly Emissive Metallacage as a Component of Theranostic Supramolecular Nanoparticles. *Proc. Natl. Acad. Sci*. **2016**, *113*, 13720–13725.
37. Li, Z.; Yan, X.; Huang, F.; Sepehrpour, H.; Stang, P. J. Near-Infrared Emissive Discrete Platinum(II) Metallacycles: Synthesis and Application in Ammonia Detection. *Org. Lett*. **2017**, *19*, 5728–5731.
38. Zhang, M.; Saha, M. L.; Wang, M.; Zhou, Z.; Song, B.; Lu, C.; Yan, X.; Li, X.; Huang, F.; Yin, S.; Stang, P. J. Multicomponent Platinum(II) Cages with Tunable Emission and Amino Acid Sensing. *J. Am. Chem. Soc.* **2017**, *139*, 5067−5074.
39. Yu, G.; Yu, S.; Saha, M. L.; Zhou, J.; Cook, T. R.; Yung, B. C.; Chen, J.; Mao, Z.; Zhang, F.; Zhou, Z.; Liu, Y.; Shao, L.; Wang, S.; Gao, C.; Huang, F.; Stang, P. J.; Chen, X. A Discrete Organoplatinum(II) Metallacage as a Multimodality Theranostic Platform for Cancer Photochemotherapy. *Nat. Commun*. **2018**, *9*, 1–18.
40. Sun, Y.; Yao, Y.; Wang, H.; Fu, W.; Chen, C.; Saha, M. L.; Zhang, M.; Datta, S.; Zhou, Z.; Yu, H.; Li, X.; Stang, P. J. Self-Assembly of Metallacages into Multidimensional Suprastructures with Tunable Emissions. *J. Am. Chem. Soc*. **2018**, *140*, 12819–12828.
41. Chang, X.; Zhou, Z.; Shang, C.; Wang, G.; Wang, Z.; Qi, Y.; Li, Z.-Y.; Wang, H.; Cao, L.; Li, X.; Fang, Y.; Stang, P. J. Coordination-Driven Self-Assembled Metallacycles Incorporating Pyrene: Fluorescence Mutability, Tunability, and Aromatic Amine Sensing. *J. Am. Chem. Soc.* **2019**, *141*, 1757–1765.
42. Chang, X.; Zhou, Z.; Shang, C.; Wang, G.; Wang, Z.; Qi, Y.; Li, Z. Y.; Wang, H.; Cao, L.; Li, X.; Fang, Y.; Stang, P. J. Coordination-Driven Self-Assembled Metallacycles Incorporating Pyrene: Fluorescence Mutability, Tunability, and Aromatic Amine Sensing. *J. Am. Chem. Soc*. **2019**, *141*, 1757–1765.
43. Sun, Y.; Chen, C.; Liu, J.; Stang, P. J. Recent Developments in the Construction and Applications of Platinum-Based Metallacycles and Metallacages Via Coordination. *Chem. Soc. Rev*. **2020**, *49*, 3889–3919.
44. Ghosh, S.; Mukherjee, P. S. Self-Assembled Pd(II) Metallocycles Using an Ambidentate Donor and the Study of Square−Triangle Equilibria. *Inorg. Chem*. **2009**, *48*, 2605–2613.
45. Bar, A. K.; Mostafa, G.; Mukherjee, P. S. A Pd_6 Molecular Cage via Multicomponent Self-Assembly Incorporating Both Neutral and Anionic Linkers. *Inorg. Chem.* **2010**, *49*, 7647–7649.
46. Samanta, D.; Shanmugaraju, S.; Joshi, S. A.; Patil, Y. P.; Nethaji, M.; Mukherjee, P. S. Pillar height dependent formation of unprecedented Pd_8 molecular swing and Pd_6 molecular boat via multicomponent self-assembly. *Chem. Commun*. **2012**, *48*, 2298–2300.
47. García-Simón, C.; Garcia-Borràs, M.; Gómez, L.; Garcia-Bosch, I.; Osuna, S.; Swart, M.; Luis, J. M.; Rovira, C.; Almedia, M.; Imaz, I.; Maspoch, D.; Costas, M.; Ribas, X. Self-Assembled Tetragonal Prismatic Molecular Cage Highly Selective for Anionic π Guests. *Chem. Eur. J.* **2013**, *19*, 1445–1456.
48. García-Simón, C.; Garcia-Borràs, M.; Gómez, L.; Parella, T.; Osuna, S.; Juanhuix, J.; Imaz, I.; Maspoch, D.; Costas, M.; Ribas, X. Sponge-like Molecular Cage for Purification of Fullerenes. *Nat. Commun.* **2014**, *5*, 5557.
49. Colomban, C.; Szalóki, G.; Allain, M.; Gómez, L.; Goeb, S.; Sallé, M.; Costas, M.; Ribas, X. Reversible C_{60} Ejection from a Metallocage through the Redox-Dependent Binding of a Competitive Guest. *Chem. Eur. J.* **2017**, *23*, 3016–3022.

50. Colomban, C.; Martin-Diaconescu, V.; Parella, T.; Goeb, S.; García-Simón, C.; Lloret-Fillol, J.; Costas, M.; Ribas, X. Design of Zn-, Cu-, and Fe-Coordination Complexes Confined in a Self-Assembled Nanocage. *Inorg. Chem.* **2018**, *57*, 3529–3539.

51. Fuertes-Espinosa, C.; Gómez-Torres, A.; Morales-Martínez, R.; Rodríguez-Fortea, A.; García-Simón, C.; Gándara, F.; Imaz, I.; Juanhuix, J.; Maspoch, D.; Poblet, J. M.; Echegoyen, L.; Ribas, X. Purification of Uranium-Based Endohedral Metallofullerenes (EMFs) by Selective Supramolecular Encapsulation and Release. *Angew. Chem. Int. Ed.* **2018**, *57*, 11294–11299.

52. Colomban, C.; Fuertes-Espinosa, C.; Goeb, S.; Sallé, M.; Costas, M.; Blancafort, L.; Ribas, X. Self-Assembled Cofacial Zinc-Porphyrin Supramolecular Nanocapsules as Tunable $^1O_2$ Photosensitizers. *Chem. Eur. J.* **2018**, *24*, 4371–4381.

53. García-Simón, C.; Monferrer, A.; Garcia-Borràs, M.; Imaz, I.; Maspoch, D.; Costas, M.; Ribas, X. Sponge-like Molecular Cage for Purification of Fullerenes. *Chem. Commun.* **2019**, *55*, 798–801.

54. Ubasart, E.; Borodin, O.; Fuertes-Espinosa, C.; Xu, Y.; García-Simón, C.; Gómez, L.; Juanhuix, J.; Gándara, F.; Imaz, I.; Maspoch, D.; Delius, M.; Ribas, X. A Three-Shell Supramolecular Complex Enables the Symmetry-Mismatched Chemo- and Regioselective Bis-Functionalization of C_{60}. *Nat. Chem*. **2021**, DOI: 10.1038/s41557-021-00658-6.

55. Yu, G.; Ye, Y.; Tong, Z.; Yang, J.; Li, Z.; Hua, B.; Shao, L.; Li, S. A Porphyrin-Based Discrete Tetragonal Prismatic Cage: Host-Guest Complexation and Its Application in Tuning Liquid-Crystalline Behavior. *Macromol. Rapid Commun*. **2016**, *37*, 1540–1547.

56. Zhao, Z.; Zhang, Z.; Wang, H.; Li, X.; Zhang, M. Multicomponent Porphyrin-Based Tetragonal Prismatic Metallacages and Their Photophysical Properties. *Isr. J. Chem.* **2019**, *59*, 299–305.

57. Eddaoudi, M.; Kim, J.; Rosi, N.; Vodak, D.; Wachter, J.; O'Keeffe, M.; Yaghi, M. Systematic Design of Pore Size and Functionality in Isoreticular MOFs and Their Application in Methane Storage. *Science* **2002**, *295*, 469–472.

58. Lipstman, S.; Goldberg, I. Hydrogen-Bonded Three-Dimensional Network of a Lanthanum(III) Exocyclic Complex with 5,10,15,20-Tetra-4-Pyridyl-Porphyrin. *Acta Cryst. Sect. C*. **2009**, *65*, 371–373.

59. Dinelli, L. R.; Von Poelhsitz, G.; Castellano, E. E.; Ellena, J.; Galembeck, S. E.; Batista, A. A. On an Electrode Modified by a Supramolecular Ruthenium Mixed Valence (Ru^{II}/Ru^{III}) Diphosphine-Porphyrin Assembly. *Inorg. Chem*. **2009**, *48*, 4692–4700.

Table of Contents

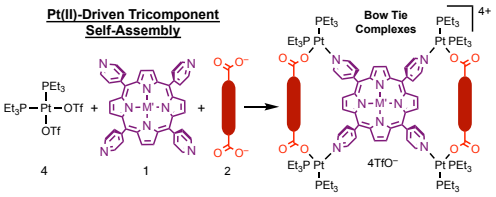

Supporting Information

Pt(II)-Coordinated Tricomponent Supramolecular Assemblies of Tetrapyridyl Porphyrin and Dicarboxylate Ligands: Are They 2D Bow Ties or 3D Prisms?

Paola A. Benavides,[†] Monica A. Gordillo,[†] Ashok Yadav,[†] M. Andrey Joaqui-Joaqui,[‡] and Sourav Saha*[,†]

[†]Department of Chemistry, Clemson University, Clemson, South Carolina 29634, United States

[‡]Department of Chemistry, University of Minnesota, Minneapolis, MN 55455, United States

*Email: souravs@clemson.edu

Table of Contents

General Materials and Methods

Reagents, starting materials, and solvents were purchased from Sigma-Aldrich, Acros Organic and TCI America. *cis*-$Pt(PEt_3)_2(OTf)_2$ and ZnTPP were prepared following reported procedures.[1,2]

The ^1H, COSY, and ROESY NMR spectra were recorded on a Bruker NEO 500 MHz NMR spectrometers. For ROESY, a mixing time of 491 ms was employed for all samples. The ^{31}P NMR spectra was recorded at 122 MHz using the same instrument.

Electrospray ionization mass spectra (ESIMS) of the M′TPP-based tricomponent bow tie complexes were recorded on a Bruker BioTOF II ESI/TOF-MS instrument at the Waters Center for Innovation in Mass Spectrometry of the Department of Chemistry at the University of Minnesota, Twin Cities.

The single crystal X-ray diffraction (SXRD) data were collected on a Bruker D8 Venture dual source diffractometer equipped with Cu and Mo radiation sources and CMOS detector. The crystal structures of bow tie complexes were solved and refined by using Bruker SHELXTL software package. The crystals of some bow tie complexes diffracted poorly, and the ethyl groups on Et_3P ligands were highly disordered due to thermal motions. These disordered ethyl groups were fixed by using the DFIX, DANG commands. In addition, the coordination of bridging XDC linkers with two Pt(II) corners also created strain and made them slightly bend and disordered in **BT3**, **BT3′**, and **BT4**. AFIX and DFIX commands were applied to fix these issues. The highly disordered triflate anions were hard to assign and omitted by PLATON/SQUEEZE in some cases, while in other cases they were assigned fully/partially using SAME/SIMU commands. ISOR and RIGU commands were applied for the atoms that were not behaving well isothermally. A SHEL cut-off was applied to remove the weak reflections in most of the structures. The disordered solvent molecules were also removed by PLATON/SQUEEZE model. The significant amount of disorder and weak diffraction of some crystals resulted in several A- and B-alerts, which have been addressed properly in the corresponding checkCIFs, while the commands applied to fix the disordered atoms and groups caused large R-values in those cases. Nevertheless, the basic bow tie skeletons of all complexes were well resolved and the disordered Et_3P groups, counter anions, and solvent molecules had practically no impact on the overall shape and geometry of these complexes.

The geometry optimized structures were calculated with semi-empirical methods using PM6 model on Gaussian software version 09.

Synthesis and Characterization

Dicarboxylate (XDC) Ligands. In general, aqueous solutions of 2.5 equiv. of KOH was added to respective dicarboxylic acids (i.e., hexane-, 4,4′-biphenyl, 1,4-benzene-, and 2,6-naphthalene dicarboxylic acids) and the resulting mixtures were stirred until the solids were fully solubilized due to salt formation. At this point, MeOH was added to the solution mixtures, which led to the precipitation of dipotassium dicarboxylate salts. The resulting solids were filtrated, washed thoroughly with cold MeOH, and recrystallized from MeOH, to remove excess of KOH and obtain pure products.

General Protocol of Tricomponent Self-Assembly of *cis*-$Pt(Et_3P)_2(TfO)_2$, M′TPP, and XDC. To a mixture of *cis*-$Pt(PEt_3)_2(OTf)_2$ (4 equiv.), M′TPP (M′ = Zn or H_2, 1 equiv.), and XDC (XDC = HDC, BPDC, BDC, and NDC, 2 equiv.) placed in a 20 mL screw-capped glass was added a 1:1:1 CH_2Cl_2/$MeNO_2$/MeCN

solvent mixture (5 mL). The reaction mixtures were then stirred at 60 °C for overnight. After allowing the reaction mixtures to cool down to room temperature, they were filtered to remove insoluble parts. Et_2O was added to the filtrates and the resulting purple precipitates were collected by centrifugation. This washing process was repeated three times to obtain pure tricomponent bow tie complexes **BT1–BT4** containing ZnTPP and **BT1′–BT4′** containing H_2TPP cores.

BT1. *cis*-Pt$(PEt_3)_2(OTf)_2$ (4.49 mg, 0.0059 mmol), ZnTPP (1 mg, 0.00147 mmol), and HDC (0.64 mg, 0.0029 mmol) in a 1:1:1 DCM/$MeNO_2$/MeCN solvent mixture (1 mL). ^{1}H NMR (500 MHz, acetone-d_6) δ = 9.28 (br s, 8H, H_a), 9.18 (s, 4H, $H_{c''}$), 8.50 (d, J = 5.8 Hz, 8H, H_b), 8.38 (s, 4H, $H_{c'}$), 2.33 – 2.15 (m, 56H, H_s and $H_{\text{-CH2-}}$), 1.65 (br s, 8H, H_t), 1.51 – 1.36 (m, 72H, $H_{\text{-CH3}}$) ppm. ^{31}P NMR (202 MHz, acetone-d_6) δ 6.23 (d, J = 20.5 Hz), 0.23 (d, J = 21.0 Hz). ESI-MS (*m/z*) Calculated for $C_{102}H_{160}F_6N_8O_{14}P_8Pt_4S_2Zn$ $[M–2TfO]^{2+}$: 1497.14. Found: 1497.09.

BT2. *cis*-Pt$(PEt_3)_2(OTf)_2$ (14.1 mg, 0.019 mmol), ZnTPP (3.3 mg, 0.0048 mmol), and BPDC (3.08 mg, 0.0096 mmol) in a 1:1:1 DCM/$MeNO_2$/MeCN solvent mixture (5 mL). ^{1}H NMR (500 MHz, acetone-d_6) δ = 9.28 (br s, 8H, H_a), 8.58 (s, 4H, $H_{c''}$), 8.38 (d, J = 5.6 Hz, 8H, H_b), 8.10 (d, J = 8.1 Hz, 8H, H_u), 7.98 (d, J = 8.2 Hz, 8H, H_v), 7.74 (s, 4H, $H_{c'}$), 2.44 – 2.18 (m, 48H, $H_{\text{-CH2-}}$), 1.58 – 1.42 (m, 72H, $H_{\text{-CH3}}$). ^{31}P NMR (122 MHz, acetone-d_6) δ 6.83 (d, J = 20.6 Hz), 1.78 (d, J = 21.2 Hz). ESI-MS (*m/z*) Calculated for $C_{118}H_{160}F_6N_8O_{14}P_8Pt_4S_2Zn$ $[M–2TfO]^{2+}$ 1593.23, Found: 1593.58.

BT3. *cis*-Pt$(PEt_3)_2(OTf)_2$ (14.1 mg, 0.019 mmol), BDC (2.34 mg, 0.0096 mmol) and ZnTPP (3.3 mg, 0.0048 mmol) in a 1:1:1 DCM/$MeNO_2$/MeCN solvent mixture (5 mL). ^{1}H NMR (500 MHz, acetone-d_6) δ = 9.35 (br s, 8H, H_a), 9.16 (s, 4H, $H_{c''}$), 8.36 (d, J = 6.3 Hz, 8H, H_b), 8.09 (s, 8H, H_w), 7.13 (s, 4H, $H_{c'}$), 2.40 – 2.19 (m, 48H, $H_{\text{-CH2-}}$), 1.57 – 1.41 (m, 72H, $H_{\text{-CH3}}$) ppm. ^{31}P NMR (203 MHz, acetone-d_6) δ = 6.02 (d, J = 20.5 Hz), 1.01 (d, J = 21.4 Hz) ppm. ESI-MS (*m/z*) Calcualted for $C_{106}H_{152}F_6N_8O_{14}P_8Pt_4S_2Zn$ $[M–2TfO]^{2+}$: 1517.13. Found: 1517.01.

BT4. *cis*-Pt$(PEt_3)_2(OTf)_2$ (14.1 mg, 0.019 mmol), BDC (2.83 mg, 0.0096 mmol) and ZnTPP (3.3 mg, 0.0048 mmol) in a 1:1:1 DCM/$MeNO_2$/MeCN solvent mixture (5 mL). ^{1}H NMR (500 MHz, acetone-d_6) δ = 9.37 (br s, 8H, H_a), 8.86 (s, 4H, $H_{c''}$), 8.71 (s, 4H, H_x), 8.26 (d, J = 5.6 Hz, 8H, H_b), 8.16 (d, J = 8.3 Hz, 4H, H_y), 8.09 (d, J = 8.4 Hz, 4H, H_z), 6.79 (s, 4H, $H_{c'}$), 2.35 – 2.24 (m, 48H, $H_{\text{-CH2-}}$), 1.49 (m, 72H, $H_{\text{-CH3}}$) ppm. ^{31}P NMR (203 MHz, acetone-d_6) δ = 6.13 (d, J = 21.0 Hz), 1.09 (d, J = 20.8 Hz) ppm. ESI-MS (*m/z*) Calculated for $C_{114}H_{156}F_6N_8O_{14}P_8Pt_4S_2Zn$ $[M–2TfO]^{2+}$: 1567.19. Found: 1567.05.

BT1′. *cis*-Pt$(PEt_3)_2(OTf)_2$ (4.47 mg, 0.0064 mmol), HDC (0.72 mg, 0.0032 mmol) and TPP (1 mg, 0.00162 mmol) in a 1:1:1 DCM/$MeNO_2$/MeCN solvent mixture (1 mL). ^{1}H NMR (500 MHz, acetone-d_6) δ = 9.39 (br s, 4H, $H_{c''}$), 9.37 – 9.31 (m, 8H, H_a), 8.59 (d, J = 6.4 Hz, 8H, H_b), 8.37 (s, 4H, $H_{c'}$), 2.40 – 2.16 (m, 56H, H_s and $H_{\text{-CH2-}}$), 1.66 (br s, 8H, H_t), 1.55 – 1.36 (m, 72H, $H_{\text{-CH3}}$), –2.97 (s, 2H, H_d). ^{31}P NMR (203 MHz, acetone-d_6) δ = 6.27 (d, J = 21.1 Hz), 0.26 (d, J = 21.2 Hz) ppm.

BT2′. *cis*-Pt$(PEt_3)_2(OTf)_2$ (14.1 mg, 0.019 mmol), BPDC (3.08 mg, 0.0096 mmol) and TPP (3.0 mg, 0.0048 mmol) in a 1:1:1 DCM/$MeNO_2$/MeCN solvent mixture (5 mL). ^{1}H NMR (500 MHz, acetone-d_6) δ = 9.34 (brs, 8H, H_a), 8.58 (s, 4H, $H_{c''}$), 8.38 (d, J = 5.6 Hz, 8H, H_b), 8.10 (d, J = 8.1 Hz, 8H, H_u), 7.98 (d, J = 8.2 Hz, 8H, H_v), 7.74 (s, 4H, $H_{c'}$), 2.44 – 2.18 (m, 48H, $H_{\text{-CH2-}}$), 1.58 – 1.42 (m, 72H, $H_{\text{-CH3}}$), –3.31 (s, 2H, H_d).

^{31}P NMR (202 MHz, acetone-d_6) δ = 6.37 (d, J = 21.0 Hz), 1.28 (d, J = 21.2 Hz) ppm. ESI-MS (*m/z*) Calculated for $C_{118}H_{162}F_6N_8O_{14}P_8Pt_4S_2$ $[M–2TfO]^{2+}$: 1561.55. Found: 1561.60.

BT3′. *cis*-$Pt(PEt_3)_2(OTf)_2$ (14.1 mg, 0.019 mmol), BDC (2.34 mg, 0.0096 mmol) and TPP (3.0 mg, 0.0048 mmol) in a 1:1:1 DCM/$MeNO_2$/MeCN solvent mixture (5 mL). ^{1}H NMR (500 MHz, acetone-d_6) δ = 9.40 (d, J = 6.1 Hz, 8H, H_a), 9.31 (s, 4H, $H_{c''}$), 8.43 (d, J = 5.5 Hz, 8H, H_b), 8.08 (s, 8H, H_w), 7.08 (s, 4H, $H_{c'}$), 2.40 – 2.18 (m, 48H, $H_{\text{-CH2-}}$), 1.61 – 1.38 (m, 72H, $H_{\text{-CH3}}$), –3.27 (s, 2H, H_d) ppm. ^{31}P NMR (122 MHz, acetone-d_6) δ = 6.73 (d, J = 20.6 Hz), 1.73 (d, J = 21.2 Hz) ppm. ESI-MS (*m/z*) Calculated for $C_{106}H_{154}F_6N_8O_{14}P_8Pt_4S_2$ $[M–2TfO]^{2+}$: 1485.45. Found: 1485.52.

BT4′. *cis*-$Pt(PEt_3)_2(OTf)_2$ (14.1 mg, 0.019 mmol), BDC (2.83 mg, 0.0096 mmol) and TPP (3.0 mg, 0.0048 mmol) in a 1:1:1 DCM/$MeNO_2$/MeCN solvent mixture (5 mL). ^{1}H NMR (500 MHz, CD_3NO_2) δ = 9.33 (br s, 8H, H_a), 8.88 (s, 4H, $H_{c''}$), 8.73 (d, J = 1.6 Hz, 4H, H_x), 8.28 (d, J = 5.5 Hz, 8H, H_b), 8.18 (d, J = 8.3 Hz, 4H, H_y), 8.11 (d, J = 8.4 Hz, 4H, H_z), 6.80 (s, 4H, $H_{c'}$), 2.29 (m, 48H, $H_{\text{-CH2-}}$), 1.53 (m, 72H, $H_{\text{-CH3}}$), –3.42 (s, 2H, H_d) ppm. ^{31}P NMR (203 MHz, CD_3NO_2) δ = 6.52 (d, J = 21.2 Hz), 1.07 (d, J = 21.1 Hz) ppm. ESI-MS (*m/z*) Calculated for $C_{114}H_{158}F_6N_8O_{14}P_8Pt_4S_2$ $[M–2TfO]^{2+}$: 1535.51. Found: 1535.60.

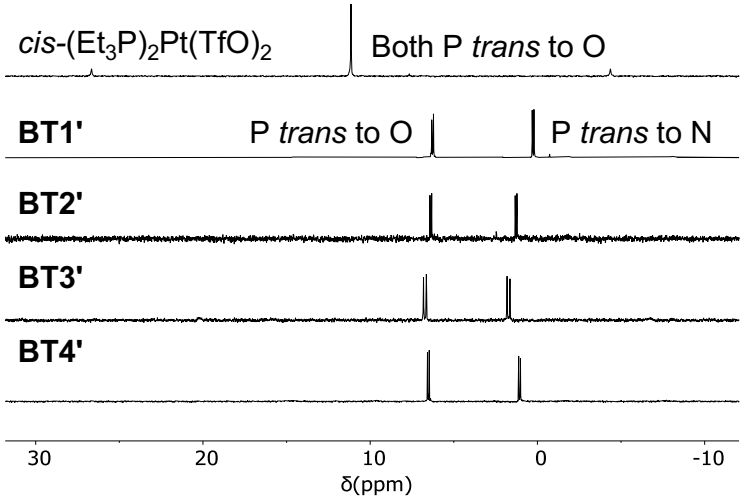

Figure S1. The ^{31}P NMR spectra (122 MHz, acetone-d_6) of *cis*-$(Et_3P)_2Pt(TfO)$, **BT1′**, **BT2′**, **BT3′**, and **BT4′** complexes reveal simultaneous coordination of carboxylate and pyridyl groups with heteroligated Pt(N,O) corners in the bow tie complexes.

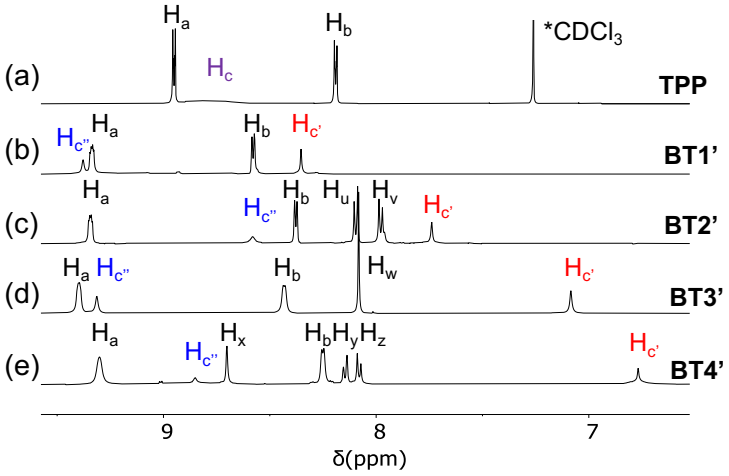

Figure S2. The partial ^{1}H NMR spectra (500 MHz) of (a) free H_2TPP ligand (in $CDCl_3$), (b) **BT1′**, (c) **BT2′**, (d) **BT3′**, and (e) **BT4′** complexes (in acetone-d_6) show that the enclosed $H_{c'}$ pyrrole protons (highlighted in red) of bow tie complexes are shifted up-field commensurately with the shielding effect of the adjacent XDC linkers, whereas the chemical shifts of exposed $H_{c''}$ pyrrole protons (highlighted in blue) vary depending on the length of XDC linkers that dictate their distances from the adjacent pyridyl rings.

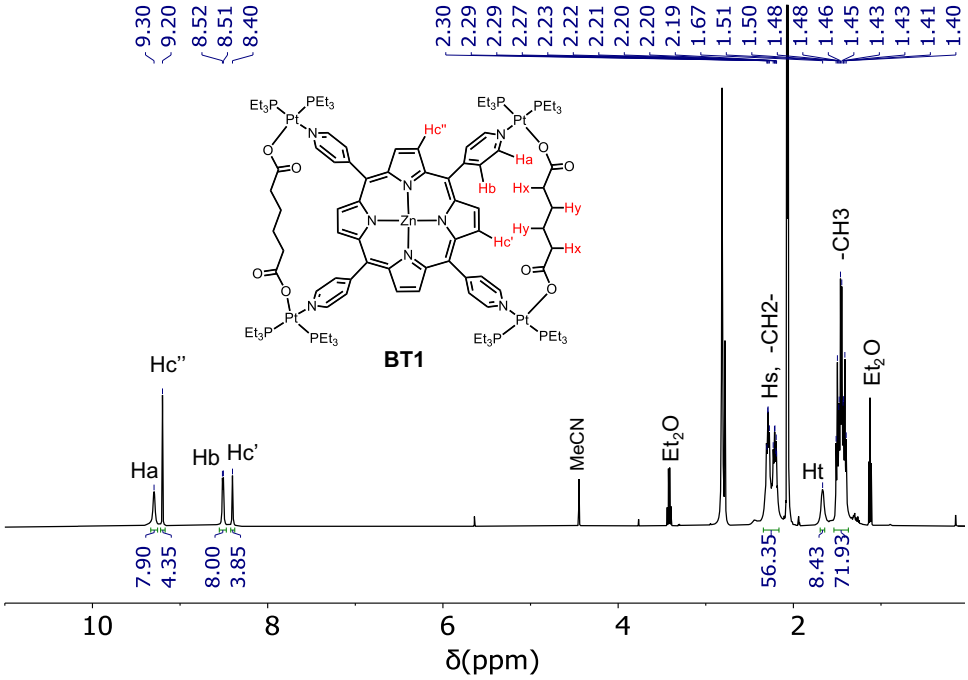
9.30 9.20 8.52 8.51 8.40
2.30 2.29 2.29 2.27 2.23 2.22 2.21 2.20 2.20 2.19 1.67 1.51 1.50 1.48 1.48 1.46 1.45 1.43 1.43 1.41 1.40
Hc"
Ha
Hb
Hx
Hy
Hy
Hx
Hc'
BT1
Hc"
Ha
Hb
Hc'
MeCN
Et2O
Hs, -CH2-
Ht
-CH3
Et2O
7.90 4.35 8.00 3.85 56.35 8.43 71.93
10
8
6
4
2
δ(ppm)

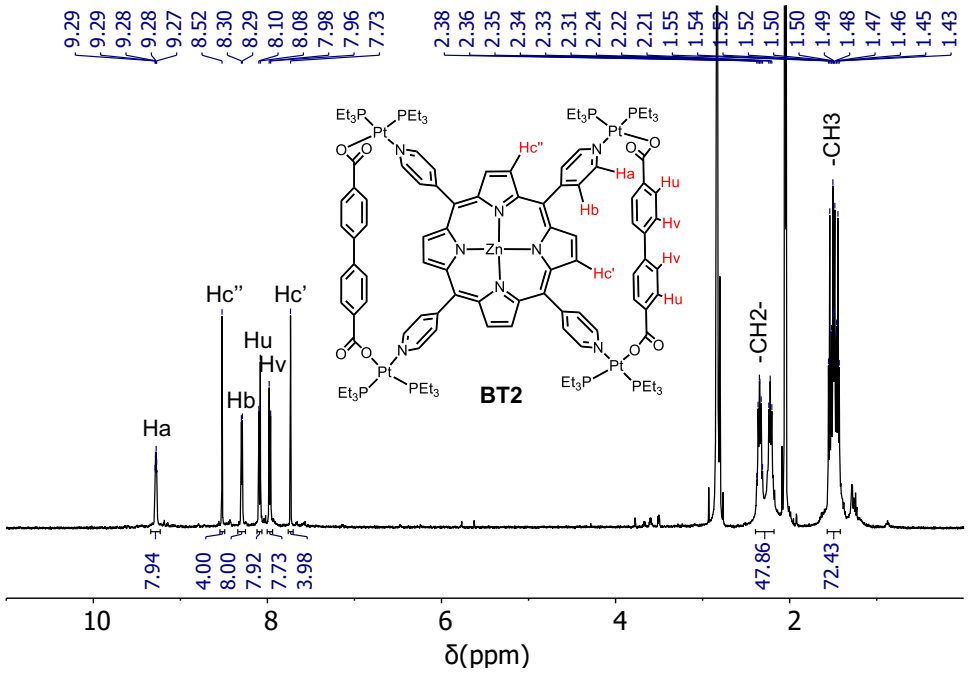
9.29 9.29 9.28 9.28 9.27 8.52 8.30 8.29 8.10 8.08 7.98 7.96 7.73
2.38 2.36 2.35 2.34 2.33 2.31 2.24 2.22 2.21 1.55 1.54 1.52 1.52 1.50 1.50 1.49 1.48 1.47 1.46 1.45 1.43
Hc"
Ha
Hb
Hu
Hv
Hv
Hu
Hc'
BT2
Hc"
Hc'
Hu
Hv
Hb
Ha
-CH2-
-CH3
7.94 4.00 8.00 7.92 7.73 3.98 47.86 72.43
10
8
6
4
2
δ(ppm)

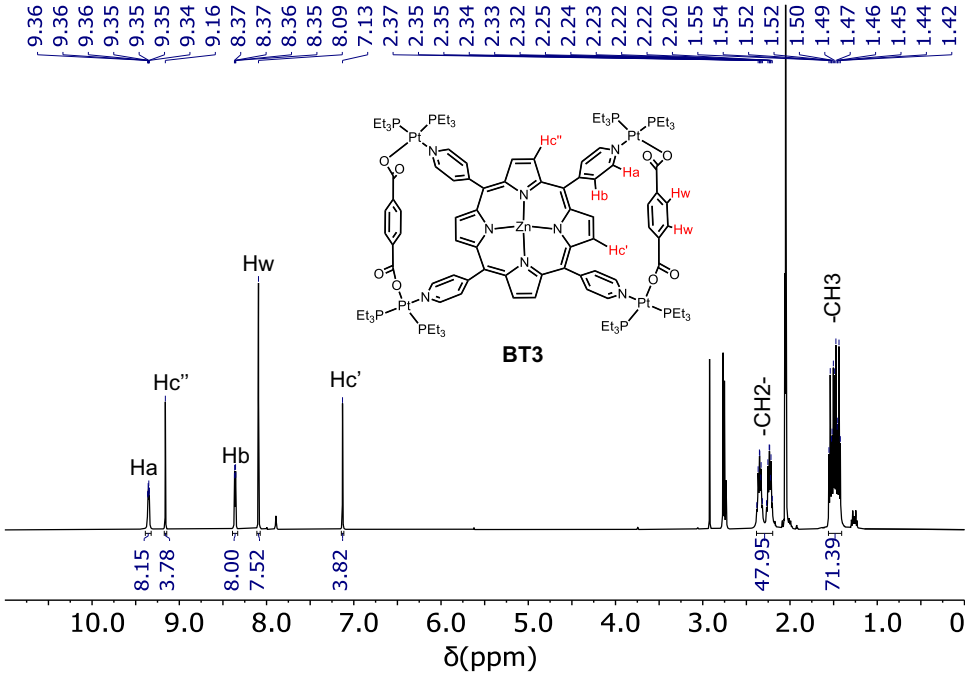
9.36 9.36 9.36 9.35 9.35 9.35 9.34 9.16 8.37 8.37 8.36 8.35 8.09 7.13 2.37 2.35 2.35 2.34 2.33 2.32 2.25 2.24 2.23 2.22 2.22 2.20 1.55 1.54 1.52 1.52 1.50 1.49 1.47 1.46 1.45 1.44 1.42
Hc"
Ha
Hb
Hw
Hw
Hc'
BT3
Hw
Hc"
Hc'
-CH2-
-CH3
Ha
Hb
8.15 3.78 8.00 7.52 3.82 47.95 71.39
10.0 9.0 8.0 7.0 6.0 5.0 4.0 3.0 2.0 1.0 0
δ(ppm)

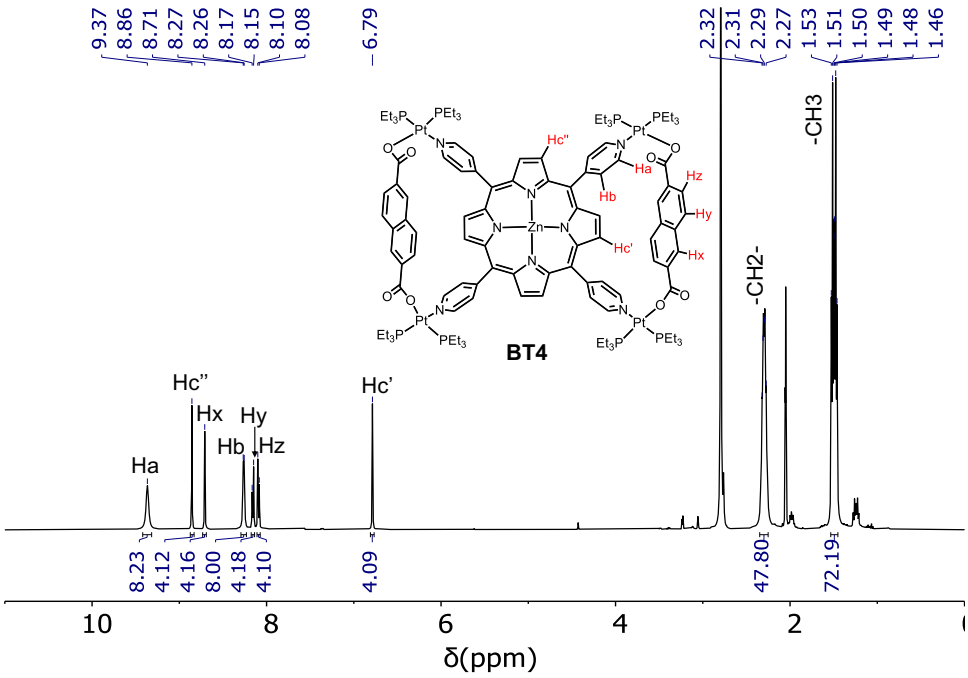
9.37 8.86 8.71 8.27 8.26 8.17 8.15 8.10 8.08 6.79 2.32 2.31 2.29 2.27 1.53 1.51 1.50 1.49 1.48 1.46
Hc"
Ha
Hb
Hz
Hy
Hx
Hc'
BT4
-CH2-
-CH3
Hc"
Hx
Hy
Hb
Hz
Ha
Hc'
8.23 4.12 4.16 8.00 4.18 4.10 4.09 47.80 72.19
10 8 6 4 2
δ(ppm)

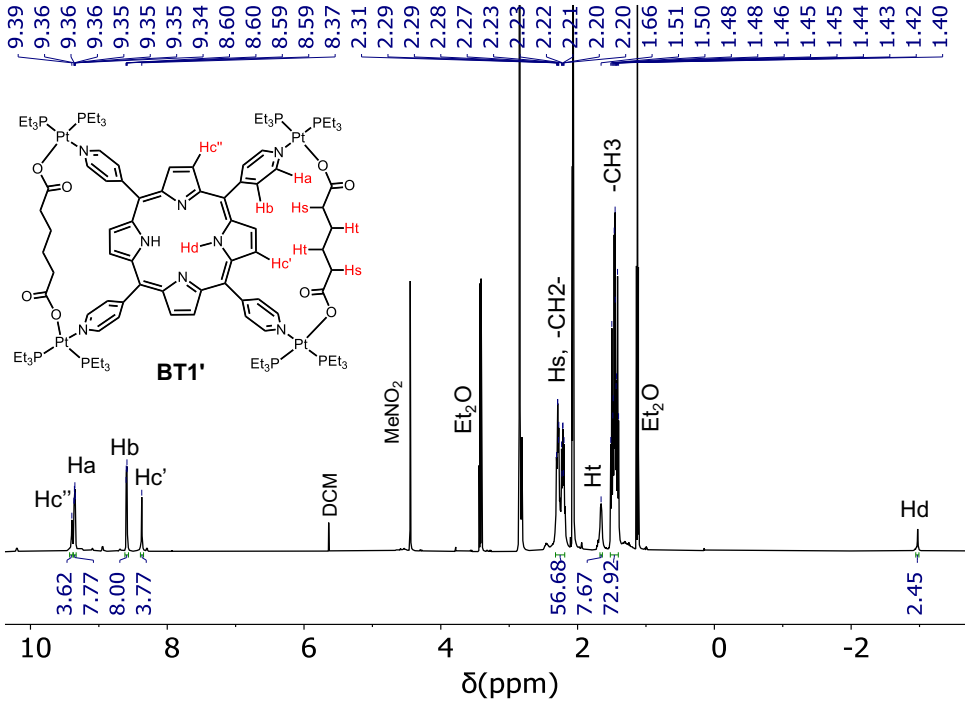
BT1'
Hc''
Ha
Hb
Hc'
DCM
MeNO2
Et2O
Hs, -CH2-
Ht
-CH3
Et2O
Hd
3.62
7.77
8.00
3.77
56.68
7.67
72.92
2.45
δ(ppm)

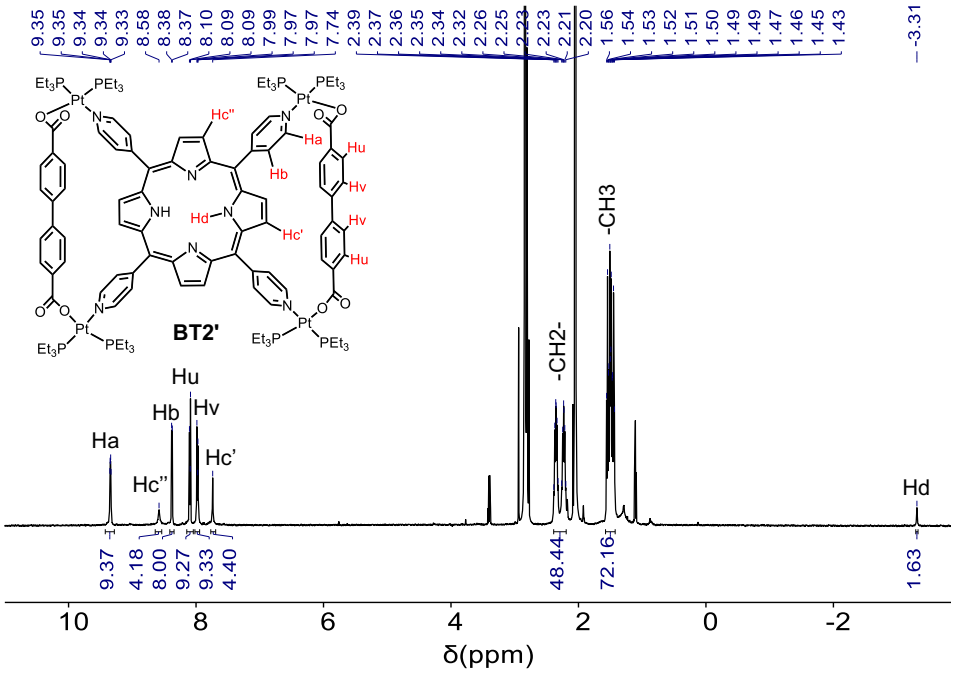
BT2'
Hc''
Ha
Hb
Hu
Hv
Hc'
-CH2-
-CH3
Hd
9.37
4.18
8.00
9.27
9.33
4.40
48.44
72.16
1.63
δ(ppm)

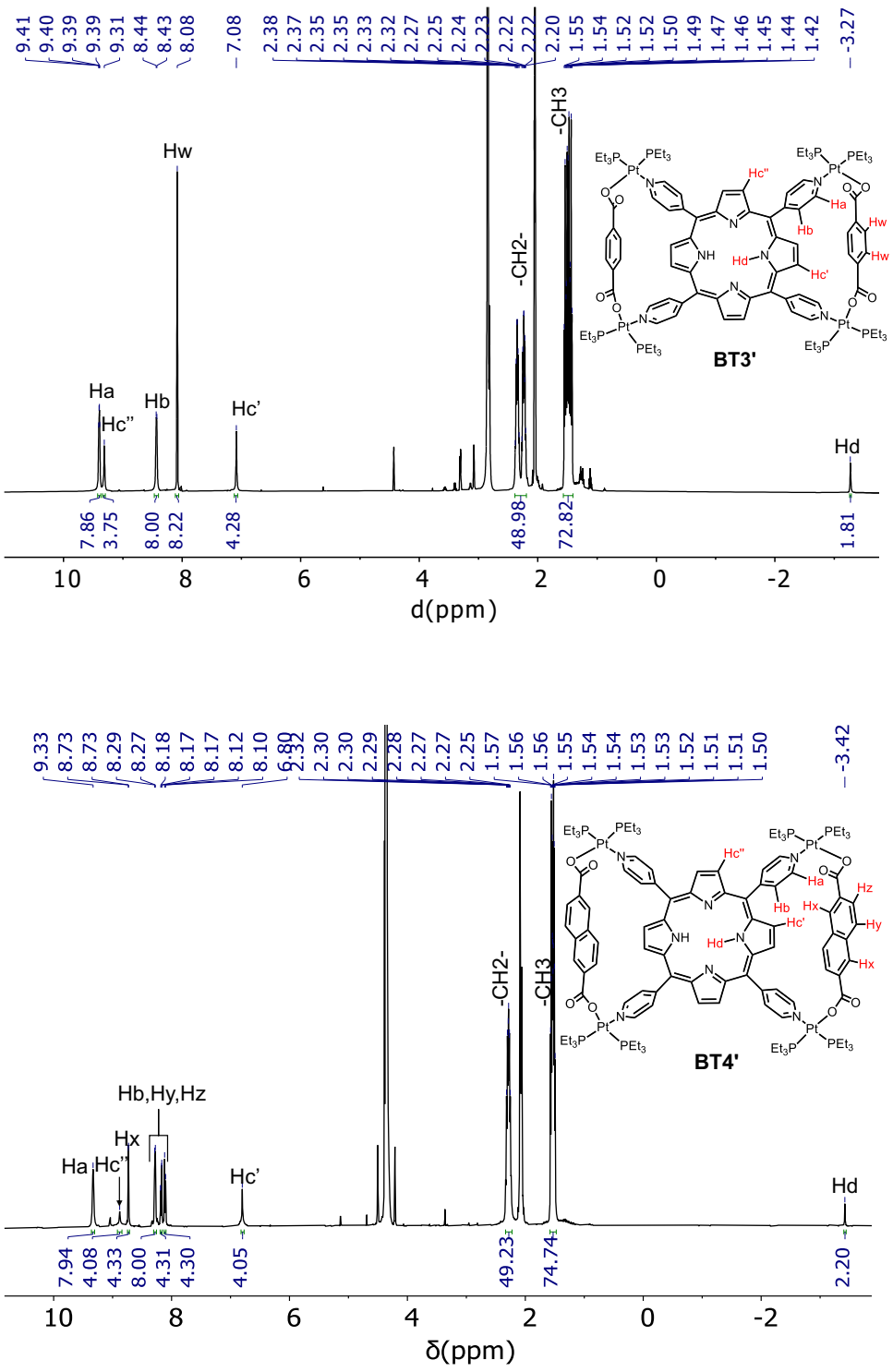

Figure S3. The ^{1}H NMR spectra (500 MHz, acetone-d_6) of **BT1**–**BT4** and **BT1′**–**BT4′** complexes.

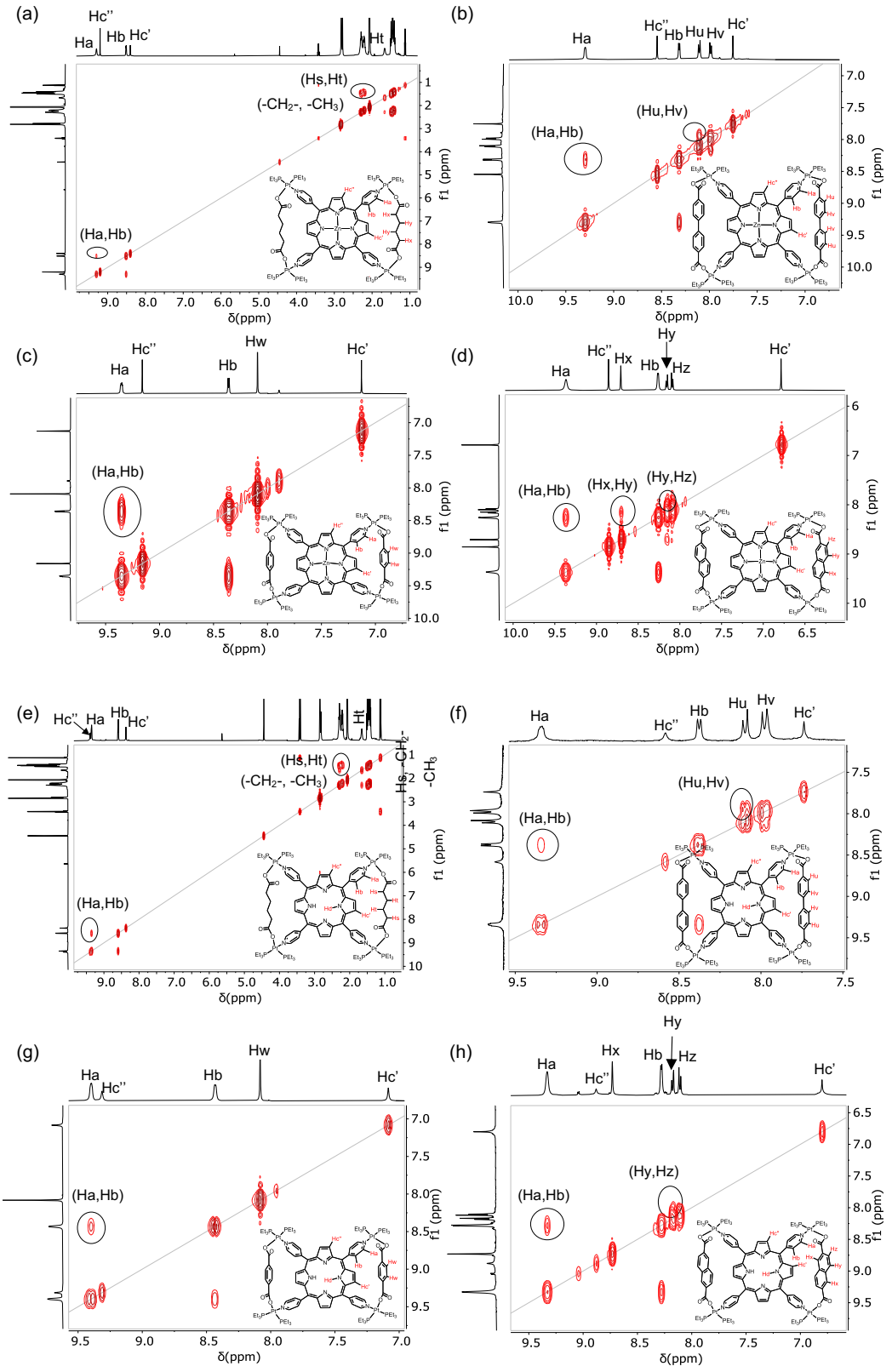

Figure S4. The ^{1}H–^{1}H COSY NMR spectra (500 MHz, acetone-d_6) of (a–d) **BT1**–**BT4** and (e–h) **BT1′**–**BT4′** complexes.

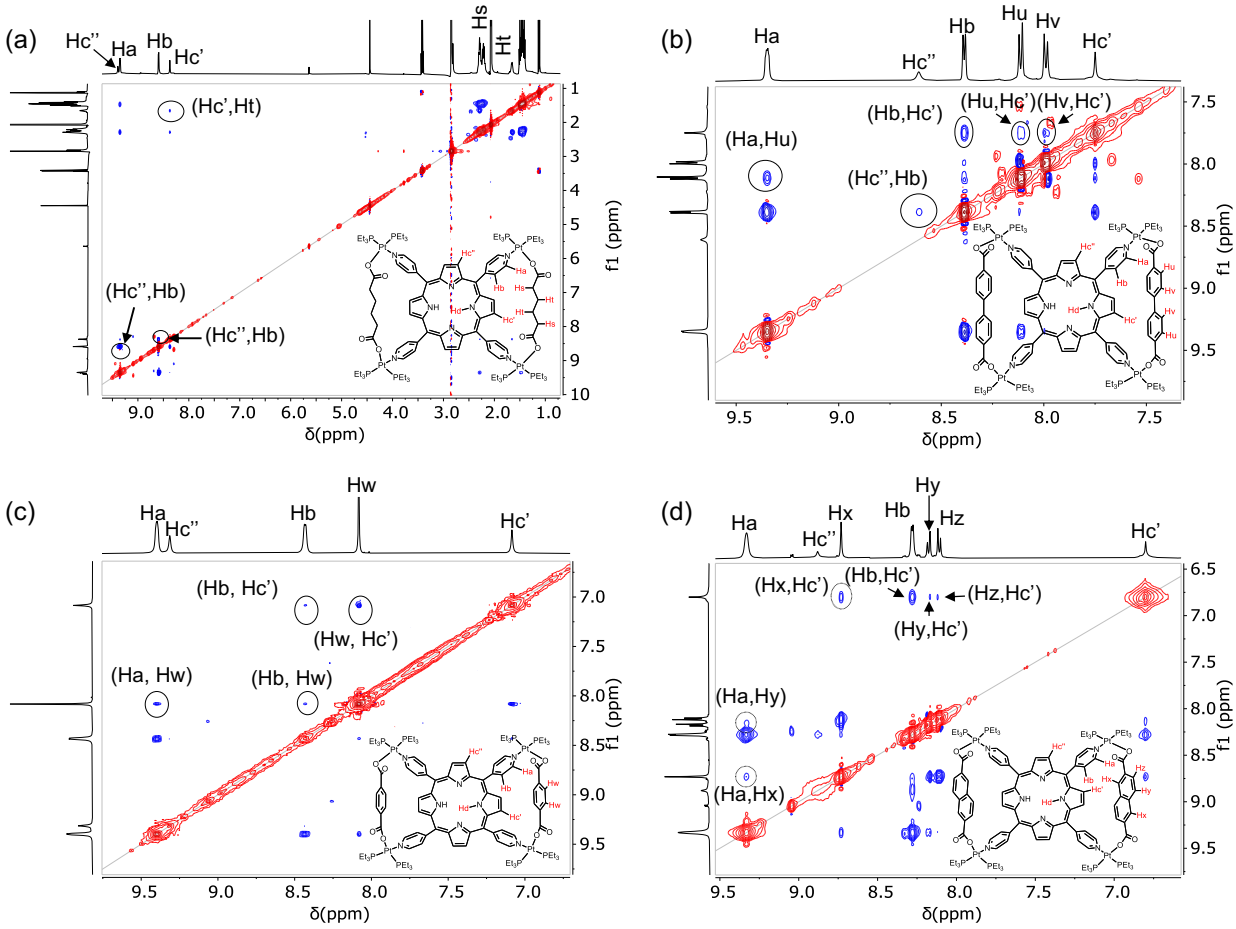

Figure S5. The ^{1}H–^{1}H ROESY NMR spectra (500 MHz, acetone-d_6) of (a) **BT1′**, (b) **BT2′**, (c) **BT3′**, and (d) **BT4′** complexes.

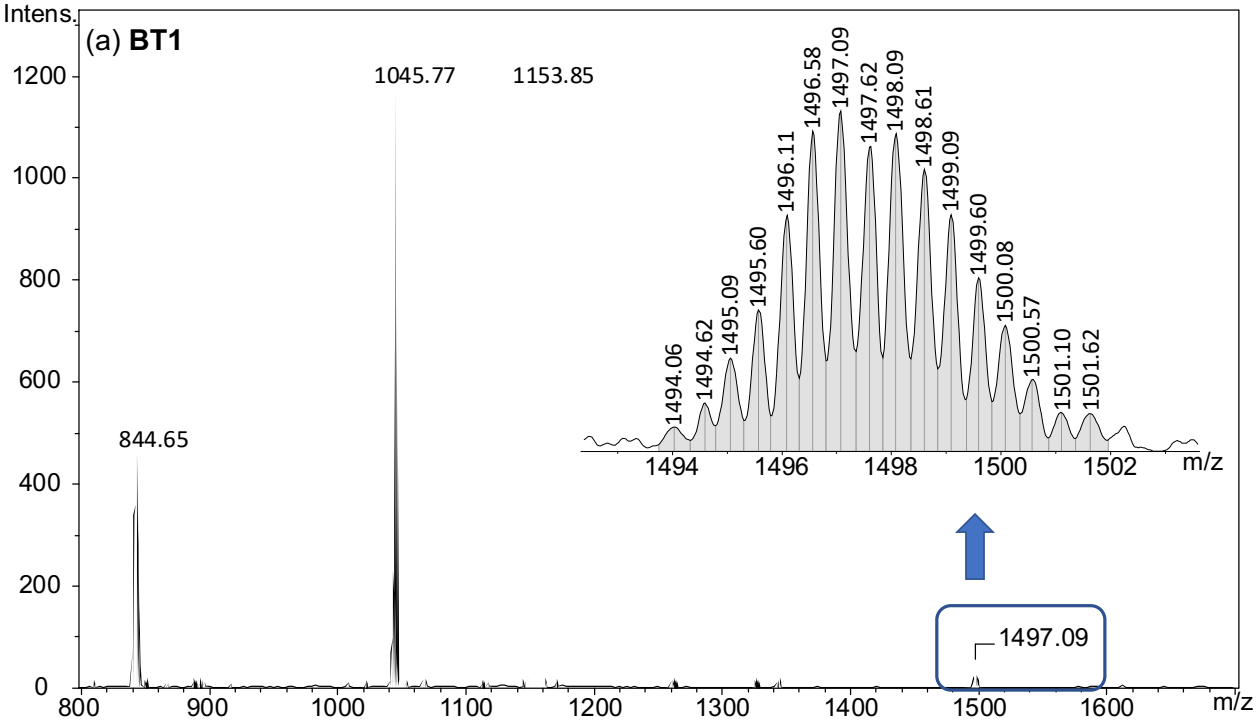
Intens.
(a) BT1
1200
1000
800
600
400
200
0
1045.77
1153.85
844.65
1494.06
1494.62
1495.09
1495.60
1496.11
1496.58
1497.09
1497.62
1498.09
1498.61
1499.09
1499.60
1500.08
1500.57
1501.10
1501.62
1494
1496
1498
1500
1502
m/z
1497.09
800
900
1000
1100
1200
1300
1400
1500
1600
m/z

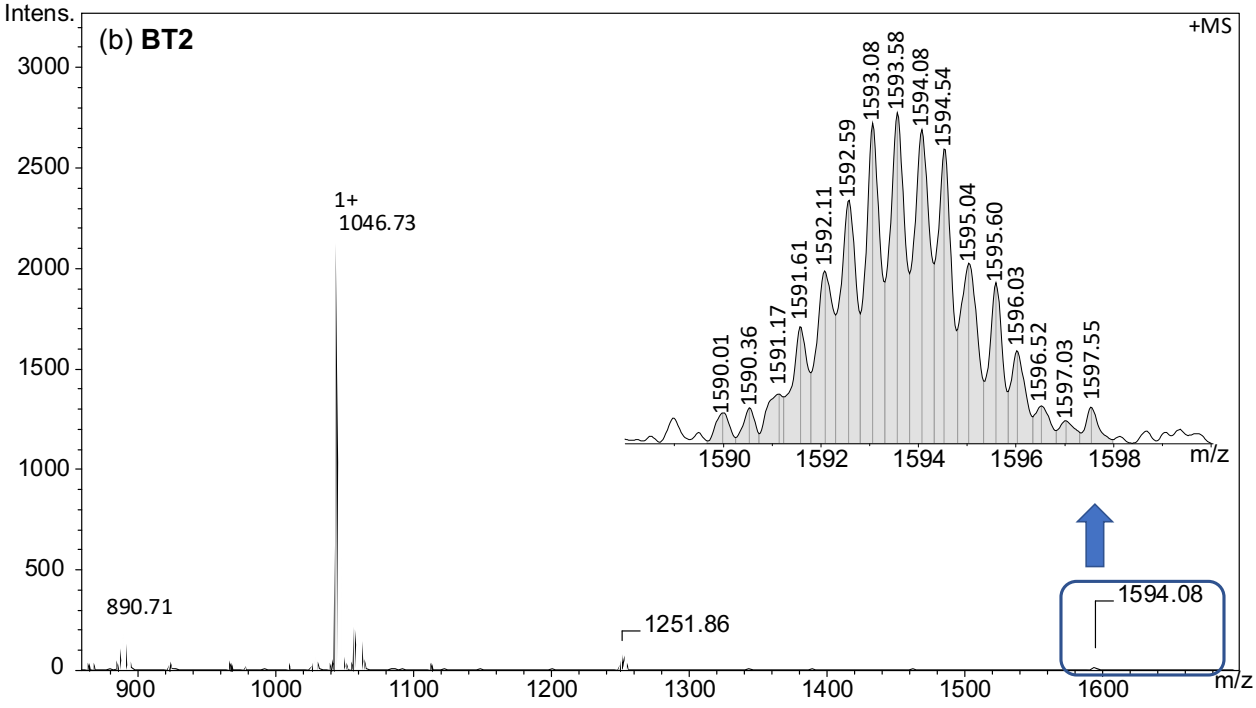
Intens.
(b) BT2
+MS
3000
2500
2000
1500
1000
500
0
1+
1046.73
890.71
1251.86
1590.01
1590.36
1591.17
1591.61
1592.11
1592.59
1593.08
1593.58
1594.08
1594.54
1595.04
1595.60
1596.03
1596.52
1597.03
1597.55
1590
1592
1594
1596
1598
m/z
1594.08
900
1000
1100
1200
1300
1400
1500
1600
m/z

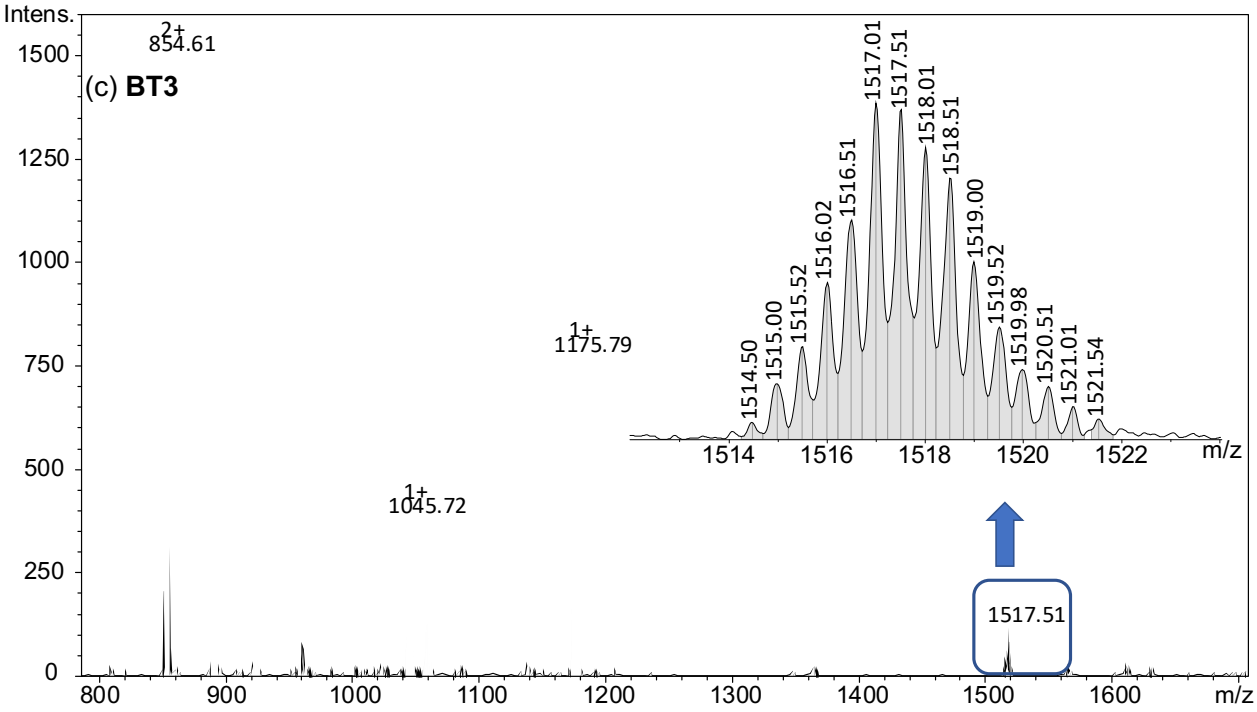
Intens.
(c) BT3
2+
854.61
1+
1175.79
1+
1045.72
1514.50
1515.00
1515.52
1516.02
1516.51
1517.01
1517.51
1518.01
1518.51
1519.00
1519.52
1519.98
1520.51
1521.01
1521.54
1517.51
m/z

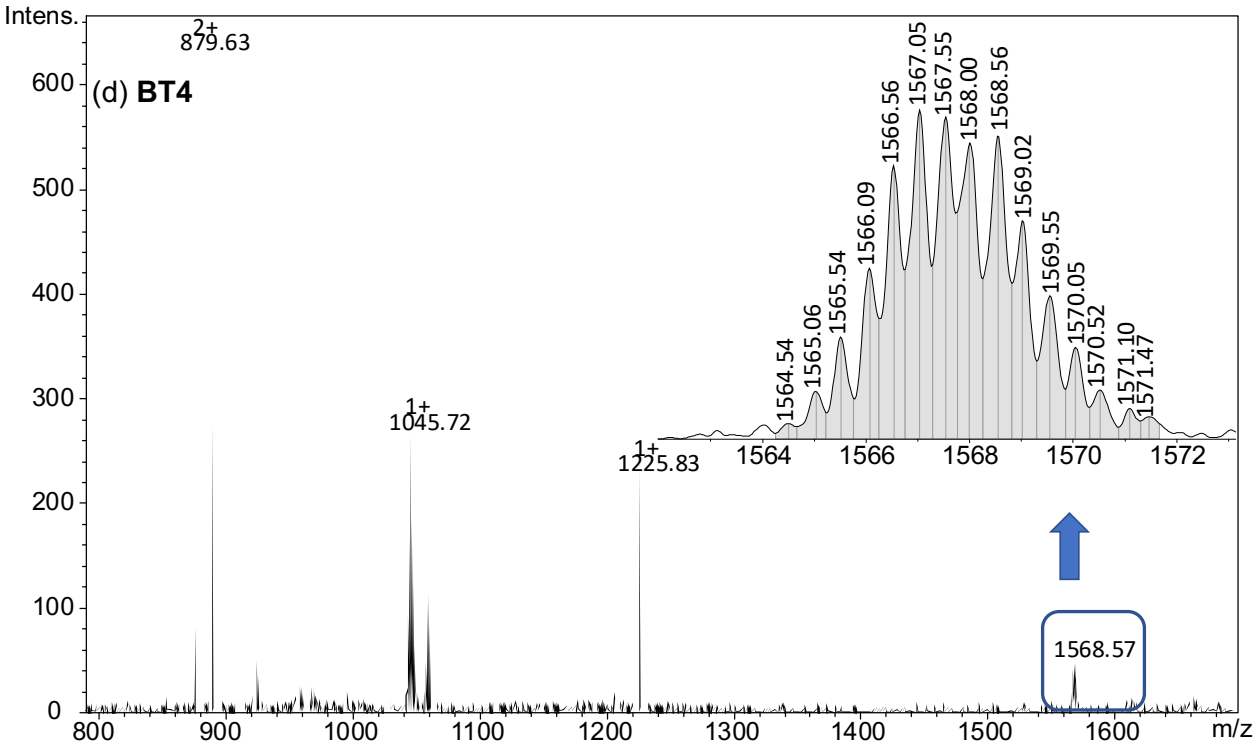
Intens.
(d) BT4
2+
879.63
1+
1045.72
1+
1225.83
1564.54
1565.06
1565.54
1566.09
1566.56
1567.05
1567.55
1568.00
1568.56
1569.02
1569.55
1570.05
1570.52
1571.10
1571.47
1568.57
m/z

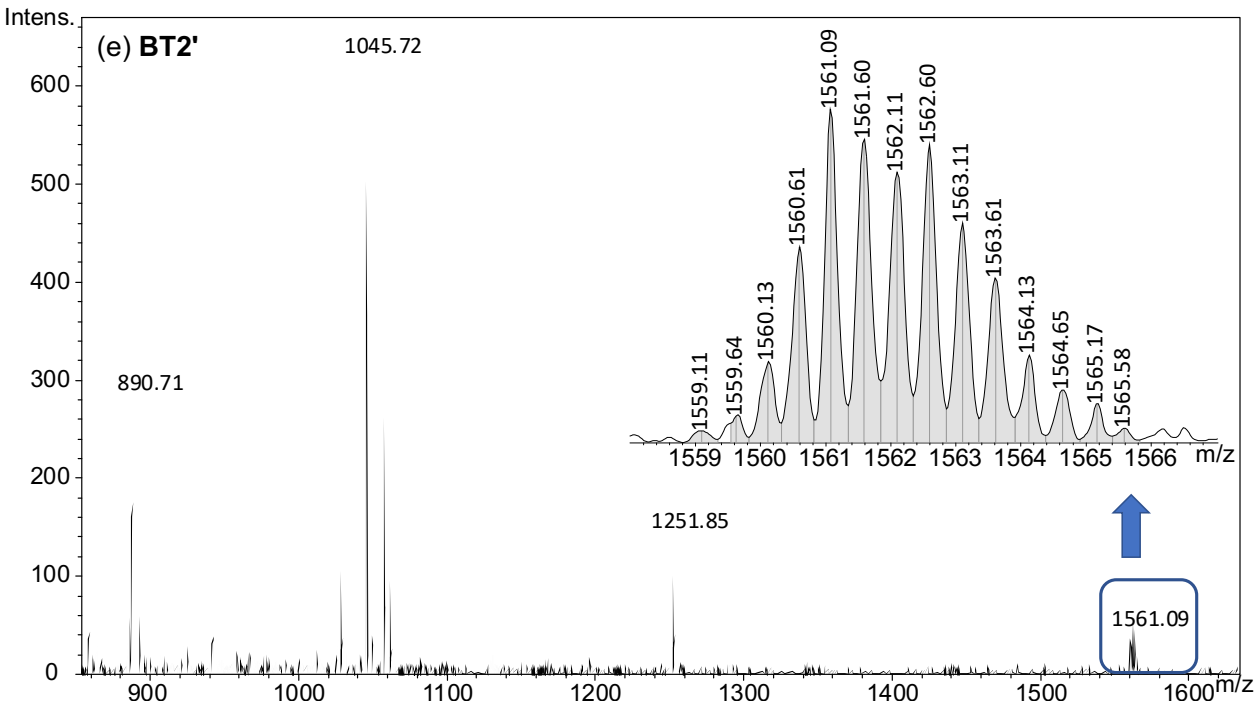
Intens.
(e) BT2'
1045.72
890.71
1251.85
1561.09
1559.11
1559.64
1560.13
1560.61
1561.09
1561.60
1562.11
1562.60
1563.11
1563.61
1564.13
1564.65
1565.17
1565.58
m/z

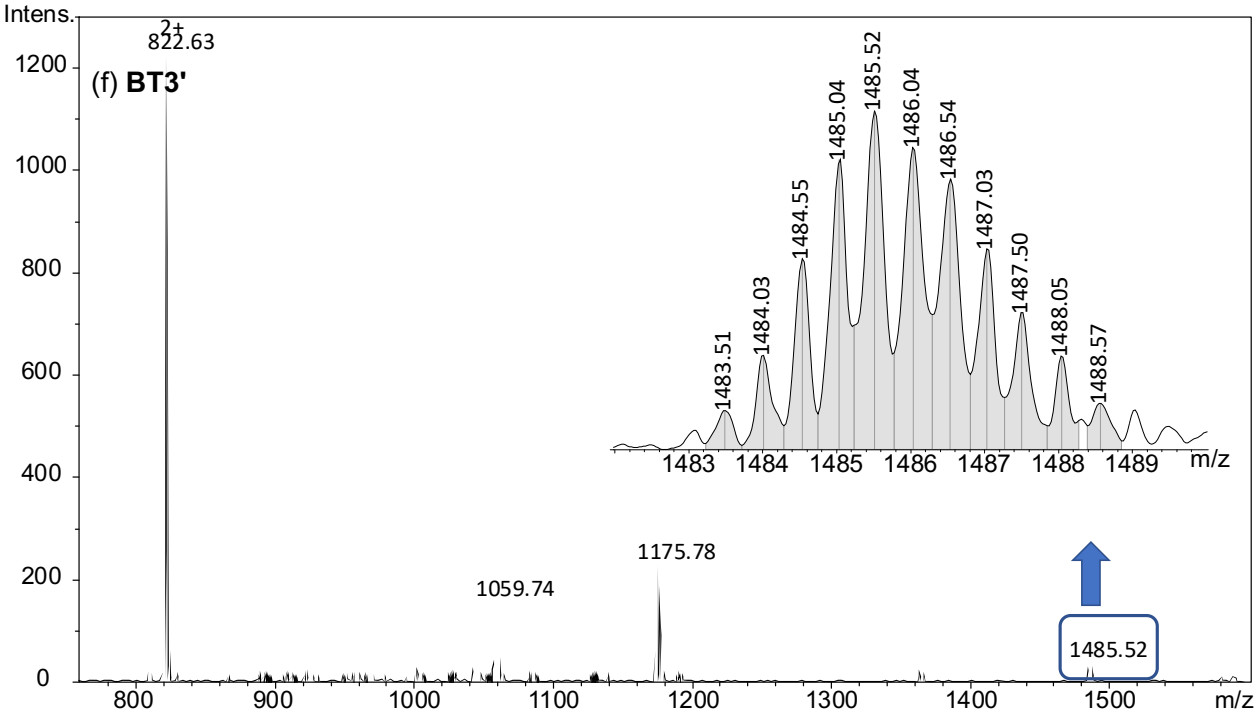
Intens.
2+
822.63
(f) BT3'
1175.78
1059.74
1485.52
1483.51
1484.03
1484.55
1485.04
1485.52
1486.04
1486.54
1487.03
1487.50
1488.05
1488.57
m/z

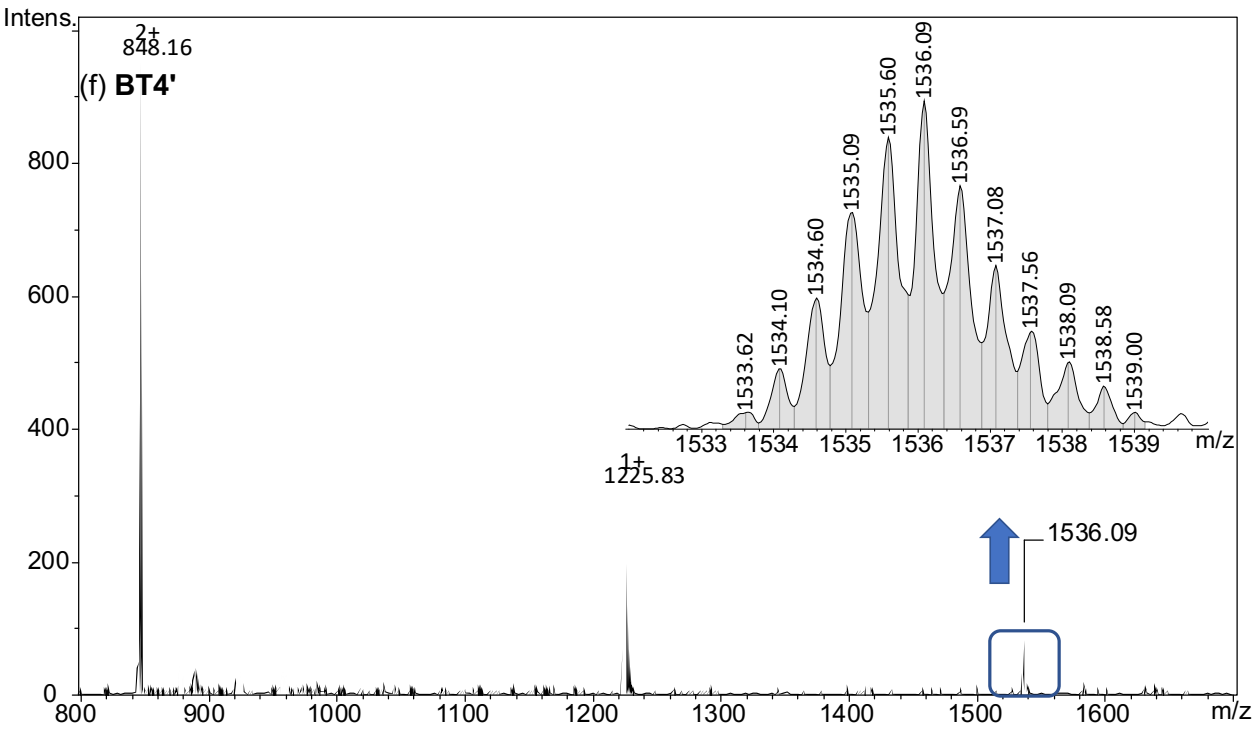

Figure S6. The ESI-MS data of (a) **BT1**, (b) **BT2**, (c) **BT3**, (d) **BT4**, (e) **BT2′**, (f) **BT3′**, and (g) **BT4′** complexes. The insets show the isotopic distributions of respective $[M - 2TfO]^{2+}$ species.

Crystallographic Data.

Table 1. Crystallographic Data for **BT2**, **BT3** and **BT4**.

Compound	**BT2**	**BT3**	**BT4**
Empirical formula	C120 H160 F12 N8 O20 P8 Pt4 S4 Zn	C108 H152 F12 N8 O20 P8 Pt4 S4 Zn	C115 H158 F12 N8 O11 P8 Pt4 S4 Zn
Formula weight	3484.28	3332.1	3278.21
Temperature	173(2) K	100(2) K	100(2) K
Wavelength	0.71073 Å	0.71073 Å	0.71073 Å
Crystal system	Triclinic	Monoclinic	Monoclinic
Space group	P -1	C 2/c	P 21/c
Unit cell dimensions	a = 14.177(3) Å α= 100.941(5)°. b = 15.762(3) Å β= 104.110(5)°. c = 20.164(4) Å γ = 95.391(6)°.	a = 30.647(10) Å α= 90°. b = 15.376(5) Å β= 104.412(8)°. c = 31.873(11) Å γ = 90°.	a = 23.980(2) Å α= 90°. b = 33.628(3) Å β= 109.469(2)°. c = 22.415(2) Å γ = 90°.
Volume	4243.8(16) $Å^3$	14547(9) $Å^3$	17042(3) $Å^3$
Z	1	4	4
Density (calculated)	1.363 Mg/m^3	1.521 Mg/m^3	1.278 Mg/m^3
Absorption coefficient	3.614 mm^{-1}	4.213 mm^{-1}	3.592 mm^{-1}
F(000)	1730	6600	6504
Crystal size	0.164 x 0.132 x 0.112 mm^3	0.350 x 0.260 x 0.020 mm^3	0.330 x 0.080 x 0.060 mm^3
Theta range for data collection	2.688 to 25.250°.	4.116 to 16.974°.	4.076 to 19.082°.
Index ranges	-17<=h<=17, -18<=k<=18, -24<=l<=24	-25<=h<=24, -12<=k<=12, -26<=l<=24	-21<=h<=21, -30<=k<=30, -20<=l<=20
Reflections collected	40383	15135	54937
Independent reflections	15172 [R(int) = 0.0832]	4045 [R(int) = 0.1205]	13508 [R(int) = 0.1416]
Completeness to theta	(25.242°) 98.7%	(16.974°) 95.8%	(19.082°) 97.1%
Absorption correction	Semi-empirical from equivalents	None	None
Refinement method	Full-matrix least-squares on F^2	Full-matrix least-squares on F^2	Full-matrix least-squares on F^2
Data / restraints / parameters	15172 / 345 / 655	4045 / 650 / 571	13508 / 3329 / 1507
Goodness-of-fit on F^2	1.047	3.652	1.022
Final R indices [I>2sigma(I)]	R1 = 0.1438, wR2 = 0.3449	R1 = 0.2450, wR2 = 0.5287	R1 = 0.1157, wR2 = 0.2864
R indices (all data)	R1 = 0.2192, wR2 = 0.4222	R1 = 0.2787, wR2 = 0.5508	R1 = 0.1868, wR2 = 0.3442
Largest diff. peak and hole	3.868 and -3.352 $e.Å^{-3}$	4.770 and -1.921 $e.Å^{-3}$	1.948 and -1.323 $e.Å^{-3}$

Table 2. Crystallographic Data for **BT2'** and **BT3'**.

Compound	**BT2'**	**BT3'**
Empirical formula	C123 H168 F12 N8 O21 P8 Pt4 S4	C108 H150 F12 N8 O20 P8 Pt4 S4
Formula weight	3479	3264.71
Temperature	100(2) K	100(2) K
Wavelength	0.71073 Å	0.71073 Å
Crystal system	Monoclinic	Tetragonal
Space group	C 2/c	I 41/a
Unit cell dimensions	a = 42.500(3) Å α= 90°. b = 17.5276(14) Å β= 107.338(2)°. c = 22.8229(18) Å γ = 90°.	a = 34.285(6) Å α= 90°. b = 34.285(6) Å β= 90°. c = 23.949(5) Å γ = 90°.
Volume	16229(2) $Å^3$	28151(11) $Å^3$
Z	4	8
Density (calculated)	1.424 Mg/m^3	1.541 Mg/m^3
Absorption coefficient	3.638 mm^{-1}	4.188 mm^{-1}
F(000)	6936	12944
Crystal size	0.160 x 0.120 x 0.030 mm^3	0.18 x 0.12 x 0.04 mm^3
Theta range for data collection	2.309 to 25.250°.	2.304 to 17.312°.
Index ranges	-50<=h<=50, -20<=k<=21, -27<=l<=27	-28<=h<=28, -28<=k<=28, -20<=l<=19
Reflections collected	48255	33537
Independent reflections	14608 [R(int) = 0.0829]	4010 [R(int) = 0.1656]
Completeness to theta	(25.242°) 99.4%	(17.312°) 92.7%
Absorption correction	Semi-empirical from equivalents	Semi-empirical from equivalents
Refinement method	Full-matrix least-squares on F^2	Full-matrix least-squares on F^2
Data / restraints / parameters	14608 / 96 / 824	4010 / 1227 / 696
Goodness-of-fit on F2	1.065	1.361
Final R indices [I>2sigma(I)]	R1 = 0.0850, wR2 = 0.1982	R1 = 0.1104, wR2 = 0.2814
R indices (all data)	R1 = 0.1100, wR2 = 0.2126	R1 = 0.1786, wR2 = 0.3603
Largest diff. peak and hole	3.151 and -3.752 e.Å-3	2.357 and -0.946 e.Å-3

Table 3. Atomic coordinates (x 10^4) and equivalent isotropic displacement parameters ($Å^2$x 10^3) for **BT2**. U(eq) is defined as one third of the trace of the orthogonalized U^{ij} tensor.

	x	y	z	U(eq)
Pt(1)	7791(1)	5049(1)	7517(1)	63(1)
Pt(2)	3947(1)	-1436(1)	1101(1)	70(1)
Zn(1)	10000	0	5000	87(2)
P(1)	6998(7)	6182(5)	7805(5)	93(3)
P(2)	9278(5)	5624(5)	8225(4)	62(2)
P(3)	4493(5)	-2410(6)	329(5)	82(2)
P(4)	2484(6)	-1474(6)	334(5)	86(3)
O(1)	6183(15)	3477(13)	7453(10)	81(4)
O(2)	6454(14)	4549(13)	6813(9)	70(4)
O(3)	3596(14)	-445(11)	1769(12)	79(4)
O(4)	2973(15)	-1373(12)	2334(12)	86(5)
N(1)	10534(15)	864(13)	5922(11)	63(5)
N(2)	8687(16)	512(15)	4855(12)	74(6)
N(3)	8275(13)	3898(11)	7029(12)	54(4)
N(4)	5266(14)	-1203(17)	1928(12)	69(5)
C(1)	11409(18)	978(17)	6387(13)	61(6)
C(2)	11493(19)	1613(19)	6990(14)	72(6)
C(3)	10665(18)	1948(19)	6923(14)	72(6)
C(4)	10039(18)	1480(19)	6230(13)	67(6)
C(5)	9068(19)	1630(17)	5941(14)	63(7)
C(6)	8453(18)	1163(18)	5286(14)	66(6)
C(7)	7461(18)	1337(18)	4973(14)	66(6)
C(8)	7080(20)	686(18)	4337(14)	68(6)
C(9)	7884(18)	219(18)	4269(13)	63(6)
C(10)	7800(20)	-453(19)	3724(13)	69(8)
C(11)	8725(16)	2421(17)	6313(13)	58(7)
C(12)	8780(30)	3140(20)	6086(17)	102(13)
C(13)	8484(16)	3931(14)	6503(15)	55(4)
C(14)	8205(16)	3181(14)	7297(15)	55(4)
C(15)	8453(17)	2389(15)	6934(11)	50(6)
C(16)	6896(16)	-677(17)	3078(12)	52(6)
C(17)	6700(20)	-200(20)	2591(16)	92(11)
C(18)	5831(17)	-440(20)	2029(15)	70(5)
C(19)	5407(17)	-1660(20)	2401(15)	69(5)
C(20)	6210(20)	-1450(20)	3002(16)	84(9)
C(21)	6110(20)	3760(20)	6923(15)	71(4)
C(22)	5520(30)	3115(16)	6249(16)	92(4)

C(23)	5470(30)	2225(15)	6229(16)	91(4)
C(24)	5090(30)	1650(20)	5586(12)	91(4)
C(25)	4740(30)	1890(16)	4957(15)	91(4)
C(26)	4770(30)	2781(15)	4991(16)	93(4)
C(27)	5180(30)	3380(20)	5627(12)	93(4)
C(28)	4289(19)	1324(17)	4297(15)	89(4)
C(29)	3712(17)	507(15)	4243(15)	89(4)
C(30)	3430(20)	-138(19)	3608(12)	89(4)
C(31)	3670(20)	10(18)	2989(15)	89(4)
C(32)	4300(20)	797(16)	3058(16)	89(4)
C(33)	4570(20)	1450(20)	3687(13)	89(4)
C(34)	3400(20)	-713(17)	2346(19)	81(4)
C(35)	10150(20)	4860(30)	8130(20)	108(9)
C(36)	11190(20)	5250(30)	8580(20)	109(9)
C(37)	9870(30)	6630(30)	8040(20)	110(10)
C(38)	10040(30)	6520(30)	7330(20)	111(10)
C(39)	9450(30)	5850(20)	9170(20)	117(10)
C(40)	8880(30)	5120(20)	9390(20)	118(10)
C(41)	5890(20)	5710(20)	7928(19)	98(8)
C(42)	6110(30)	5420(20)	8611(18)	98(8)
C(43)	7580(30)	7110(20)	8480(20)	130(11)
C(44)	6820(30)	7850(30)	8520(20)	131(11)
C(45)	6620(30)	6610(30)	7048(19)	125(11)
C(46)	7230(30)	6950(30)	6770(20)	126(11)
C(47)	1560(20)	-2430(20)	225(19)	108(10)
C(48)	1450(30)	-2600(20)	927(19)	111(10)
C(49)	1930(30)	-510(20)	620(30)	190(20)
C(50)	980(30)	-480(30)	60(30)	190(20)
C(51)	2440(40)	-1470(30)	-582(17)	184(18)
C(52)	3030(40)	-640(30)	-650(30)	186(18)
C(53)	3690(40)	-3400(30)	-100(30)	153(13)
C(54)	3170(40)	-3980(30)	270(30)	153(13)
C(56)	5850(30)	-1170(30)	90(20)	134(11)
C(55)	5210(30)	-2060(30)	-240(20)	135(11)
C(57)	5500(40)	-2920(30)	880(20)	140(12)
C(58)	5840(40)	-3660(30)	430(20)	143(12)

Table 4. Bond lengths [Å] and angles [º] for **BT2**.

Pt(1)-O(2)	2.052(19)
Pt(1)-N(3)	2.148(17)
Pt(1)-P(2)	2.233(7)
Pt(1)-P(1)	2.258(7)
Pt(2)-O(3)	2.044(19)
Pt(2)-N(4)	2.13(2)
Pt(2)-P(4)	2.253(8)
Pt(2)-P(3)	2.298(9)
Zn(1)-N(1)#1	2.011(18)
Zn(1)-N(1)	2.011(18)
Zn(1)-N(2)#1	2.08(2)
Zn(1)-N(2)	2.08(2)
P(1)-C(41)	1.77(3)
P(1)-C(45)	1.77(3)
P(1)-C(43)	1.77(3)
P(2)-C(39)	1.81(4)
P(2)-C(35)	1.82(4)
P(2)-C(37)	1.87(3)
P(3)-C(53)	1.78(5)
P(3)-C(55)	1.83(4)
P(3)-C(57)	1.92(5)
P(4)-C(51)	1.83(3)
P(4)-C(49)	1.83(3)
P(4)-C(47)	1.84(2)
O(1)-C(21)	1.22(3)
O(2)-C(21)	1.37(4)
O(3)-C(34)	1.39(4)
O(4)-C(34)	1.15(3)
N(1)-C(1)	1.33(3)
N(1)-C(4)	1.39(3)
N(2)-C(6)	1.34(3)
N(2)-C(9)	1.39(3)
N(3)-C(13)	1.18(3)
N(3)-C(14)	1.35(3)
N(4)-C(19)	1.29(4)
N(4)-C(18)	1.33(4)
C(1)-C(2)	1.39(3)
C(1)-C(10)#1	1.49(3)
C(2)-C(3)	1.32(3)
C(2)-H(2)	0.95

C(3)-C(4)	1.47(3)
C(3)-H(3)	0.95
C(4)-C(5)	1.42(3)
C(5)-C(6)	1.41(4)
C(5)-C(11)	1.51(3)
C(6)-C(7)	1.47(4)
C(7)-C(8)	1.43(3)
C(7)-H(7)	0.95
C(8)-C(9)	1.44(4)
C(8)-H(8)	0.95
C(9)-C(10)	1.35(3)
C(10)-C(16)	1.55(3)
C(11)-C(12)	1.31(4)
C(11)-C(15)	1.40(3)
C(12)-C(13)	1.52(3)
C(12)-H(12)	0.95
C(13)-H(13)	0.95
C(14)-C(15)	1.44(3)
C(14)-H(14)	0.95
C(15)-H(15)	0.95
C(16)-C(17)	1.34(4)
C(16)-C(20)	1.45(4)
C(17)-C(18)	1.42(4)
C(17)-H(17)	0.95
C(18)-H(18)	0.95
C(19)-C(20)	1.40(4)
C(19)-H(19)	0.95
C(20)-H(20)	0.95
C(21)-C(22)	1.53(4)
C(22)-C(27)	1.388(18)
C(22)-C(23)	1.389(18)
C(23)-C(24)	1.386(18)
C(23)-H(23)	0.95
C(24)-C(25)	1.384(18)
C(24)-H(24)	0.95
C(25)-C(26)	1.389(18)
C(25)-C(28)	1.42(4)
C(26)-C(27)	1.398(18)
C(26)-H(26)	0.95
C(27)-H(27)	0.95
C(28)-C(33)	1.425(18)
C(28)-C(29)	1.431(18)
C(29)-C(30)	1.418(18)

C(29)-H(29)	0.95
C(30)-C(31)	1.424(18)
C(30)-H(30)	0.95
C(31)-C(32)	1.421(18)
C(31)-C(34)	1.50(4)
C(32)-C(33)	1.417(18)
C(32)-H(32)	0.95
C(33)-H(33)	0.95
C(35)-C(36)	1.52(5)
C(35)-H(35A)	0.99
C(35)-H(35B)	0.99
C(36)-H(36A)	0.98
C(36)-H(36B)	0.98
C(36)-H(36C)	0.98
C(37)-C(38)	1.49(5)
C(37)-H(37A)	0.99
C(37)-H(37B)	0.99
C(38)-H(38A)	0.98
C(38)-H(38B)	0.98
C(38)-H(38C)	0.98
C(39)-C(40)	1.53(5)
C(39)-H(39A)	0.99
C(39)-H(39B)	0.99
C(40)-H(40A)	0.98
C(40)-H(40B)	0.98
C(40)-H(40C)	0.98
C(41)-C(42)	1.50(5)
C(41)-H(41A)	0.99
C(41)-H(41B)	0.99
C(42)-H(42A)	0.98
C(42)-H(42B)	0.98
C(42)-H(42C)	0.98
C(43)-C(44)	1.66(5)
C(43)-H(43A)	0.99
C(43)-H(43B)	0.99
C(44)-H(44A)	0.98
C(44)-H(44B)	0.98
C(44)-H(44C)	0.98
C(45)-C(46)	1.27(5)
C(45)-H(45A)	0.99
C(45)-H(45B)	0.99
C(46)-H(46A)	0.98
C(46)-H(46B)	0.98

C(46)-H(46C)	0.98
C(47)-C(48)	1.532(10)
C(47)-H(47A)	0.99
C(47)-H(47B)	0.99
C(48)-H(48A)	0.98
C(48)-H(48B)	0.98
C(48)-H(48C)	0.98
C(49)-C(50)	1.534(10)
C(49)-H(49A)	0.99
C(49)-H(49B)	0.99
C(50)-H(50A)	0.98
C(50)-H(50B)	0.98
C(50)-H(50C)	0.98
C(51)-C(52)	1.531(10)
C(51)-H(51A)	0.99
C(51)-H(51B)	0.99
C(52)-H(52A)	0.98
C(52)-H(52B)	0.98
C(52)-H(52C)	0.98
C(53)-C(54)	1.529(10)
C(53)-H(53A)	0.99
C(53)-H(53B)	0.99
C(54)-H(54A)	0.98
C(54)-H(54B)	0.98
C(54)-H(54C)	0.98
C(56)-C(55)	1.530(10)
C(56)-H(56A)	0.98
C(56)-H(56B)	0.98
C(56)-H(56C)	0.98
C(55)-H(55A)	0.99
C(55)-H(55B)	0.99
C(57)-C(58)	1.531(10)
C(57)-H(57A)	0.99
C(57)-H(57B)	0.99
C(58)-H(58A)	0.98
C(58)-H(58B)	0.98
C(58)-H(58C)	0.98

O(2)-Pt(1)-N(3)	84.8(7)
O(2)-Pt(1)-P(2)	176.2(6)
N(3)-Pt(1)-P(2)	94.5(6)
O(2)-Pt(1)-P(1)	82.8(5)
N(3)-Pt(1)-P(1)	167.0(6)

P(2)-Pt(1)-P(1)	97.6(3)
O(3)-Pt(2)-N(4)	81.6(8)
O(3)-Pt(2)-P(4)	88.4(6)
N(4)-Pt(2)-P(4)	170.0(6)
O(3)-Pt(2)-P(3)	172.3(5)
N(4)-Pt(2)-P(3)	95.7(6)
P(4)-Pt(2)-P(3)	94.0(3)
N(1)#1-Zn(1)-N(1)	180
N(1)#1-Zn(1)-N(2)#1	89.8(8)
N(1)-Zn(1)-N(2)#1	90.2(8)
N(1)#1-Zn(1)-N(2)	90.2(8)
N(1)-Zn(1)-N(2)	89.8(8)
N(2)#1-Zn(1)-N(2)	180
C(41)-P(1)-C(45)	104(2)
C(41)-P(1)-C(43)	112(2)
C(45)-P(1)-C(43)	104(2)
C(41)-P(1)-Pt(1)	105.1(13)
C(45)-P(1)-Pt(1)	107.3(15)
C(43)-P(1)-Pt(1)	122.1(15)
C(39)-P(2)-C(35)	101(2)
C(39)-P(2)-C(37)	105.9(19)
C(35)-P(2)-C(37)	103.1(18)
C(39)-P(2)-Pt(1)	119.1(15)
C(35)-P(2)-Pt(1)	110.2(13)
C(37)-P(2)-Pt(1)	115.8(13)
C(53)-P(3)-C(55)	111(2)
C(53)-P(3)-C(57)	97(2)
C(55)-P(3)-C(57)	97(2)
C(53)-P(3)-Pt(2)	116.9(17)
C(55)-P(3)-Pt(2)	122.5(14)
C(57)-P(3)-Pt(2)	107.2(12)
C(51)-P(4)-C(49)	104(3)
C(51)-P(4)-C(47)	101.3(18)
C(49)-P(4)-C(47)	106(2)
C(51)-P(4)-Pt(2)	119(2)
C(49)-P(4)-Pt(2)	109.7(11)
C(47)-P(4)-Pt(2)	115.6(13)
C(21)-O(2)-Pt(1)	110.0(18)
C(34)-O(3)-Pt(2)	111.9(16)
C(1)-N(1)-C(4)	103.6(18)
C(1)-N(1)-Zn(1)	129.8(15)
C(4)-N(1)-Zn(1)	126.6(17)
C(6)-N(2)-C(9)	108(2)

C(6)-N(2)-Zn(1)	127.6(18)
C(9)-N(2)-Zn(1)	124.3(16)
C(13)-N(3)-C(14)	126(2)
C(13)-N(3)-Pt(1)	115.5(16)
C(14)-N(3)-Pt(1)	118.2(16)
C(19)-N(4)-C(18)	120(2)
C(19)-N(4)-Pt(2)	122.1(19)
C(18)-N(4)-Pt(2)	116(2)
N(1)-C(1)-C(2)	113(2)
N(1)-C(1)-C(10)#1	123(2)
C(2)-C(1)-C(10)#1	124(2)
C(3)-C(2)-C(1)	109(2)
C(3)-C(2)-H(2)	125.7
C(1)-C(2)-H(2)	125.7
C(2)-C(3)-C(4)	105(2)
C(2)-C(3)-H(3)	127.6
C(4)-C(3)-H(3)	127.6
N(1)-C(4)-C(5)	126(2)
N(1)-C(4)-C(3)	110(2)
C(5)-C(4)-C(3)	124(2)
C(6)-C(5)-C(4)	124(2)
C(6)-C(5)-C(11)	118(2)
C(4)-C(5)-C(11)	117(2)
N(2)-C(6)-C(5)	125(2)
N(2)-C(6)-C(7)	110(2)
C(5)-C(6)-C(7)	125(2)
C(8)-C(7)-C(6)	106(2)
C(8)-C(7)-H(7)	126.9
C(6)-C(7)-H(7)	126.9
C(7)-C(8)-C(9)	105(2)
C(7)-C(8)-H(8)	127.7
C(9)-C(8)-H(8)	127.7
C(10)-C(9)-N(2)	127(2)
C(10)-C(9)-C(8)	122(2)
N(2)-C(9)-C(8)	111(2)
C(9)-C(10)-C(1)#1	125(2)
C(9)-C(10)-C(16)	122(2)
C(1)#1-C(10)-C(16)	111.6(19)
C(12)-C(11)-C(15)	122(2)
C(12)-C(11)-C(5)	119(3)
C(15)-C(11)-C(5)	119(3)
C(11)-C(12)-C(13)	117(3)
C(11)-C(12)-H(12)	121.7

C(13)-C(12)-H(12)	121.7
N(3)-C(13)-C(12)	121(3)
N(3)-C(13)-H(13)	119.7
C(12)-C(13)-H(13)	119.7
N(3)-C(14)-C(15)	118(2)
N(3)-C(14)-H(14)	121
C(15)-C(14)-H(14)	121
C(11)-C(15)-C(14)	117(2)
C(11)-C(15)-H(15)	121.5
C(14)-C(15)-H(15)	121.5
C(17)-C(16)-C(20)	118(2)
C(17)-C(16)-C(10)	124(2)
C(20)-C(16)-C(10)	117(2)
C(16)-C(17)-C(18)	120(3)
C(16)-C(17)-H(17)	120
C(18)-C(17)-H(17)	120
N(4)-C(18)-C(17)	121(3)
N(4)-C(18)-H(18)	119.7
C(17)-C(18)-H(18)	119.7
N(4)-C(19)-C(20)	123(3)
N(4)-C(19)-H(19)	118.3
C(20)-C(19)-H(19)	118.3
C(19)-C(20)-C(16)	117(3)
C(19)-C(20)-H(20)	121.7
C(16)-C(20)-H(20)	121.7
O(1)-C(21)-O(2)	132(3)
O(1)-C(21)-C(22)	114(3)
O(2)-C(21)-C(22)	113(3)
C(27)-C(22)-C(23)	119(3)
C(27)-C(22)-C(21)	122(2)
C(23)-C(22)-C(21)	119(2)
C(24)-C(23)-C(22)	118(3)
C(24)-C(23)-H(23)	120.9
C(22)-C(23)-H(23)	120.9
C(25)-C(24)-C(23)	125(3)
C(25)-C(24)-H(24)	117.7
C(23)-C(24)-H(24)	117.7
C(24)-C(25)-C(26)	116(3)
C(24)-C(25)-C(28)	127(2)
C(26)-C(25)-C(28)	117(2)
C(25)-C(26)-C(27)	120(3)
C(25)-C(26)-H(26)	119.8
C(27)-C(26)-H(26)	119.8

C(22)-C(27)-C(26)	122(3)
C(22)-C(27)-H(27)	119.2
C(26)-C(27)-H(27)	119.2
C(25)-C(28)-C(33)	121(2)
C(25)-C(28)-C(29)	121(2)
C(33)-C(28)-C(29)	117(3)
C(30)-C(29)-C(28)	121(3)
C(30)-C(29)-H(29)	119.4
C(28)-C(29)-H(29)	119.4
C(29)-C(30)-C(31)	122(3)
C(29)-C(30)-H(30)	119.1
C(31)-C(30)-H(30)	119.1
C(32)-C(31)-C(30)	117(3)
C(32)-C(31)-C(34)	123(2)
C(30)-C(31)-C(34)	119(2)
C(33)-C(32)-C(31)	121(3)
C(33)-C(32)-H(32)	119.3
C(31)-C(32)-H(32)	119.3
C(32)-C(33)-C(28)	122(3)
C(32)-C(33)-H(33)	119.1
C(28)-C(33)-H(33)	119.1
O(4)-C(34)-O(3)	126(3)
O(4)-C(34)-C(31)	121(3)
O(3)-C(34)-C(31)	113(2)
C(36)-C(35)-P(2)	112(3)
C(36)-C(35)-H(35A)	109.3
P(2)-C(35)-H(35A)	109.3
C(36)-C(35)-H(35B)	109.3
P(2)-C(35)-H(35B)	109.3
H(35A)-C(35)-H(35B)	108
C(35)-C(36)-H(36A)	109.5
C(35)-C(36)-H(36B)	109.5
H(36A)-C(36)-H(36B)	109.5
C(35)-C(36)-H(36C)	109.5
H(36A)-C(36)-H(36C)	109.5
H(36B)-C(36)-H(36C)	109.5
C(38)-C(37)-P(2)	115(3)
C(38)-C(37)-H(37A)	108.6
P(2)-C(37)-H(37A)	108.6
C(38)-C(37)-H(37B)	108.6
P(2)-C(37)-H(37B)	108.6
H(37A)-C(37)-H(37B)	107.6
C(37)-C(38)-H(38A)	109.5

C(37)-C(38)-H(38B)	109.5
H(38A)-C(38)-H(38B)	109.5
C(37)-C(38)-H(38C)	109.5
H(38A)-C(38)-H(38C)	109.5
H(38B)-C(38)-H(38C)	109.5
C(40)-C(39)-P(2)	112(2)
C(40)-C(39)-H(39A)	109.3
P(2)-C(39)-H(39A)	109.3
C(40)-C(39)-H(39B)	109.3
P(2)-C(39)-H(39B)	109.3
H(39A)-C(39)-H(39B)	107.9
C(39)-C(40)-H(40A)	109.5
C(39)-C(40)-H(40B)	109.5
H(40A)-C(40)-H(40B)	109.5
C(39)-C(40)-H(40C)	109.5
H(40A)-C(40)-H(40C)	109.5
H(40B)-C(40)-H(40C)	109.5
C(42)-C(41)-P(1)	109(2)
C(42)-C(41)-H(41A)	109.8
P(1)-C(41)-H(41A)	109.8
C(42)-C(41)-H(41B)	109.8
P(1)-C(41)-H(41B)	109.8
H(41A)-C(41)-H(41B)	108.3
C(41)-C(42)-H(42A)	109.5
C(41)-C(42)-H(42B)	109.5
H(42A)-C(42)-H(42B)	109.5
C(41)-C(42)-H(42C)	109.5
H(42A)-C(42)-H(42C)	109.5
H(42B)-C(42)-H(42C)	109.5
C(44)-C(43)-P(1)	110(3)
C(44)-C(43)-H(43A)	109.7
P(1)-C(43)-H(43A)	109.7
C(44)-C(43)-H(43B)	109.7
P(1)-C(43)-H(43B)	109.7
H(43A)-C(43)-H(43B)	108.2
C(43)-C(44)-H(44A)	109.5
C(43)-C(44)-H(44B)	109.5
H(44A)-C(44)-H(44B)	109.5
C(43)-C(44)-H(44C)	109.5
H(44A)-C(44)-H(44C)	109.5
H(44B)-C(44)-H(44C)	109.5
C(46)-C(45)-P(1)	122(4)
C(46)-C(45)-H(45A)	106.8

P(1)-C(45)-H(45A)	106.8
C(46)-C(45)-H(45B)	106.8
P(1)-C(45)-H(45B)	106.8
H(45A)-C(45)-H(45B)	106.6
C(45)-C(46)-H(46A)	109.5
C(45)-C(46)-H(46B)	109.5
H(46A)-C(46)-H(46B)	109.5
C(45)-C(46)-H(46C)	109.5
H(46A)-C(46)-H(46C)	109.5
H(46B)-C(46)-H(46C)	109.5
C(48)-C(47)-P(4)	113(2)
C(48)-C(47)-H(47A)	109.1
P(4)-C(47)-H(47A)	109.1
C(48)-C(47)-H(47B)	109.1
P(4)-C(47)-H(47B)	109.1
H(47A)-C(47)-H(47B)	107.8
C(47)-C(48)-H(48A)	109.5
C(47)-C(48)-H(48B)	109.5
H(48A)-C(48)-H(48B)	109.5
C(47)-C(48)-H(48C)	109.5
H(48A)-C(48)-H(48C)	109.5
H(48B)-C(48)-H(48C)	109.5
C(50)-C(49)-P(4)	110(3)
C(50)-C(49)-H(49A)	109.6
P(4)-C(49)-H(49A)	109.6
C(50)-C(49)-H(49B)	109.6
P(4)-C(49)-H(49B)	109.6
H(49A)-C(49)-H(49B)	108.1
C(49)-C(50)-H(50A)	109.5
C(49)-C(50)-H(50B)	109.5
H(50A)-C(50)-H(50B)	109.5
C(49)-C(50)-H(50C)	109.5
H(50A)-C(50)-H(50C)	109.5
H(50B)-C(50)-H(50C)	109.5
C(52)-C(51)-P(4)	112(3)
C(52)-C(51)-H(51A)	109.2
P(4)-C(51)-H(51A)	109.2
C(52)-C(51)-H(51B)	109.2
P(4)-C(51)-H(51B)	109.2
H(51A)-C(51)-H(51B)	107.9
C(51)-C(52)-H(52A)	109.5
C(51)-C(52)-H(52B)	109.5
H(52A)-C(52)-H(52B)	109.5

C(51)-C(52)-H(52C)	109.5
H(52A)-C(52)-H(52C)	109.5
H(52B)-C(52)-H(52C)	109.5
C(54)-C(53)-P(3)	124(4)
C(54)-C(53)-H(53A)	106.3
P(3)-C(53)-H(53A)	106.3
C(54)-C(53)-H(53B)	106.3
P(3)-C(53)-H(53B)	106.3
H(53A)-C(53)-H(53B)	106.4
C(53)-C(54)-H(54A)	109.5
C(53)-C(54)-H(54B)	109.5
H(54A)-C(54)-H(54B)	109.5
C(53)-C(54)-H(54C)	109.5
H(54A)-C(54)-H(54C)	109.5
H(54B)-C(54)-H(54C)	109.5
C(55)-C(56)-H(56A)	109.5
C(55)-C(56)-H(56B)	109.5
H(56A)-C(56)-H(56B)	109.5
C(55)-C(56)-H(56C)	109.5
H(56A)-C(56)-H(56C)	109.5
H(56B)-C(56)-H(56C)	109.5
C(56)-C(55)-P(3)	113(3)
C(56)-C(55)-H(55A)	109
P(3)-C(55)-H(55A)	109
C(56)-C(55)-H(55B)	109
P(3)-C(55)-H(55B)	109
H(55A)-C(55)-H(55B)	107.8
C(58)-C(57)-P(3)	113(3)
C(58)-C(57)-H(57A)	109.1
P(3)-C(57)-H(57A)	109.1
C(58)-C(57)-H(57B)	109.1
P(3)-C(57)-H(57B)	109.1
H(57A)-C(57)-H(57B)	107.8
C(57)-C(58)-H(58A)	109.5
C(57)-C(58)-H(58B)	109.5
H(58A)-C(58)-H(58B)	109.5
C(57)-C(58)-H(58C)	109.5
H(58A)-C(58)-H(58C)	109.5
H(58B)-C(58)-H(58C)	109.5

Symmetry transformations used to generate equivalent atoms:

#1 -x+2,-y,-z+1

Table 5. Atomic coordinates (x 10^4) and equivalent isotropic displacement parameters ($Å^2$x 10^3) for **BT3**. U(eq) is defined as one third of the trace of the orthogonalized U^{ij} tensor.

	x	y	z	U(eq)
Pt(1)	6023(1)	5750(2)	4546(1)	92(2)
O(1)	4438(16)	2350(40)	2539(18)	90(14)
O(2)	3772(14)	2770(30)	2624(17)	108(12)
C(23)	4860(20)	4450(30)	3644(15)	87(13)
C(24)	5107(14)	4030(40)	3390(20)	89(14)
C(25)	4890(20)	3490(30)	3055(18)	90(14)
C(26)	4430(20)	3370(30)	2970(16)	87(13)
C(27)	4180(15)	3790(40)	3220(20)	92(14)
C(28)	4400(20)	4330(30)	3559(18)	88(14)
P(1)	6486(9)	6353(17)	5153(10)	103(7)
Pt(2)	3342(2)	1949(4)	2203(2)	141(3)
P(2)	6004(9)	6885(14)	4089(9)	91(7)
Zn(03)	5000	0	5000	82(5)
O(3)	5615(18)	5070(30)	4027(17)	81(9)
C(2)	5586(12)	4390(30)	5084(15)	67(12)
N(5)	5949(12)	4570(20)	4908(13)	47(8)
C(3)	6177(11)	3890(30)	4767(13)	34(8)
C(4)	6043(14)	3040(20)	4803(15)	55(12)
C(5)	5681(15)	2860(20)	4979(16)	67(11)
C(6)	5453(13)	3540(30)	5120(16)	72(13)
O(4)	4957(18)	5350(40)	4230(20)	100(15)
P(3)	3184(10)	2970(20)	1691(9)	124(7)
P(4)	2867(11)	990(30)	1891(13)	171(13)
C(7)	5530(20)	2030(50)	5030(30)	66(12)
C(8)	5628(18)	1590(30)	5365(14)	69(12)
C(9)	5949(18)	1840(30)	5750(17)	71(15)
C(10)	5968(17)	1170(40)	6062(13)	74(15)
C(11)	5659(18)	510(30)	5870(17)	74(14)
N(3)	5449(15)	770(30)	5439(15)	65(11)
C(12)	5208(18)	1790(40)	4631(16)	80(13)
C(13)	5100(20)	2270(30)	4240(20)	84(15)
C(14)	4760(20)	1820(40)	3935(15)	81(15)
C(15)	4655(17)	1060(30)	4139(19)	79(13)
N(2)	4931(18)	1040(30)	4569(17)	75(7)
C(16)	4430(30)	360(60)	3980(30)	77(9)
C(17)	4180(30)	450(60)	3560(30)	75(14)

C(18)	4180(30)	300(60)	3180(30)	85(14)
C(19)	3990(30)	580(70)	2800(30)	96(15)
N(4)	3640(30)	1130(60)	2740(30)	118(15)
C(21)	3470(30)	1290(60)	3080(30)	98(16)
C(20)	3760(30)	940(50)	3510(30)	76(14)
C(1A)	5710(30)	7640(50)	4100(30)	105(14)
C(2A)	5190(30)	7550(60)	3970(40)	140(30)
C(38)	5910(30)	6620(50)	3500(30)	110(14)
C(39)	6150(30)	5760(50)	3430(30)	120(20)
C(3A)	6650(30)	7160(50)	4170(30)	118(16)
C(49)	2940(30)	-160(70)	2110(40)	170(20)
C(52)	5090(30)	5050(40)	3980(20)	86(12)
C(53)	4161(17)	2750(50)	2650(20)	90(13)
C(9A)	3390(20)	2420(50)	1260(20)	125(9)
C(12A)	6440(30)	5740(70)	5680(20)	128(17)
C(13A)	3880(20)	2320(70)	1230(30)	136(12)
C(14A)	6983(18)	6420(70)	4340(40)	160(30)
C(15A)	5820(20)	7440(60)	5270(30)	110(16)
C(16A)	6700(30)	6050(60)	6130(30)	130(30)
C(17A)	6320(20)	7450(30)	5270(30)	96(13)
C(19A)	2570(40)	-850(50)	1930(40)	200(40)
C(22A)	1980(30)	1010(100)	2120(50)	240(40)
C(23A)	2360(30)	730(90)	1910(40)	200(20)
C(25A)	7054(17)	6250(40)	5080(30)	119(15)
C(28A)	7330(20)	5410(60)	5130(40)	170(40)
C(29A)	2400(40)	710(80)	950(20)	210(40)
C(31A)	2800(30)	570(70)	1348(19)	174(19)
C(32A)	2890(30)	3870(50)	1360(30)	136(17)
C(33A)	3060(40)	4330(70)	1000(30)	190(40)
C(34A)	3530(20)	3940(30)	1720(30)	136(16)
C(35A)	3420(30)	4870(30)	1830(30)	150(20)

Table 6. Bond lengths [Å] and angles [º] for **BT3**.

Pt(1)-O(3)	2.09(6)
Pt(1)-N(5)	2.19(3)
Pt(1)-P(2)	2.26(2)
Pt(1)-P(1)	2.29(3)
O(1)-C(53)	1.17(2)
O(2)-C(53)	1.18(2)
O(2)-Pt(2)	2.06(2)
C(23)-C(24)	1.39

C(23)-C(28)	1.39
C(23)-C(52)	1.46(2)
C(24)-C(25)	1.39
C(24)-H(24)	0.95
C(25)-C(26)	1.39
C(25)-H(25)	0.95
C(26)-C(27)	1.39
C(26)-C(53)	1.48(2)
C(27)-C(28)	1.39
C(27)-H(27)	0.95
C(28)-H(28)	0.95
P(1)-C(25A)	1.82(2)
P(1)-C(17A)	1.83(2)
P(1)-C(12A)	1.96(7)
Pt(2)-N(4)	2.13(9)
Pt(2)-P(4)	2.13(3)
Pt(2)-P(3)	2.23(3)
P(2)-C(1A)	1.48(8)
P(2)-C(38)	1.87(9)
P(2)-C(3A)	1.96(9)
Zn(03)-N(3)#1	2.07(4)
Zn(03)-N(3)	2.07(4)
Zn(03)-N(2)	2.08(4)
Zn(03)-N(2)#1	2.08(4)
O(3)-C(52)	1.58(10)
C(2)-N(5)	1.39
C(2)-C(6)	1.39
C(2)-H(2)	0.95
N(5)-C(3)	1.39
C(3)-C(4)	1.39
C(3)-H(3)	0.95
C(4)-C(5)	1.39
C(4)-H(4)	0.95
C(5)-C(7)	1.37(8)
C(5)-C(6)	1.39
C(6)-H(6)	0.95
O(4)-C(52)	1.07(8)
P(3)-C(34A)	1.83(2)
P(3)-C(9A)	1.85(2)
P(3)-C(32A)	1.83(7)
P(4)-C(23A)	1.63(9)
P(4)-C(31A)	1.81(2)
P(4)-C(49)	1.90(10)

C(7)-C(8)	1.23(8)
C(7)-C(12)	1.46(8)
C(8)-N(3)	1.42
C(8)-C(9)	1.42
C(9)-C(10)	1.42
C(9)-H(9)	0.95
C(10)-C(11)	1.42
C(10)-H(10)	0.95
C(11)-N(3)	1.42
C(11)-C(16)#1	1.46(9)
C(12)-C(13)	1.42
C(12)-N(2)	1.42
C(13)-C(14)	1.42
C(13)-H(13)	0.95
C(14)-C(15)	1.42
C(14)-H(14)	0.95
C(15)-C(16)	1.31(9)
C(15)-N(2)	1.42
C(16)-C(17)	1.38(10)
C(17)-C(18)	1.22(10)
C(17)-C(20)	1.46(10)
C(18)-C(19)	1.28(10)
C(18)-H(18)	0.95
C(19)-N(4)	1.35(11)
C(19)-H(19)	0.95
N(4)-C(21)	1.33(11)
C(21)-C(20)	1.54(10)
C(21)-H(21)	0.95
C(20)-H(20)	0.95
C(1A)-C(2A)	1.54(2)
C(1A)-H(1A1)	0.99
C(1A)-H(1A2)	0.99
C(2A)-H(2A1)	0.989
C(2A)-H(2A2)	0.9894
C(2A)-H(2A3)	0.9893
C(38)-C(39)	1.54(2)
C(38)-H(38A)	0.99
C(38)-H(38B)	0.99
C(39)-C(35A)#2	2.20(11)
C(39)-H(39A)	1.0085
C(39)-H(39B)	1.0091
C(39)-H(39C)	1.0095
C(3A)-C(14A)	1.54(2)

C(3A)-H(3A1)	0.99
C(3A)-H(3A2)	0.99
C(49)-C(19A)	1.54(2)
C(49)-H(49A)	0.99
C(49)-H(49B)	0.99
C(9A)-C(13A)	1.55(2)
C(9A)-H(9A1)	0.99
C(9A)-H(9A2)	0.99
C(12A)-C(16A)	1.54(2)
C(12A)-H(12A)	0.99
C(12A)-H(12B)	0.99
C(13A)-H(13A)	0.999
C(13A)-H(13B)	0.9967
C(13A)-H(13C)	0.996
C(14A)-H(14A)	0.9801
C(14A)-H(14B)	0.9801
C(14A)-H(14C)	0.9801
C(15A)-C(17A)	1.53(2)
C(15A)-H(15A)	0.98
C(15A)-H(15B)	0.98
C(15A)-H(15C)	0.98
C(16A)-H(16A)	0.9802
C(16A)-H(16B)	0.9802
C(16A)-H(16C)	0.9802
C(17A)-H(17A)	0.99
C(17A)-H(17B)	0.99
C(19A)-H(19A)	1.0149
C(19A)-H(19B)	1.0127
C(19A)-H(19C)	1.0131
C(22A)-C(23A)	1.54(2)
C(22A)-H(22A)	1.1408
C(22A)-H(22B)	1.1551
C(22A)-H(22C)	1.1401
C(23A)-H(23A)	0.99
C(23A)-H(23B)	0.99
C(25A)-C(28A)	1.53(2)
C(25A)-H(25A)	0.99
C(25A)-H(25B)	0.99
C(28A)-H(28A)	1.0135
C(28A)-H(28B)	1.0125
C(28A)-H(28C)	1.0124
C(29A)-C(31A)	1.54(2)
C(29A)-H(29A)	1.0091

C(29A)-H(29B)	1.0093
C(29A)-H(29C)	1.0078
C(31A)-H(31A)	0.99
C(31A)-H(31B)	0.99
C(32A)-C(33A)	1.55(2)
C(32A)-H(32A)	0.99
C(32A)-H(32B)	0.99
C(33A)-H(33A)	1.0001
C(33A)-H(33B)	1.0009
C(33A)-H(33C)	0.9989
C(34A)-C(35A)	1.53(2)
C(34A)-H(34A)	0.99
C(34A)-H(34B)	0.99
C(35A)-H(35A)	0.9801
C(35A)-H(35B)	0.9801
C(35A)-H(35C)	0.9801

O(3)-Pt(1)-N(5)	83.3(16)
O(3)-Pt(1)-P(2)	87.9(15)
N(5)-Pt(1)-P(2)	170.8(13)
O(3)-Pt(1)-P(1)	173.8(15)
N(5)-Pt(1)-P(1)	90.8(12)
P(2)-Pt(1)-P(1)	98.1(10)
C(53)-O(2)-Pt(2)	120(3)
C(24)-C(23)-C(28)	120
C(24)-C(23)-C(52)	120(6)
C(28)-C(23)-C(52)	120(6)
C(25)-C(24)-C(23)	120
C(25)-C(24)-H(24)	120
C(23)-C(24)-H(24)	120
C(24)-C(25)-C(26)	120
C(24)-C(25)-H(25)	120
C(26)-C(25)-H(25)	120
C(25)-C(26)-C(27)	120
C(25)-C(26)-C(53)	125(5)
C(27)-C(26)-C(53)	115(5)
C(28)-C(27)-C(26)	120
C(28)-C(27)-H(27)	120
C(26)-C(27)-H(27)	120
C(27)-C(28)-C(23)	120
C(27)-C(28)-H(28)	120
C(23)-C(28)-H(28)	120
C(25A)-P(1)-C(17A)	116(3)

C(25A)-P(1)-C(12A)	110(3)
C(17A)-P(1)-C(12A)	101(4)
C(25A)-P(1)-Pt(1)	106(4)
C(17A)-P(1)-Pt(1)	113(3)
C(12A)-P(1)-Pt(1)	111(3)
O(2)-Pt(2)-N(4)	76(3)
O(2)-Pt(2)-P(4)	168(2)
N(4)-Pt(2)-P(4)	94(2)
O(2)-Pt(2)-P(3)	91.9(19)
N(4)-Pt(2)-P(3)	167(2)
P(4)-Pt(2)-P(3)	98.3(13)
C(1A)-P(2)-C(38)	105(5)
C(1A)-P(2)-C(3A)	116(4)
C(38)-P(2)-C(3A)	94(5)
C(1A)-P(2)-Pt(1)	120(4)
C(38)-P(2)-Pt(1)	117(3)
C(3A)-P(2)-Pt(1)	103(2)
N(3)#1-Zn(03)-N(3)	180(5)
N(3)#1-Zn(03)-N(2)	93(5)
N(3)-Zn(03)-N(2)	87(2)
N(3)#1-Zn(03)-N(2)#1	87(7)
N(3)-Zn(03)-N(2)#1	93(6)
N(2)-Zn(03)-N(2)#1	180(6)
C(52)-O(3)-Pt(1)	118(3)
N(5)-C(2)-C(6)	120
N(5)-C(2)-H(2)	120
C(6)-C(2)-H(2)	120
C(2)-N(5)-C(3)	120
C(2)-N(5)-Pt(1)	125(2)
C(3)-N(5)-Pt(1)	109(2)
N(5)-C(3)-C(4)	120
N(5)-C(3)-H(3)	120
C(4)-C(3)-H(3)	120
C(5)-C(4)-C(3)	120
C(5)-C(4)-H(4)	120
C(3)-C(4)-H(4)	120
C(7)-C(5)-C(4)	123(5)
C(7)-C(5)-C(6)	117(5)
C(4)-C(5)-C(6)	120
C(5)-C(6)-C(2)	120
C(5)-C(6)-H(6)	120
C(2)-C(6)-H(6)	120
C(34A)-P(3)-C(9A)	96(2)

C(34A)-P(3)-C(32A)	67(4)
C(9A)-P(3)-C(32A)	97(3)
C(34A)-P(3)-Pt(2)	121(3)
C(9A)-P(3)-Pt(2)	100(3)
C(32A)-P(3)-Pt(2)	160(3)
C(23A)-P(4)-C(31A)	94(5)
C(23A)-P(4)-C(49)	77(6)
C(31A)-P(4)-C(49)	89(6)
C(23A)-P(4)-Pt(2)	135(4)
C(31A)-P(4)-Pt(2)	126(4)
C(49)-P(4)-Pt(2)	118(3)
C(8)-C(7)-C(5)	127(7)
C(8)-C(7)-C(12)	125(7)
C(5)-C(7)-C(12)	108(6)
C(7)-C(8)-N(3)	128(6)
C(7)-C(8)-C(9)	124(6)
N(3)-C(8)-C(9)	108
C(8)-C(9)-C(10)	108
C(8)-C(9)-H(9)	126
C(10)-C(9)-H(9)	126
C(9)-C(10)-C(11)	108
C(9)-C(10)-H(10)	126
C(11)-C(10)-H(10)	126
N(3)-C(11)-C(10)	108
N(3)-C(11)-C(16)#1	119(5)
C(10)-C(11)-C(16)#1	132(5)
C(8)-N(3)-C(11)	108
C(8)-N(3)-Zn(03)	128(3)
C(11)-N(3)-Zn(03)	124(3)
C(13)-C(12)-N(2)	108
C(13)-C(12)-C(7)	126(5)
N(2)-C(12)-C(7)	126(5)
C(12)-C(13)-C(14)	108
C(12)-C(13)-H(13)	126
C(14)-C(13)-H(13)	126
C(15)-C(14)-C(13)	108
C(15)-C(14)-H(14)	126
C(13)-C(14)-H(14)	126
C(16)-C(15)-C(14)	132(6)
C(16)-C(15)-N(2)	119(6)
C(14)-C(15)-N(2)	108
C(15)-N(2)-C(12)	108
C(15)-N(2)-Zn(03)	126(4)

C(12)-N(2)-Zn(03)	125(3)
C(15)-C(16)-C(17)	113(8)
C(15)-C(16)-C(11)#1	139(8)
C(17)-C(16)-C(11)#1	108(7)
C(18)-C(17)-C(16)	144(10)
C(18)-C(17)-C(20)	102(9)
C(16)-C(17)-C(20)	114(8)
C(17)-C(18)-C(19)	140(10)
C(17)-C(18)-H(18)	110.4
C(19)-C(18)-H(18)	110.1
C(18)-C(19)-N(4)	120(10)
C(18)-C(19)-H(19)	119.9
N(4)-C(19)-H(19)	120
C(21)-N(4)-C(19)	117(9)
C(21)-N(4)-Pt(2)	112(8)
C(19)-N(4)-Pt(2)	131(8)
N(4)-C(21)-C(20)	114(9)
N(4)-C(21)-H(21)	123.1
C(20)-C(21)-H(21)	123.2
C(17)-C(20)-C(21)	125(9)
C(17)-C(20)-H(20)	117.6
C(21)-C(20)-H(20)	117.4
P(2)-C(1A)-C(2A)	121(6)
P(2)-C(1A)-H(1A1)	107
C(2A)-C(1A)-H(1A1)	106.9
P(2)-C(1A)-H(1A2)	107
C(2A)-C(1A)-H(1A2)	107
H(1A1)-C(1A)-H(1A2)	106.8
C(1A)-C(2A)-H(2A1)	110.1
C(1A)-C(2A)-H(2A2)	110.6
H(2A1)-C(2A)-H(2A2)	108.5
C(1A)-C(2A)-H(2A3)	110.4
H(2A1)-C(2A)-H(2A3)	108.6
H(2A2)-C(2A)-H(2A3)	108.6
C(39)-C(38)-P(2)	112(6)
C(39)-C(38)-H(38A)	109.1
P(2)-C(38)-H(38A)	109.4
C(39)-C(38)-H(38B)	109.3
P(2)-C(38)-H(38B)	109.3
H(38A)-C(38)-H(38B)	107.9
C(38)-C(39)-C(35A)#2	159(7)
C(38)-C(39)-H(39A)	112.1
C(35A)#2-C(39)-H(39A)	61.4

C(38)-C(39)-H(39B)	112.3
C(35A)#2-C(39)-H(39B)	56
H(39A)-C(39)-H(39B)	106.6
C(38)-C(39)-H(39C)	112.5
C(35A)#2-C(39)-H(39C)	88.7
H(39A)-C(39)-H(39C)	106.5
H(39B)-C(39)-H(39C)	106.5
C(14A)-C(3A)-P(2)	117(5)
C(14A)-C(3A)-H(3A1)	108.3
P(2)-C(3A)-H(3A1)	108.2
C(14A)-C(3A)-H(3A2)	108.2
P(2)-C(3A)-H(3A2)	107.9
H(3A1)-C(3A)-H(3A2)	107.3
C(19A)-C(49)-P(4)	120(6)
C(19A)-C(49)-H(49A)	107.5
P(4)-C(49)-H(49A)	107.5
C(19A)-C(49)-H(49B)	106.9
P(4)-C(49)-H(49B)	107.3
H(49A)-C(49)-H(49B)	106.9
O(4)-C(52)-C(23)	128(9)
O(4)-C(52)-O(3)	119(6)
C(23)-C(52)-O(3)	111(7)
O(1)-C(53)-O(2)	142(5)
O(1)-C(53)-C(26)	104(5)
O(2)-C(53)-C(26)	114(4)
C(13A)-C(9A)-P(3)	127(3)
C(13A)-C(9A)-H(9A1)	106.3
P(3)-C(9A)-H(9A1)	105.7
C(13A)-C(9A)-H(9A2)	104.7
P(3)-C(9A)-H(9A2)	105.6
H(9A1)-C(9A)-H(9A2)	106.1
C(16A)-C(12A)-P(1)	121(6)
C(16A)-C(12A)-H(12A)	107.2
P(1)-C(12A)-H(12A)	107.2
C(16A)-C(12A)-H(12B)	106.9
P(1)-C(12A)-H(12B)	107
H(12A)-C(12A)-H(12B)	106.8
C(9A)-C(13A)-H(13A)	112.2
C(9A)-C(13A)-H(13B)	110.9
H(13A)-C(13A)-H(13B)	107.9
C(9A)-C(13A)-H(13C)	110.4
H(13A)-C(13A)-H(13C)	107.5
H(13B)-C(13A)-H(13C)	107.9

C(3A)-C(14A)-H(14A)	109.6
C(3A)-C(14A)-H(14B)	109.3
H(14A)-C(14A)-H(14B)	109.5
C(3A)-C(14A)-H(14C)	109.6
H(14A)-C(14A)-H(14C)	109.5
H(14B)-C(14A)-H(14C)	109.5
C(17A)-C(15A)-H(15A)	109.5
C(17A)-C(15A)-H(15B)	109.5
H(15A)-C(15A)-H(15B)	109.5
C(17A)-C(15A)-H(15C)	109.4
H(15A)-C(15A)-H(15C)	109.5
H(15B)-C(15A)-H(15C)	109.5
C(12A)-C(16A)-H(16A)	109.3
C(12A)-C(16A)-H(16B)	109.6
H(16A)-C(16A)-H(16B)	109.5
C(12A)-C(16A)-H(16C)	109.5
H(16A)-C(16A)-H(16C)	109.4
H(16B)-C(16A)-H(16C)	109.5
C(15A)-C(17A)-P(1)	109(5)
C(15A)-C(17A)-H(17A)	110
P(1)-C(17A)-H(17A)	109.8
C(15A)-C(17A)-H(17B)	109.9
P(1)-C(17A)-H(17B)	110.1
H(17A)-C(17A)-H(17B)	108.3
C(49)-C(19A)-H(19A)	113.2
C(49)-C(19A)-H(19B)	112.5
H(19A)-C(19A)-H(19B)	106.1
C(49)-C(19A)-H(19C)	112.6
H(19A)-C(19A)-H(19C)	105.9
H(19B)-C(19A)-H(19C)	106.1
C(23A)-C(22A)-H(22A)	125.4
C(23A)-C(22A)-H(22B)	127.3
H(22A)-C(22A)-H(22B)	88.7
C(23A)-C(22A)-H(22C)	124.6
H(22A)-C(22A)-H(22C)	89.7
H(22B)-C(22A)-H(22C)	89.3
C(22A)-C(23A)-P(4)	142(10)
C(22A)-C(23A)-H(23A)	101.6
P(4)-C(23A)-H(23A)	102.1
C(22A)-C(23A)-H(23B)	101.5
P(4)-C(23A)-H(23B)	101.1
H(23A)-C(23A)-H(23B)	104.6
C(28A)-C(25A)-P(1)	126(3)

C(28A)-C(25A)-H(25A)	106.1
P(1)-C(25A)-H(25A)	105.9
C(28A)-C(25A)-H(25B)	105.8
P(1)-C(25A)-H(25B)	105.9
H(25A)-C(25A)-H(25B)	106.2
C(25A)-C(28A)-H(28A)	112.9
C(25A)-C(28A)-H(28B)	112.6
H(28A)-C(28A)-H(28B)	106.1
C(25A)-C(28A)-H(28C)	112.6
H(28A)-C(28A)-H(28C)	106
H(28B)-C(28A)-H(28C)	106.1
C(31A)-C(29A)-H(29A)	112.3
C(31A)-C(29A)-H(29B)	112.4
H(29A)-C(29A)-H(29B)	106.5
C(31A)-C(29A)-H(29C)	112.1
H(29A)-C(29A)-H(29C)	106.7
H(29B)-C(29A)-H(29C)	106.5
C(29A)-C(31A)-P(4)	127(4)
C(29A)-C(31A)-H(31A)	105.7
P(4)-C(31A)-H(31A)	105.5
C(29A)-C(31A)-H(31B)	105.5
P(4)-C(31A)-H(31B)	105.6
H(31A)-C(31A)-H(31B)	106.1
C(33A)-C(32A)-P(3)	124(5)
C(33A)-C(32A)-H(32A)	106.8
P(3)-C(32A)-H(32A)	106.2
C(33A)-C(32A)-H(32B)	105.9
P(3)-C(32A)-H(32B)	106.2
H(32A)-C(32A)-H(32B)	106.4
C(32A)-C(33A)-H(33A)	111.5
C(32A)-C(33A)-H(33B)	111.9
H(33A)-C(33A)-H(33B)	107.4
C(32A)-C(33A)-H(33C)	110.8
H(33A)-C(33A)-H(33C)	107.4
H(33B)-C(33A)-H(33C)	107.6
C(35A)-C(34A)-P(3)	128(4)
C(35A)-C(34A)-H(34A)	104.9
P(3)-C(34A)-H(34A)	105.3
C(35A)-C(34A)-H(34B)	105.7
P(3)-C(34A)-H(34B)	105.4
H(34A)-C(34A)-H(34B)	106
C(34A)-C(35A)-C(39)#2	108(6)
C(34A)-C(35A)-H(35A)	109.3

C(39)#2-C(35A)-H(35A)	133.6
C(34A)-C(35A)-H(35B)	109.1
C(39)#2-C(35A)-H(35B)	30.7
H(35A)-C(35A)-H(35B)	109.5
C(34A)-C(35A)-H(35C)	110
C(39)#2-C(35A)-H(35C)	81.8
H(35A)-C(35A)-H(35C)	109.5
H(35B)-C(35A)-H(35C)	109.5

Symmetry transformations used to generate equivalent atoms:

#1 -x+1,-y,-z+1 #2 -x+1,y,-z+1/2

Table 7. Atomic coordinates (x 10^4) and equivalent isotropic displacement parameters ($Å^2$x 10^3) for **BT4**. U(eq) is defined as one third of the trace of the orthogonalized U^{ij} tensor.

	x	y	z	U(eq)
Pt(1)	11311(1)	5735(1)	5811(1)	95(1)
Pt(2)	7728(1)	7226(1)	636(1)	127(1)
Pt(3)	2824(1)	6741(1)	3123(1)	203(1)
Pt(4)	6519(1)	5208(1)	8238(1)	172(1)
Zn(1)	7006(1)	6042(1)	4265(2)	83(1)
P(4)	6875(7)	7432(6)	-16(7)	196(6)
P(5)	2678(7)	7130(8)	2258(11)	270(12)
P(6)	1911(7)	6815(10)	3164(12)	349(17)
P(7)	6053(8)	5041(7)	8926(8)	220(8)
P(8)	7423(9)	5218(10)	8884(10)	311(15)
O(1)	11074(9)	5931(6)	4915(11)	96(5)
O(2)	10664(9)	5368(7)	4489(10)	98(6)
O(3)	8509(10)	7020(8)	1324(13)	123(7)
O(4)	8572(12)	7579(9)	1931(14)	143(9)
O(5)	3110(11)	6473(12)	4045(15)	164(10)
O(6)	3109(16)	5833(13)	3583(19)	197(13)
O(8)	5735(12)	4709(9)	7128(15)	148(9)
O(9W)	6813(10)	5532(6)	3685(14)	134(8)
N(5)	10369(10)	5770(5)	5630(12)	79(6)
C(29)	7265(11)	6464(5)	1929(12)	118(9)
C(26)	7189(10)	6720(7)	2383(9)	101(7)
C(27)	7199(10)	7129(6)	2297(10)	109(8)
C(28)	7284(10)	7282(5)	1757(12)	118(9)
N(6)	7360(9)	7025(7)	1304(9)	112(7)
C(30)	7350(10)	6616(7)	1390(10)	118(9)
P(1)	11480(4)	5553(3)	6803(6)	118(3)

N(8)	6769(10)	5365(8)	7456(9)	131(8)
C(36)	6914(10)	5087(6)	7073(12)	133(10)
C(37)	6976(10)	5206(7)	6504(11)	120(9)
C(38)	6892(10)	5602(8)	6318(10)	113(8)
C(39)	6747(10)	5880(6)	6702(13)	124(9)
C(40)	6685(10)	5761(7)	7271(11)	134(9)
C(34)	4679(16)	6780(13)	3820(20)	151(12)
C(31)	4895(14)	6427(11)	3566(19)	105(8)
C(32)	4492(15)	6219(12)	3203(19)	118(9)
C(33)	3891(15)	6298(13)	3047(19)	121(10)
N(7)	3724(13)	6654(12)	3245(17)	133(9)
C(35)	4153(17)	6884(14)	3650(20)	153(12)
P(2)	12265(4)	5759(3)	5846(6)	118(4)
N(1)	7590(7)	5853(6)	5128(8)	92(6)
C(1)	7465(6)	5726(6)	5673(10)	85(7)
C(2)	8009(8)	5627(6)	6147(8)	76(6)
C(4)	8470(6)	5693(6)	5894(10)	83(7)
C(4')	8212(8)	5833(6)	5264(9)	82(6)
P(3)	8330(7)	7402(4)	65(7)	156(5)
C(13)	5808(7)	6451(6)	3392(9)	76(6)
C(3)	5593(6)	6646(7)	2798(10)	95(8)
C(11)	6080(9)	6714(7)	2584(8)	94(8)
C(3')	6596(7)	6560(6)	3047(10)	79(6)
N(3)	6427(7)	6397(5)	3546(8)	73(5)
C(5)	8552(12)	5945(8)	4904(16)	81(6)
N(2)	7717(7)	6223(6)	3999(9)	79(5)
C(6)	8320(8)	6119(7)	4300(9)	91(7)
C(7)	8642(6)	6242(7)	3903(11)	99(8)
C(8)	8237(8)	6422(6)	3356(9)	86(7)
C(9)	7666(7)	6410(6)	3415(9)	81(7)
C(10)	7149(13)	6555(9)	2988(16)	91(7)
C(14)	5528(12)	6340(9)	3760(15)	82(7)
N(4)	6333(7)	6041(6)	4657(9)	85(6)
C(16)	5732(8)	6151(6)	4362(8)	83(7)
C(17)	5416(6)	6041(6)	4772(10)	80(7)
C(18)	5822(8)	5864(6)	5320(8)	76(7)
C(19)	6389(7)	5864(6)	5249(9)	82(7)
C(21)	9180(12)	5890(8)	5118(15)	76(7)
C(22)	9434(13)	5513(8)	5232(15)	83(8)
C(23)	10027(11)	5454(7)	5472(13)	61(7)
C(24)	10169(12)	6134(7)	5516(14)	67(7)
C(25)	9561(12)	6201(9)	5268(15)	83(7)
C(41)	10723(15)	5746(12)	4433(19)	92(8)

C(42)	10358(14)	5954(11)	3887(18)	90(7)
C(43)	10256(12)	6374(10)	3935(16)	90(7)
C(44)	9597(10)	6379(5)	2847(12)	93(7)
C(45)	9869(8)	6578(7)	3413(10)	92(7)
C(48)	9762(9)	6981(7)	3463(9)	88(7)
C(49)	9382(10)	7184(5)	2947(12)	119(9)
C(51)	9110(9)	6985(7)	2381(10)	102(8)
C(52)	9218(9)	6583(7)	2331(9)	103(8)
C(46)	9652(14)	5960(10)	2799(17)	95(7)
C(47)	10059(16)	5748(12)	3337(19)	113(9)
C(55)	3886(18)	5607(15)	4740(20)	139(10)
C(57)	3190(20)	6070(20)	4010(30)	146(11)
C(58)	3887(19)	6255(16)	5190(20)	148(11)
C(59)	3675(17)	5986(16)	4710(20)	130(9)
C(60)	4285(10)	5464(10)	5327(11)	128(9)
C(61)	4482(12)	5072(9)	5406(12)	142(10)
C(62)	4888(12)	4951(6)	5980(14)	132(10)
C(63)	5097(9)	5221(9)	6473(10)	105(8)
C(56)	4900(11)	5613(8)	6394(12)	106(8)
C(56')	4494(11)	5734(7)	5821(15)	123(9)
C(65)	11822(17)	5084(12)	7020(20)	128(10)
C(66)	11570(20)	4771(14)	6640(20)	168(17)
C(67)	10812(14)	5521(15)	7030(20)	168(12)
C(71)	12810(14)	5513(13)	6450(20)	155(11)
C(72)	13459(15)	5528(14)	6470(30)	185(18)
C(73)	12240(19)	5220(15)	5030(30)	184(16)
C(75)	12520(20)	6325(14)	6010(40)	230(20)
C(76)	12210(20)	6609(14)	5720(40)	230(20)
C(77)	8840(20)	7775(13)	510(20)	160(10)
C(78)	8592(19)	8141(13)	680(30)	172(16)
C(79)	8860(20)	7002(14)	140(20)	169(12)
C(200)	6918(13)	5727(9)	5708(17)	93(7)
C(304)	6980(30)	8163(17)	550(30)	219(19)
C(303)	6810(20)	8015(18)	-90(30)	208(13)
C(307)	1650(30)	6080(30)	3310(40)	390(30)
C(306)	1680(30)	6480(20)	3670(30)	360(20)
O(305)	5715(10)	5266(8)	7593(12)	125(7)
C(302)	8580(20)	7631(17)	-1050(30)	220(20)
C(301)	8150(20)	7594(14)	-630(20)	171(11)
C(308)	1350(20)	6910(30)	2500(30)	360(20)
C(311)	2390(30)	7660(20)	2310(40)	303(19)
C(313)	11910(20)	5911(14)	7410(20)	164(12)
C(314)	8695(18)	7239(14)	1910(20)	121(9)

C(315)	4316(17)	6143(13)	5800(20)	133(10)
C(316)	5529(17)	5070(14)	7060(20)	104(8)
C(317)	12319(19)	5645(14)	5110(20)	157(11)
C(318)	11650(30)	6355(12)	7320(30)	250(30)
C(319)	10240(20)	5760(20)	6910(40)	310(30)
C(4S)	2200(30)	7030(20)	1540(30)	298(18)
C(8S)	3460(30)	7620(20)	1780(40)	340(30)
C(10S)	2810(30)	7850(20)	2920(40)	320(30)
C(12S)	5280(20)	5310(20)	8690(30)	250(16)
C(14S)	5920(20)	4510(10)	8790(30)	269(16)
C(18S)	3430(20)	7270(20)	2210(30)	288(18)
C(19S)	2370(30)	7260(30)	4370(30)	450(40)
C(20S)	6620(30)	7000(20)	-850(30)	270(20)
C(29S)	6390(30)	5030(20)	9730(30)	264(16)
C(34S)	5950(30)	4880(30)	10060(30)	330(30)
C(35S)	4840(20)	5110(20)	8990(30)	310(30)
C(36S)	6430(40)	4205(15)	9010(50)	400(40)
C(37S)	6540(30)	7450(20)	-800(30)	243(15)
C(38S)	6278(18)	7360(20)	260(20)	224(14)
C(39S)	5639(16)	7510(20)	-50(30)	290(30)
C(40S)	1880(20)	7205(17)	3720(30)	380(20)
C(41S)	760(20)	6990(30)	2610(30)	370(30)
C(43S)	2410(40)	6610(20)	1410(40)	350(30)
C(44S)	7570(40)	4340(14)	9050(50)	470(40)
C(45S)	7560(30)	5614(15)	9470(30)	340(20)
C(46S)	8050(30)	5390(30)	8750(30)	360(20)
C(47S)	7780(30)	4767(14)	9270(30)	370(20)
C(48S)	8650(20)	5520(30)	9230(30)	390(30)
C(49S)	7810(40)	5940(30)	9140(40)	410(40)
C(50S)	8590(30)	6631(15)	-130(30)	199(18)
S(500)	10652(8)	7317(6)	5641(10)	232(8)
O(501)	10572(18)	7669(9)	5930(18)	286(18)
O(502)	11123(15)	7081(12)	6002(19)	318(19)
O(503)	10155(12)	7112(10)	5271(16)	225(14)
C(500)	10932(15)	7505(11)	4981(18)	288(14)
F(501)	11410(19)	7735(16)	5310(20)	440(30)
F(502)	11071(19)	7143(13)	4770(20)	368(19)
F(503)	10440(20)	7703(13)	4582(18)	380(20)
S(501)	6390(20)	6855(10)	7370(20)	590(30)
O(504)	6740(30)	6817(15)	6990(30)	600(40)
O(505)	6220(30)	6505(12)	7600(30)	640(40)
O(506)	6490(30)	7187(14)	7760(30)	580(40)
C(501)	5640(30)	7003(16)	6760(30)	650(30)

F(504)	5490(30)	6650(20)	6430(40)	720(40)
F(505)	5330(30)	7090(20)	7180(40)	730(40)
F(506)	5810(30)	7320(17)	6470(30)	630(40)
S(502)	9350(30)	5084(15)	7750(30)	750(40)
O(507)	8970(40)	5320(20)	7950(40)	700(40)
O(508)	9500(40)	4713(16)	8030(40)	720(40)
O(509)	9310(40)	5110(20)	7110(30)	710(50)
C(502)	10080(30)	5370(20)	8130(40)	770(40)
F(507)	10210(40)	5250(30)	8760(30)	790(50)
F(508)	10420(40)	5210(30)	7790(50)	770(50)
F(509)	9870(50)	5755(17)	7970(50)	820(50)
S(503)	4020(40)	7247(17)	-230(40)	1090(60)
O(510)	3960(60)	7000(20)	250(60)	1060(70)
O(511)	4530(50)	7210(30)	-380(70)	1100(70)
O(512)	3500(50)	7330(30)	-720(60)	1080(70)
C(503)	4160(40)	7752(18)	200(50)	1090(70)
F(510)	4750(50)	7710(20)	580(70)	1050(70)
F(511)	3740(60)	7750(20)	500(70)	1060(70)
F(512)	4060(60)	8010(20)	-310(50)	1140(70)

Table 8. Bond lengths [Å] and angles [º] for **BT4**.

Pt(1)-O(1)	2.01(2)
Pt(1)-N(5)	2.16(2)
Pt(1)-P(1)	2.207(12)
Pt(1)-P(2)	2.264(9)
Pt(2)-N(6)	2.088(15)
Pt(2)-O(3)	2.11(3)
Pt(2)-P(4)	2.194(15)
Pt(2)-P(3)	2.302(12)
Pt(3)-N(7)	2.10(3)
Pt(3)-O(5)	2.15(3)
Pt(3)-P(6)	2.236(14)
Pt(3)-P(5)	2.266(16)
Pt(4)-O(305)	2.00(3)
Pt(4)-N(8)	2.100(17)
Pt(4)-P(8)	2.17(2)
Pt(4)-P(7)	2.256(14)
Zn(1)-N(1)	2.072(16)
Zn(1)-N(2)	2.077(13)
Zn(1)-N(4)	2.080(13)
Zn(1)-O(9W)	2.11(2)

Zn(1)-N(3)	2.113(15)
P(4)-C(37S)	1.68(5)
P(4)-C(38S)	1.76(5)
P(4)-C(303)	1.97(6)
P(4)-C(20S)	2.29(7)
P(5)-C(4S)	1.67(7)
P(5)-C(18S)	1.90(5)
P(5)-C(311)	1.92(7)
P(6)-C(308)	1.67(6)
P(6)-C(306)	1.82(2)
P(6)-C(40S)	1.83(2)
P(7)-C(29S)	1.72(5)
P(7)-C(14S)	1.82(2)
P(7)-C(12S)	1.97(6)
P(8)-C(46S)	1.72(6)
P(8)-C(47S)	1.81(2)
P(8)-C(45S)	1.82(2)
O(1)-C(41)	1.29(4)
O(2)-C(41)	1.29(4)
O(3)-C(314)	1.44(5)
O(4)-C(314)	1.19(4)
O(5)-C(57)	1.37(6)
O(6)-C(57)	1.21(6)
O(8)-C(316)	1.30(4)
N(5)-C(24)	1.31(3)
N(5)-C(23)	1.32(3)
C(29)-C(26)	1.39
C(29)-C(30)	1.39
C(29)-H(29)	0.95
C(26)-C(27)	1.39
C(26)-C(10)	1.50(3)
C(27)-C(28)	1.39
C(27)-H(27)	0.95
C(28)-N(6)	1.39
C(28)-H(28)	0.95
N(6)-C(30)	1.39
C(30)-H(500)	0.95
P(1)-C(65)	1.77(4)
P(1)-C(67)	1.840(19)
P(1)-C(313)	1.85(4)
N(8)-C(36)	1.39
N(8)-C(40)	1.39
C(36)-C(37)	1.39

C(36)-H(36)	0.95
C(37)-C(38)	1.39
C(37)-H(37)	0.95
C(38)-C(39)	1.39
C(38)-C(200)	1.45(3)
C(39)-C(40)	1.39
C(39)-H(39)	0.95
C(40)-H(40)	0.95
C(34)-C(35)	1.24(4)
C(34)-C(31)	1.49(5)
C(34)-H(34)	0.95
C(31)-C(32)	1.25(4)
C(31)-C(14)	1.46(4)
C(32)-C(33)	1.39(4)
C(32)-H(32)	0.95
C(33)-N(7)	1.38(5)
C(33)-H(33)	0.95
N(7)-C(35)	1.36(5)
C(35)-H(35)	0.95
P(2)-C(71)	1.74(4)
P(2)-C(317)	1.75(5)
P(2)-C(75)	1.99(5)
N(1)-C(1)	1.42
N(1)-C(4')	1.42
C(1)-C(200)	1.34(3)
C(1)-C(2)	1.42
C(2)-C(4)	1.42
C(2)-H(2)	0.95
C(4)-C(4')	1.42
C(4)-H(4)	0.95
C(4')-C(5)	1.38(3)
P(3)-C(301)	1.61(4)
P(3)-C(77)	1.80(5)
P(3)-C(79)	1.81(4)
C(13)-C(14)	1.28(3)
C(13)-C(3)	1.42
C(13)-N(3)	1.42
C(3)-C(11)	1.42
C(3)-H(3)	0.95
C(11)-C(3')	1.42
C(11)-H(11)	0.95
C(3')-C(10)	1.38(3)
C(3')-N(3)	1.42

C(5)-C(6)	1.41(3)
C(5)-C(21)	1.43(4)
N(2)-C(9)	1.42
N(2)-C(6)	1.42
C(6)-C(7)	1.42
C(7)-C(8)	1.42
C(7)-H(7)	0.95
C(8)-C(9)	1.42
C(8)-H(8)	0.95
C(9)-C(10)	1.38(3)
C(14)-C(16)	1.42(3)
N(4)-C(19)	1.42
N(4)-C(16)	1.42
C(16)-C(17)	1.42
C(17)-C(18)	1.42
C(17)-H(17)	0.95
C(18)-C(19)	1.42
C(18)-H(18)	0.95
C(19)-C(200)	1.42(3)
C(21)-C(25)	1.36(4)
C(21)-C(22)	1.39(4)
C(22)-C(23)	1.36(3)
C(22)-H(22)	0.95
C(23)-H(23)	0.95
C(24)-C(25)	1.39(3)
C(24)-H(24)	0.95
C(25)-H(25)	0.95
C(41)-C(42)	1.43(4)
C(42)-C(47)	1.39(5)
C(42)-C(43)	1.45(4)
C(43)-C(45)	1.41(3)
C(43)-H(43)	0.95
C(44)-C(45)	1.39
C(44)-C(52)	1.39
C(44)-C(46)	1.42(3)
C(45)-C(48)	1.39
C(48)-C(49)	1.39
C(48)-H(48)	0.95
C(49)-C(51)	1.39
C(49)-H(49)	0.95
C(51)-C(52)	1.39
C(51)-C(314)	1.46(4)
C(52)-H(52)	0.95

C(46)-C(47)	1.46(4)
C(46)-H(46)	0.95
C(47)-H(47)	0.95
C(55)-C(59)	1.36(6)
C(55)-C(60)	1.43(4)
C(55)-H(55)	0.95
C(57)-C(59)	1.63(7)
C(58)-C(59)	1.38(6)
C(58)-C(315)	1.46(5)
C(58)-H(58)	0.95
C(60)-C(61)	1.39
C(60)-C(56')	1.39
C(61)-C(62)	1.39
C(61)-H(61)	0.95
C(62)-C(63)	1.39
C(62)-H(62)	0.95
C(63)-C(56)	1.39
C(63)-C(316)	1.47(5)
C(56)-C(56')	1.39
C(56)-H(56)	0.95
C(56')-C(315)	1.44(4)
C(65)-C(66)	1.36(5)
C(65)-H(65A)	0.99
C(65)-H(65B)	0.99
C(66)-H(66A)	0.98
C(66)-H(66B)	0.98
C(66)-H(66C)	0.98
C(67)-C(319)	1.54(2)
C(67)-H(67A)	0.99
C(67)-H(67B)	0.99
C(71)-C(72)	1.54(4)
C(71)-H(71A)	0.99
C(71)-H(71B)	0.99
C(72)-H(72A)	0.98
C(72)-H(72B)	0.98
C(72)-H(72C)	0.98
C(73)-C(317)	1.44(5)
C(73)-H(73A)	0.98
C(73)-H(73B)	0.98
C(73)-H(73C)	0.98
C(75)-C(76)	1.26(6)
C(75)-H(75A)	0.99
C(75)-H(75B)	0.99

C(76)-H(76A)	0.9818
C(76)-H(76B)	0.9818
C(76)-H(76C)	0.9818
C(77)-C(78)	1.47(5)
C(77)-H(77A)	0.99
C(77)-H(77B)	0.99
C(78)-H(78A)	0.98
C(78)-H(78B)	0.98
C(78)-H(78C)	0.98
C(79)-C(50S)	1.44(6)
C(79)-H(79A)	0.99
C(79)-H(79B)	0.99
C(304)-C(303)	1.44(7)
C(304)-H(501)	0.98
C(304)-H(502)	0.98
C(304)-H(30C)	0.98
C(303)-H(503)	0.99
C(303)-H(504)	0.99
C(307)-C(306)	1.55(2)
C(307)-H(30D)	1.1182
C(307)-H(30E)	1.1157
C(307)-H(30F)	1.1154
C(306)-H(30G)	0.99
C(306)-H(30H)	0.99
O(305)-C(316)	1.30(4)
C(302)-C(301)	1.60(5)
C(302)-H(505)	0.9802
C(302)-H(506)	0.9802
C(302)-H(30I)	0.9802
C(301)-H(30J)	0.99
C(301)-H(30K)	0.99
C(308)-C(41S)	1.55(2)
C(308)-H(30L)	0.99
C(308)-H(30M)	0.99
C(311)-C(10S)	1.55(2)
C(311)-H(31A)	0.99
C(311)-H(31B)	0.99
C(313)-C(318)	1.61(6)
C(313)-H(317)	0.99
C(313)-H(318)	0.99
C(315)-H(400)	0.95
C(317)-H(315)	0.99
C(317)-H(316)	0.99

C(318)-H(310)	0.98
C(318)-H(311)	0.98
C(318)-H(312)	0.98
C(319)-H(313)	0.98
C(319)-H(31E)	0.98
C(319)-H(31F)	0.98
C(4S)-C(43S)	1.54(2)
C(4S)-H(4S1)	0.99
C(4S)-H(4S2)	0.99
C(8S)-C(18S)	1.55(2)
C(8S)-H(8S1)	1.0258
C(8S)-H(8S2)	1.026
C(8S)-H(8S3)	1.0253
C(10S)-H(10A)	0.9944
C(10S)-H(10B)	0.9947
C(10S)-H(10C)	0.9948
C(12S)-C(35S)	1.55(2)
C(12S)-H(12A)	0.99
C(12S)-H(12B)	0.99
C(14S)-C(36S)	1.55(2)
C(14S)-H(14A)	0.99
C(14S)-H(14B)	0.99
C(18S)-H(18A)	0.99
C(18S)-H(18B)	0.99
C(19S)-C(40S)	1.55(2)
C(19S)-H(19A)	0.9813
C(19S)-H(19B)	0.9813
C(19S)-H(19C)	0.9813
C(20S)-C(37S)	1.54(2)
C(20S)-H(20A)	0.98
C(20S)-H(20B)	0.98
C(20S)-H(20C)	0.98
C(29S)-C(34S)	1.54(2)
C(29S)-H(29A)	0.99
C(29S)-H(29B)	0.99
C(34S)-H(34A)	1.0196
C(34S)-H(34B)	1.0208
C(34S)-H(34C)	1.0179
C(35S)-H(35A)	0.9807
C(35S)-H(35B)	0.9806
C(35S)-H(35C)	0.9806
C(36S)-H(36A)	0.9989
C(36S)-H(36B)	0.9994

C(36S)-H(36C)	0.9989
C(37S)-H(37A)	0.99
C(37S)-H(37B)	0.99
C(38S)-C(39S)	1.55(2)
C(38S)-H(38A)	0.99
C(38S)-H(38B)	0.99
C(39S)-H(39A)	0.98
C(39S)-H(39B)	0.98
C(39S)-H(39C)	0.98
C(40S)-H(40A)	0.99
C(40S)-H(40B)	0.99
C(41S)-H(41A)	0.9992
C(41S)-H(41B)	0.9988
C(41S)-H(41C)	0.999
C(43S)-H(43A)	1.0837
C(43S)-H(43B)	1.0856
C(43S)-H(43C)	1.0826
C(44S)-C(47S)	1.55(2)
C(44S)-H(44A)	0.9814
C(44S)-H(44B)	0.9814
C(44S)-H(44C)	0.9815
C(45S)-C(49S)	1.54(2)
C(45S)-H(45A)	0.99
C(45S)-H(45B)	0.99
C(46S)-C(48S)	1.54(2)
C(46S)-H(46A)	0.99
C(46S)-H(46B)	0.99
C(47S)-H(47A)	0.99
C(47S)-H(47B)	0.99
C(48S)-H(48A)	0.98
C(48S)-H(48B)	0.98
C(48S)-H(48C)	0.98
C(49S)-H(49A)	1.0063
C(49S)-H(49B)	1.0073
C(49S)-H(49C)	1.0067
C(50S)-H(50A)	0.98
C(50S)-H(50B)	0.98
C(50S)-H(50C)	0.98
S(500)-O(503)	1.387(19)
S(500)-O(501)	1.392(19)
S(500)-O(502)	1.396(19)
S(500)-C(500)	1.92(5)
C(500)-F(501)	1.375(19)

C(500)-F(502)	1.39(2)
C(500)-F(503)	1.40(2)
S(501)-O(504)	1.391(19)
S(501)-O(506)	1.393(19)
S(501)-O(505)	1.40(2)
S(501)-C(501)	1.93(5)
C(501)-F(506)	1.38(2)
C(501)-F(504)	1.39(2)
C(501)-F(505)	1.39(2)
S(502)-O(508)	1.39(2)
S(502)-O(507)	1.39(2)
S(502)-O(509)	1.40(2)
S(502)-C(502)	1.93(5)
C(502)-F(507)	1.39(2)
C(502)-F(508)	1.39(2)
C(502)-F(509)	1.40(2)
S(503)-O(510)	1.39(2)
S(503)-O(512)	1.39(2)
S(503)-O(511)	1.39(2)
S(503)-C(503)	1.92(5)
C(503)-F(510)	1.39(2)
C(503)-F(511)	1.39(2)
C(503)-F(512)	1.39(2)

O(1)-Pt(1)-N(5)	82.2(9)
O(1)-Pt(1)-P(1)	173.5(6)
N(5)-Pt(1)-P(1)	91.9(7)
O(1)-Pt(1)-P(2)	88.2(6)
N(5)-Pt(1)-P(2)	170.1(7)
P(1)-Pt(1)-P(2)	97.6(4)
N(6)-Pt(2)-O(3)	81.6(8)
N(6)-Pt(2)-P(4)	93.2(7)
O(3)-Pt(2)-P(4)	174.8(7)
N(6)-Pt(2)-P(3)	167.2(7)
O(3)-Pt(2)-P(3)	85.6(7)
P(4)-Pt(2)-P(3)	99.6(5)
N(7)-Pt(3)-O(5)	80.3(11)
N(7)-Pt(3)-P(6)	170.6(11)
O(5)-Pt(3)-P(6)	90.6(8)
N(7)-Pt(3)-P(5)	92.9(10)
O(5)-Pt(3)-P(5)	167.0(12)
P(6)-Pt(3)-P(5)	95.6(6)
O(305)-Pt(4)-N(8)	81.2(8)

O(305)-Pt(4)-P(8)	172.1(9)
N(8)-Pt(4)-P(8)	93.0(7)
O(305)-Pt(4)-P(7)	86.7(7)
N(8)-Pt(4)-P(7)	167.8(8)
P(8)-Pt(4)-P(7)	99.2(6)
N(1)-Zn(1)-N(2)	89.7(8)
N(1)-Zn(1)-N(4)	89.1(8)
N(2)-Zn(1)-N(4)	161.6(8)
N(1)-Zn(1)-O(9W)	105.5(9)
N(2)-Zn(1)-O(9W)	95.4(9)
N(4)-Zn(1)-O(9W)	102.6(9)
N(1)-Zn(1)-N(3)	162.3(8)
N(2)-Zn(1)-N(3)	90.5(7)
N(4)-Zn(1)-N(3)	85.3(7)
O(9W)-Zn(1)-N(3)	92.1(9)
C(37S)-P(4)-C(38S)	102(3)
C(37S)-P(4)-C(303)	83(3)
C(38S)-P(4)-C(303)	97(3)
C(37S)-P(4)-Pt(2)	137(2)
C(38S)-P(4)-Pt(2)	113.8(15)
C(303)-P(4)-Pt(2)	113.7(19)
C(37S)-P(4)-C(20S)	42.3(16)
C(38S)-P(4)-C(20S)	100(3)
C(303)-P(4)-C(20S)	125(2)
Pt(2)-P(4)-C(20S)	106.1(19)
C(4S)-P(5)-C(18S)	111(3)
C(4S)-P(5)-C(311)	96(3)
C(18S)-P(5)-C(311)	98(3)
C(4S)-P(5)-Pt(3)	125(3)
C(18S)-P(5)-Pt(3)	108.2(16)
C(311)-P(5)-Pt(3)	116(2)
C(308)-P(6)-C(306)	111(3)
C(308)-P(6)-C(40S)	105(4)
C(306)-P(6)-C(40S)	86(4)
C(308)-P(6)-Pt(3)	119.2(18)
C(306)-P(6)-Pt(3)	118(2)
C(40S)-P(6)-Pt(3)	112(2)
C(29S)-P(7)-C(14S)	99(3)
C(29S)-P(7)-C(12S)	111(3)
C(14S)-P(7)-C(12S)	108(3)
C(29S)-P(7)-Pt(4)	124.3(19)
C(14S)-P(7)-Pt(4)	103(2)
C(12S)-P(7)-Pt(4)	110.2(16)

C(46S)-P(8)-C(47S)	93(5)
C(46S)-P(8)-C(45S)	86(4)
C(47S)-P(8)-C(45S)	109(3)
C(46S)-P(8)-Pt(4)	129(2)
C(47S)-P(8)-Pt(4)	121(2)
C(45S)-P(8)-Pt(4)	113(3)
C(41)-O(1)-Pt(1)	125(2)
C(314)-O(3)-Pt(2)	115(2)
C(57)-O(5)-Pt(3)	111(3)
C(24)-N(5)-C(23)	123(2)
C(24)-N(5)-Pt(1)	112.4(16)
C(23)-N(5)-Pt(1)	121.6(16)
C(26)-C(29)-C(30)	120
C(26)-C(29)-H(29)	120
C(30)-C(29)-H(29)	120
C(27)-C(26)-C(29)	120
C(27)-C(26)-C(10)	120(2)
C(29)-C(26)-C(10)	120(2)
C(26)-C(27)-C(28)	120
C(26)-C(27)-H(27)	120
C(28)-C(27)-H(27)	120
N(6)-C(28)-C(27)	120
N(6)-C(28)-H(28)	120
C(27)-C(28)-H(28)	120
C(30)-N(6)-C(28)	120
C(30)-N(6)-Pt(2)	116.7(13)
C(28)-N(6)-Pt(2)	120.9(14)
N(6)-C(30)-C(29)	120
N(6)-C(30)-H(500)	120
C(29)-C(30)-H(500)	120
C(65)-P(1)-C(67)	104(2)
C(65)-P(1)-C(313)	106(2)
C(67)-P(1)-C(313)	100(2)
C(65)-P(1)-Pt(1)	116.0(15)
C(67)-P(1)-Pt(1)	114.3(15)
C(313)-P(1)-Pt(1)	115.2(17)
C(36)-N(8)-C(40)	120
C(36)-N(8)-Pt(4)	123.2(15)
C(40)-N(8)-Pt(4)	115.9(15)
N(8)-C(36)-C(37)	120
N(8)-C(36)-H(36)	120
C(37)-C(36)-H(36)	120
C(36)-C(37)-C(38)	120

C(36)-C(37)-H(37)	120
C(38)-C(37)-H(37)	120
C(39)-C(38)-C(37)	120
C(39)-C(38)-C(200)	119(2)
C(37)-C(38)-C(200)	121(2)
C(38)-C(39)-C(40)	120
C(38)-C(39)-H(39)	120
C(40)-C(39)-H(39)	120
C(39)-C(40)-N(8)	120
C(39)-C(40)-H(40)	120
N(8)-C(40)-H(40)	120
C(35)-C(34)-C(31)	124(4)
C(35)-C(34)-H(34)	118.2
C(31)-C(34)-H(34)	118.2
C(32)-C(31)-C(14)	126(4)
C(32)-C(31)-C(34)	114(3)
C(14)-C(31)-C(34)	120(3)
C(31)-C(32)-C(33)	125(4)
C(31)-C(32)-H(32)	117.7
C(33)-C(32)-H(32)	117.6
N(7)-C(33)-C(32)	118(4)
N(7)-C(33)-H(33)	120.9
C(32)-C(33)-H(33)	120.9
C(35)-N(7)-C(33)	118(3)
C(35)-N(7)-Pt(3)	122(3)
C(33)-N(7)-Pt(3)	118(3)
C(34)-C(35)-N(7)	121(4)
C(34)-C(35)-H(35)	119.5
N(7)-C(35)-H(35)	119.5
C(71)-P(2)-C(317)	111(2)
C(71)-P(2)-C(75)	102(3)
C(317)-P(2)-C(75)	106(3)
C(71)-P(2)-Pt(1)	119.9(13)
C(317)-P(2)-Pt(1)	110.7(15)
C(75)-P(2)-Pt(1)	106.4(14)
C(1)-N(1)-C(4')	108
C(1)-N(1)-Zn(1)	128.7(11)
C(4')-N(1)-Zn(1)	123.3(11)
C(200)-C(1)-C(2)	129(2)
C(200)-C(1)-N(1)	123(2)
C(2)-C(1)-N(1)	108
C(1)-C(2)-C(4)	108
C(1)-C(2)-H(2)	126

C(4)-C(2)-H(2)	126
C(4')-C(4)-C(2)	108
C(4')-C(4)-H(4)	126
C(2)-C(4)-H(4)	126
C(5)-C(4')-C(4)	121.7(19)
C(5)-C(4')-N(1)	130.2(19)
C(4)-C(4')-N(1)	108
C(301)-P(3)-C(77)	100(2)
C(301)-P(3)-C(79)	110(2)
C(77)-P(3)-C(79)	98(3)
C(301)-P(3)-Pt(2)	129.0(18)
C(77)-P(3)-Pt(2)	108.0(15)
C(79)-P(3)-Pt(2)	107.6(13)
C(14)-C(13)-C(3)	129.4(19)
C(14)-C(13)-N(3)	122.5(19)
C(3)-C(13)-N(3)	108
C(13)-C(3)-C(11)	108
C(13)-C(3)-H(3)	126
C(11)-C(3)-H(3)	126
C(3)-C(11)-C(3')	108
C(3)-C(11)-H(11)	126
C(3')-C(11)-H(11)	126
C(10)-C(3')-N(3)	127.4(19)
C(10)-C(3')-C(11)	124.5(19)
N(3)-C(3')-C(11)	108
C(3')-N(3)-C(13)	108
C(3')-N(3)-Zn(1)	122.2(10)
C(13)-N(3)-Zn(1)	128.7(10)
C(4')-C(5)-C(6)	124(2)
C(4')-C(5)-C(21)	122(3)
C(6)-C(5)-C(21)	114(2)
C(9)-N(2)-C(6)	108
C(9)-N(2)-Zn(1)	124.6(11)
C(6)-N(2)-Zn(1)	126.4(11)
C(5)-C(6)-C(7)	127.0(17)
C(5)-C(6)-N(2)	124.9(17)
C(7)-C(6)-N(2)	108
C(6)-C(7)-C(8)	108
C(6)-C(7)-H(7)	126
C(8)-C(7)-H(7)	126
C(7)-C(8)-C(9)	108
C(7)-C(8)-H(8)	126
C(9)-C(8)-H(8)	126

C(10)-C(9)-N(2)	125.3(18)
C(10)-C(9)-C(8)	126.7(18)
N(2)-C(9)-C(8)	108
C(3')-C(10)-C(9)	128(3)
C(3')-C(10)-C(26)	116(2)
C(9)-C(10)-C(26)	116(2)
C(13)-C(14)-C(16)	131(2)
C(13)-C(14)-C(31)	118(3)
C(16)-C(14)-C(31)	111(2)
C(19)-N(4)-C(16)	108
C(19)-N(4)-Zn(1)	123.4(11)
C(16)-N(4)-Zn(1)	127.9(11)
C(17)-C(16)-N(4)	108
C(17)-C(16)-C(14)	129.9(16)
N(4)-C(16)-C(14)	122.1(16)
C(18)-C(17)-C(16)	108
C(18)-C(17)-H(17)	126
C(16)-C(17)-H(17)	126
C(19)-C(18)-C(17)	108
C(19)-C(18)-H(18)	126
C(17)-C(18)-H(18)	126
N(4)-C(19)-C(18)	108
N(4)-C(19)-C(200)	126.6(18)
C(18)-C(19)-C(200)	125.3(18)
C(25)-C(21)-C(22)	116(3)
C(25)-C(21)-C(5)	122(3)
C(22)-C(21)-C(5)	122(3)
C(23)-C(22)-C(21)	123(3)
C(23)-C(22)-H(22)	118.5
C(21)-C(22)-H(22)	118.5
N(5)-C(23)-C(22)	118(2)
N(5)-C(23)-H(23)	121.2
C(22)-C(23)-H(23)	121.2
N(5)-C(24)-C(25)	120(2)
N(5)-C(24)-H(24)	120.1
C(25)-C(24)-H(24)	120.1
C(21)-C(25)-C(24)	120(3)
C(21)-C(25)-H(25)	120
C(24)-C(25)-H(25)	119.9
O(1)-C(41)-O(2)	117(3)
O(1)-C(41)-C(42)	122(4)
O(2)-C(41)-C(42)	121(4)
C(47)-C(42)-C(41)	120(4)

C(47)-C(42)-C(43)	120(3)
C(41)-C(42)-C(43)	119(4)
C(45)-C(43)-C(42)	120(3)
C(45)-C(43)-H(43)	120.1
C(42)-C(43)-H(43)	120.1
C(45)-C(44)-C(52)	120
C(45)-C(44)-C(46)	121(2)
C(52)-C(44)-C(46)	118(2)
C(48)-C(45)-C(44)	120
C(48)-C(45)-C(43)	120(2)
C(44)-C(45)-C(43)	120(2)
C(49)-C(48)-C(45)	120
C(49)-C(48)-H(48)	120
C(45)-C(48)-H(48)	120
C(48)-C(49)-C(51)	120
C(48)-C(49)-H(49)	120
C(51)-C(49)-H(49)	120
C(49)-C(51)-C(52)	120
C(49)-C(51)-C(314)	112(3)
C(52)-C(51)-C(314)	128(3)
C(51)-C(52)-C(44)	120
C(51)-C(52)-H(52)	120
C(44)-C(52)-H(52)	120
C(44)-C(46)-C(47)	118(3)
C(44)-C(46)-H(46)	120.9
C(47)-C(46)-H(46)	120.8
C(42)-C(47)-C(46)	120(4)
C(42)-C(47)-H(47)	120.1
C(46)-C(47)-H(47)	120.2
C(59)-C(55)-C(60)	119(5)
C(59)-C(55)-H(55)	120.4
C(60)-C(55)-H(55)	120.4
O(6)-C(57)-O(5)	136(6)
O(6)-C(57)-C(59)	121(6)
O(5)-C(57)-C(59)	101(5)
C(59)-C(58)-C(315)	122(5)
C(59)-C(58)-H(58)	119
C(315)-C(58)-H(58)	119
C(55)-C(59)-C(58)	123(5)
C(55)-C(59)-C(57)	111(5)
C(58)-C(59)-C(57)	127(5)
C(61)-C(60)-C(56')	120
C(61)-C(60)-C(55)	122(3)

C(56')-C(60)-C(55)	118(3)
C(60)-C(61)-C(62)	120
C(60)-C(61)-H(61)	120
C(62)-C(61)-H(61)	120
C(61)-C(62)-C(63)	120
C(61)-C(62)-H(62)	120
C(63)-C(62)-H(62)	120
C(56)-C(63)-C(62)	120
C(56)-C(63)-C(316)	123(3)
C(62)-C(63)-C(316)	117(3)
C(63)-C(56)-C(56')	120
C(63)-C(56)-H(56)	120
C(56')-C(56)-H(56)	120
C(56)-C(56')-C(60)	120
C(56)-C(56')-C(315)	115(3)
C(60)-C(56')-C(315)	125(3)
C(66)-C(65)-P(1)	116(3)
C(66)-C(65)-H(65A)	108.2
P(1)-C(65)-H(65A)	108.2
C(66)-C(65)-H(65B)	108.1
P(1)-C(65)-H(65B)	108.1
H(65A)-C(65)-H(65B)	107.3
C(65)-C(66)-H(66A)	109.5
C(65)-C(66)-H(66B)	109.5
H(66A)-C(66)-H(66B)	109.5
C(65)-C(66)-H(66C)	109.4
H(66A)-C(66)-H(66C)	109.5
H(66B)-C(66)-H(66C)	109.5
C(319)-C(67)-P(1)	137(4)
C(319)-C(67)-H(67A)	103.1
P(1)-C(67)-H(67A)	102.9
C(319)-C(67)-H(67B)	103
P(1)-C(67)-H(67B)	103
H(67A)-C(67)-H(67B)	105.1
C(72)-C(71)-P(2)	120(3)
C(72)-C(71)-H(71A)	107.2
P(2)-C(71)-H(71A)	107.3
C(72)-C(71)-H(71B)	107.3
P(2)-C(71)-H(71B)	107.2
H(71A)-C(71)-H(71B)	106.9
C(71)-C(72)-H(72A)	109.4
C(71)-C(72)-H(72B)	109.6
H(72A)-C(72)-H(72B)	109.5

C(71)-C(72)-H(72C)	109.4
H(72A)-C(72)-H(72C)	109.5
H(72B)-C(72)-H(72C)	109.5
C(317)-C(73)-H(73A)	109.5
C(317)-C(73)-H(73B)	109.4
H(73A)-C(73)-H(73B)	109.5
C(317)-C(73)-H(73C)	109.4
H(73A)-C(73)-H(73C)	109.5
H(73B)-C(73)-H(73C)	109.5
C(76)-C(75)-P(2)	122(5)
C(76)-C(75)-H(75A)	106.6
P(2)-C(75)-H(75A)	106.8
C(76)-C(75)-H(75B)	106.8
P(2)-C(75)-H(75B)	106.7
H(75A)-C(75)-H(75B)	106.6
C(75)-C(76)-H(76A)	109.7
C(75)-C(76)-H(76B)	109.6
H(76A)-C(76)-H(76B)	109.2
C(75)-C(76)-H(76C)	109.8
H(76A)-C(76)-H(76C)	109.2
H(76B)-C(76)-H(76C)	109.3
C(78)-C(77)-P(3)	118(4)
C(78)-C(77)-H(77A)	107.7
P(3)-C(77)-H(77A)	107.9
C(78)-C(77)-H(77B)	107.9
P(3)-C(77)-H(77B)	107.9
H(77A)-C(77)-H(77B)	107.2
C(77)-C(78)-H(78A)	109.4
C(77)-C(78)-H(78B)	109.5
H(78A)-C(78)-H(78B)	109.5
C(77)-C(78)-H(78C)	109.5
H(78A)-C(78)-H(78C)	109.5
H(78B)-C(78)-H(78C)	109.5
C(50S)-C(79)-P(3)	114(4)
C(50S)-C(79)-H(79A)	108.7
P(3)-C(79)-H(79A)	108.7
C(50S)-C(79)-H(79B)	108.8
P(3)-C(79)-H(79B)	108.8
H(79A)-C(79)-H(79B)	107.6
C(1)-C(200)-C(19)	128(3)
C(1)-C(200)-C(38)	114(3)
C(19)-C(200)-C(38)	118(2)
C(303)-C(304)-H(501)	109.5

C(303)-C(304)-H(502)	109.5
H(501)-C(304)-H(502)	109.5
C(303)-C(304)-H(30C)	109.4
H(501)-C(304)-H(30C)	109.5
H(502)-C(304)-H(30C)	109.5
C(304)-C(303)-P(4)	106(3)
C(304)-C(303)-H(503)	110.6
P(4)-C(303)-H(503)	110.6
C(304)-C(303)-H(504)	110.5
P(4)-C(303)-H(504)	110.6
H(503)-C(303)-H(504)	108.7
C(306)-C(307)-H(30D)	123
C(306)-C(307)-H(30E)	122.6
H(30D)-C(307)-H(30E)	93.4
C(306)-C(307)-H(30F)	122.6
H(30D)-C(307)-H(30F)	93.5
H(30E)-C(307)-H(30F)	93.6
C(307)-C(306)-P(6)	101(5)
C(307)-C(306)-H(30G)	111.7
P(6)-C(306)-H(30G)	111.5
C(307)-C(306)-H(30H)	111.5
P(6)-C(306)-H(30H)	111.6
H(30G)-C(306)-H(30H)	109.4
C(316)-O(305)-Pt(4)	125(3)
C(301)-C(302)-H(505)	109.4
C(301)-C(302)-H(506)	109.4
H(505)-C(302)-H(506)	109.5
C(301)-C(302)-H(30I)	109.7
H(505)-C(302)-H(30I)	109.5
H(506)-C(302)-H(30I)	109.5
C(302)-C(301)-P(3)	126(4)
C(302)-C(301)-H(30J)	105.7
P(3)-C(301)-H(30J)	105.9
C(302)-C(301)-H(30K)	106
P(3)-C(301)-H(30K)	106
H(30J)-C(301)-H(30K)	106.2
C(41S)-C(308)-P(6)	113(4)
C(41S)-C(308)-H(30L)	109
P(6)-C(308)-H(30L)	108.8
C(41S)-C(308)-H(30M)	108.8
P(6)-C(308)-H(30M)	109
H(30L)-C(308)-H(30M)	107.7
C(10S)-C(311)-P(5)	108(4)

C(10S)-C(311)-H(31A)	110.2
P(5)-C(311)-H(31A)	110.2
C(10S)-C(311)-H(31B)	110
P(5)-C(311)-H(31B)	110.1
H(31A)-C(311)-H(31B)	108.5
C(318)-C(313)-P(1)	114(3)
C(318)-C(313)-H(317)	108.7
P(1)-C(313)-H(317)	108.7
C(318)-C(313)-H(318)	108.7
P(1)-C(313)-H(318)	108.8
H(317)-C(313)-H(318)	107.7
O(4)-C(314)-O(3)	121(4)
O(4)-C(314)-C(51)	131(5)
O(3)-C(314)-C(51)	107(4)
C(56')-C(315)-C(58)	113(4)
C(56')-C(315)-H(400)	123.6
C(58)-C(315)-H(400)	123.6
O(8)-C(316)-O(305)	112(4)
O(8)-C(316)-C(63)	123(4)
O(305)-C(316)-C(63)	125(4)
C(73)-C(317)-P(2)	106(4)
C(73)-C(317)-H(315)	110.5
P(2)-C(317)-H(315)	110.5
C(73)-C(317)-H(316)	110.5
P(2)-C(317)-H(316)	110.5
H(315)-C(317)-H(316)	108.7
C(313)-C(318)-H(310)	109.4
C(313)-C(318)-H(311)	109.6
H(310)-C(318)-H(311)	109.5
C(313)-C(318)-H(312)	109.4
H(310)-C(318)-H(312)	109.5
H(311)-C(318)-H(312)	109.5
C(67)-C(319)-H(313)	109.5
C(67)-C(319)-H(31E)	109.6
H(313)-C(319)-H(31E)	109.5
C(67)-C(319)-H(31F)	109.4
H(313)-C(319)-H(31F)	109.5
H(31E)-C(319)-H(31F)	109.5
C(43S)-C(4S)-P(5)	102(4)
C(43S)-C(4S)-H(4S1)	111.3
P(5)-C(4S)-H(4S1)	111.2
C(43S)-C(4S)-H(4S2)	111.5
P(5)-C(4S)-H(4S2)	111.4

H(4S1)-C(4S)-H(4S2)	109.2
C(18S)-C(8S)-H(8S1)	114.2
C(18S)-C(8S)-H(8S2)	113.7
H(8S1)-C(8S)-H(8S2)	104.7
C(18S)-C(8S)-H(8S3)	113.7
H(8S1)-C(8S)-H(8S3)	104.7
H(8S2)-C(8S)-H(8S3)	104.8
C(311)-C(10S)-H(10A)	110.7
C(311)-C(10S)-H(10B)	110.9
H(10A)-C(10S)-H(10B)	108.1
C(311)-C(10S)-H(10C)	111
H(10A)-C(10S)-H(10C)	108
H(10B)-C(10S)-H(10C)	108
C(35S)-C(12S)-P(7)	114(4)
C(35S)-C(12S)-H(12A)	108.3
P(7)-C(12S)-H(12A)	108.7
C(35S)-C(12S)-H(12B)	109.5
P(7)-C(12S)-H(12B)	108.7
H(12A)-C(12S)-H(12B)	107.7
C(36S)-C(14S)-P(7)	121(3)
C(36S)-C(14S)-H(14A)	107.2
P(7)-C(14S)-H(14A)	107
C(36S)-C(14S)-H(14B)	107
P(7)-C(14S)-H(14B)	107.1
H(14A)-C(14S)-H(14B)	106.8
C(8S)-C(18S)-P(5)	118(3)
C(8S)-C(18S)-H(18A)	107.6
P(5)-C(18S)-H(18A)	107.5
C(8S)-C(18S)-H(18B)	108
P(5)-C(18S)-H(18B)	108
H(18A)-C(18S)-H(18B)	107.1
C(40S)-C(19S)-H(19A)	109.6
C(40S)-C(19S)-H(19B)	109.6
H(19A)-C(19S)-H(19B)	109.3
C(40S)-C(19S)-H(19C)	109.6
H(19A)-C(19S)-H(19C)	109.4
H(19B)-C(19S)-H(19C)	109.3
C(37S)-C(20S)-P(4)	47(3)
C(37S)-C(20S)-H(20A)	109.5
P(4)-C(20S)-H(20A)	67.8
C(37S)-C(20S)-H(20B)	109.5
P(4)-C(20S)-H(20B)	145.3
H(20A)-C(20S)-H(20B)	109.5

C(37S)-C(20S)-H(20C)	109.4
P(4)-C(20S)-H(20C)	103.5
H(20A)-C(20S)-H(20C)	109.5
H(20B)-C(20S)-H(20C)	109.5
C(34S)-C(29S)-P(7)	111(4)
C(34S)-C(29S)-H(29A)	109.1
P(7)-C(29S)-H(29A)	109.6
C(34S)-C(29S)-H(29B)	109.5
P(7)-C(29S)-H(29B)	109.5
H(29A)-C(29S)-H(29B)	108.1
C(29S)-C(34S)-H(34A)	113.4
C(29S)-C(34S)-H(34B)	113.7
H(34A)-C(34S)-H(34B)	105.3
C(29S)-C(34S)-H(34C)	112.9
H(34A)-C(34S)-H(34C)	105.4
H(34B)-C(34S)-H(34C)	105.5
C(12S)-C(35S)-H(35A)	110.1
C(12S)-C(35S)-H(35B)	109.7
H(35A)-C(35S)-H(35B)	109.4
C(12S)-C(35S)-H(35C)	108.9
H(35A)-C(35S)-H(35C)	109.4
H(35B)-C(35S)-H(35C)	109.4
C(14S)-C(36S)-H(36A)	111.2
C(14S)-C(36S)-H(36B)	111.5
H(36A)-C(36S)-H(36B)	107.5
C(14S)-C(36S)-H(36C)	111.2
H(36A)-C(36S)-H(36C)	107.6
H(36B)-C(36S)-H(36C)	107.6
C(20S)-C(37S)-P(4)	90(4)
C(20S)-C(37S)-H(37A)	113.6
P(4)-C(37S)-H(37A)	113.6
C(20S)-C(37S)-H(37B)	113.5
P(4)-C(37S)-H(37B)	113.6
H(37A)-C(37S)-H(37B)	110.9
C(39S)-C(38S)-P(4)	126(4)
C(39S)-C(38S)-H(38A)	105.8
P(4)-C(38S)-H(38A)	105.9
C(39S)-C(38S)-H(38B)	105.8
P(4)-C(38S)-H(38B)	105.9
H(38A)-C(38S)-H(38B)	106.2
C(38S)-C(39S)-H(39A)	109.5
C(38S)-C(39S)-H(39B)	109.5
H(39A)-C(39S)-H(39B)	109.5

C(38S)-C(39S)-H(39C)	109.4
H(39A)-C(39S)-H(39C)	109.5
H(39B)-C(39S)-H(39C)	109.5
C(19S)-C(40S)-P(6)	122(3)
C(19S)-C(40S)-H(40A)	106.8
P(6)-C(40S)-H(40A)	106.8
C(19S)-C(40S)-H(40B)	106.9
P(6)-C(40S)-H(40B)	106.9
H(40A)-C(40S)-H(40B)	106.7
C(308)-C(41S)-H(41A)	111.4
C(308)-C(41S)-H(41B)	111.2
H(41A)-C(41S)-H(41B)	107.6
C(308)-C(41S)-H(41C)	111.3
H(41A)-C(41S)-H(41C)	107.5
H(41B)-C(41S)-H(41C)	107.6
C(4S)-C(43S)-H(43A)	119.6
C(4S)-C(43S)-H(43B)	119.8
H(43A)-C(43S)-H(43B)	97.6
C(4S)-C(43S)-H(43C)	119.4
H(43A)-C(43S)-H(43C)	97.8
H(43B)-C(43S)-H(43C)	97.6
C(47S)-C(44S)-H(44A)	109.5
C(47S)-C(44S)-H(44B)	109.6
H(44A)-C(44S)-H(44B)	109.3
C(47S)-C(44S)-H(44C)	109.7
H(44A)-C(44S)-H(44C)	109.3
H(44B)-C(44S)-H(44C)	109.3
C(49S)-C(45S)-P(8)	101(6)
C(49S)-C(45S)-H(45A)	111.6
P(8)-C(45S)-H(45A)	111.6
C(49S)-C(45S)-H(45B)	111.7
P(8)-C(45S)-H(45B)	111.8
H(45A)-C(45S)-H(45B)	109.5
C(48S)-C(46S)-P(8)	130(5)
C(48S)-C(46S)-H(46A)	104.9
P(8)-C(46S)-H(46A)	104.9
C(48S)-C(46S)-H(46B)	104.7
P(8)-C(46S)-H(46B)	104.7
H(46A)-C(46S)-H(46B)	105.8
C(44S)-C(47S)-P(8)	125(3)
C(44S)-C(47S)-H(47A)	106
P(8)-C(47S)-H(47A)	106.1
C(44S)-C(47S)-H(47B)	106.2

P(8)-C(47S)-H(47B)	106.1
H(47A)-C(47S)-H(47B)	106.3
C(46S)-C(48S)-H(48A)	109.5
C(46S)-C(48S)-H(48B)	109.5
H(48A)-C(48S)-H(48B)	109.5
C(46S)-C(48S)-H(48C)	109.3
H(48A)-C(48S)-H(48C)	109.5
H(48B)-C(48S)-H(48C)	109.5
C(45S)-C(49S)-H(49A)	111.9
C(45S)-C(49S)-H(49B)	112.3
H(49A)-C(49S)-H(49B)	106.7
C(45S)-C(49S)-H(49C)	112
H(49A)-C(49S)-H(49C)	106.8
H(49B)-C(49S)-H(49C)	106.8
C(79)-C(50S)-H(50A)	109.4
C(79)-C(50S)-H(50B)	109.5
H(50A)-C(50S)-H(50B)	109.5
C(79)-C(50S)-H(50C)	109.5
H(50A)-C(50S)-H(50C)	109.5
H(50B)-C(50S)-H(50C)	109.5
O(503)-S(500)-O(501)	118(2)
O(503)-S(500)-O(502)	116(2)
O(501)-S(500)-O(502)	115(2)
O(503)-S(500)-C(500)	98.9(18)
O(501)-S(500)-C(500)	102.6(19)
O(502)-S(500)-C(500)	102.2(19)
F(501)-C(500)-F(502)	115(2)
F(501)-C(500)-F(503)	117(2)
F(502)-C(500)-F(503)	117(2)
F(501)-C(500)-S(500)	102(2)
F(502)-C(500)-S(500)	99(2)
F(503)-C(500)-S(500)	102(2)
O(504)-S(501)-O(506)	117(2)
O(504)-S(501)-O(505)	117(2)
O(506)-S(501)-O(505)	117(2)
O(504)-S(501)-C(501)	101(2)
O(506)-S(501)-C(501)	99(2)
O(505)-S(501)-C(501)	98(2)
F(506)-C(501)-F(504)	119(2)
F(506)-C(501)-F(505)	117(2)
F(504)-C(501)-F(505)	116(2)
F(506)-C(501)-S(501)	100(2)
F(504)-C(501)-S(501)	100(2)

F(505)-C(501)-S(501)	99(2)
O(508)-S(502)-O(507)	118(2)
O(508)-S(502)-O(509)	116(2)
O(507)-S(502)-O(509)	117(2)
O(508)-S(502)-C(502)	100(2)
O(507)-S(502)-C(502)	99(2)
O(509)-S(502)-C(502)	99(2)
F(507)-C(502)-F(508)	118(2)
F(507)-C(502)-F(509)	117(2)
F(508)-C(502)-F(509)	117(2)
F(507)-C(502)-S(502)	100(2)
F(508)-C(502)-S(502)	100(2)
F(509)-C(502)-S(502)	99(2)
O(510)-S(503)-O(512)	117(2)
O(510)-S(503)-O(511)	117(2)
O(512)-S(503)-O(511)	116(2)
O(510)-S(503)-C(503)	101(2)
O(512)-S(503)-C(503)	100(2)
O(511)-S(503)-C(503)	100(2)
F(510)-C(503)-F(511)	117(2)
F(510)-C(503)-F(512)	116(2)
F(511)-C(503)-F(512)	117(2)
F(510)-C(503)-S(503)	101(2)
F(511)-C(503)-S(503)	101(2)
F(512)-C(503)-S(503)	100(2)

Table 9. Atomic coordinates (x 10^4) and equivalent isotropic displacement parameters ($Å^2$x 10^3) for **BT2'**. U(eq) is defined as one third of the trace of the orthogonalized U^{ij} tensor.

	x	y	z	U(eq)
Pt(1)	5816(1)	3577(1)	4430(1)	28(1)
Pt(2)	6648(1)	10841(1)	7624(1)	31(1)
S(1)	5841(1)	9864(3)	4772(2)	56(1)
S(2)	6862(1)	5026(3)	1953(3)	72(2)
P(1)	5391(1)	2790(2)	4385(2)	34(1)
P(2)	6120(1)	2824(2)	4013(2)	34(1)
P(3)	6376(1)	11249(2)	8280(2)	44(1)
P(4)	6983(1)	11847(3)	7697(2)	51(1)
F(1)	5361(5)	9151(11)	4997(14)	198(12)
F(2)	5351(4)	10414(11)	5084(9)	143(8)
F(3)	5690(7)	9795(14)	5788(10)	208(13)

F(4)	7043(4)	4415(7)	2994(7)	124(7)
F(5)	6475(4)	4441(7)	2572(5)	94(4)
F(6)	6715(3)	5486(6)	2935(4)	79(4)
O(1)	5589(2)	4297(5)	4910(5)	37(2)
O(2)	5375(3)	5114(7)	4130(6)	62(4)
O(3)	6341(3)	9883(6)	7490(5)	40(2)
O(4)	6775(3)	9106(6)	8007(5)	49(3)
O(5)	6032(4)	10497(7)	5080(8)	106(7)
O(6)	5652(4)	9994(11)	4157(6)	110(7)
O(7)	6012(3)	9150(7)	4900(7)	77(4)
O(8)	6882(4)	4286(6)	1720(5)	76(5)
O(9)	6565(3)	5436(10)	1586(6)	82(5)
O(10)	7132(3)	5512(7)	2125(6)	65(4)
N(1)	7384(3)	6487(5)	4577(5)	24(2)
N(2)	7052(2)	7543(6)	5213(4)	21(2)
N(3)	6147(3)	4493(7)	4539(5)	30(3)
N(4)	6837(3)	10267(6)	6993(5)	26(2)
C(1)	7563(3)	6036(7)	4309(6)	27(3)
C(2)	7417(4)	5304(8)	4162(7)	35(3)
C(3)	7131(4)	5312(8)	4311(7)	36(3)
C(4)	7108(3)	6066(7)	4572(5)	23(3)
C(5)	6850(3)	6281(7)	4797(6)	28(3)
C(6)	6824(3)	6951(7)	5093(6)	23(3)
C(7)	6564(3)	7184(8)	5345(7)	34(3)
C(8)	6646(3)	7859(7)	5629(6)	31(3)
C(9)	6956(3)	8109(7)	5545(6)	22(3)
C(10)	7131(3)	8765(7)	5781(6)	26(3)
C(11)	6589(3)	5705(8)	4721(6)	30(3)
C(12)	6365(3)	5563(8)	4146(6)	28(3)
C(13)	6146(3)	4972(8)	4068(6)	28(3)
C(14)	6348(3)	4656(8)	5104(6)	33(3)
C(15)	6571(3)	5236(8)	5203(6)	30(3)
C(16)	7014(3)	9274(7)	6190(6)	24(3)
C(17)	6723(3)	9692(7)	6005(6)	26(3)
C(18)	6646(3)	10159(7)	6413(6)	31(3)
C(19)	7112(3)	9847(8)	7168(6)	32(3)
C(20)	7210(3)	9369(8)	6786(6)	28(3)
C(21)	5508(4)	4973(10)	4671(9)	49(4)
C(22)	5612(3)	5615(8)	5126(7)	34(3)
C(23)	5792(4)	5456(9)	5739(8)	47(4)
C(24)	5929(4)	6049(9)	6139(8)	49(4)
C(25)	5869(3)	6809(9)	5948(7)	35(3)
C(26)	5688(3)	6960(9)	5357(7)	40(4)

C(27)	5563(3)	6372(9)	4939(7)	40(4)
C(28)	6023(4)	7410(8)	6385(6)	32(3)
C(29)	6341(4)	7337(8)	6797(7)	37(3)
C(30)	6485(4)	7922(8)	7199(6)	35(3)
C(31)	6332(4)	8582(8)	7182(6)	33(3)
C(32)	6023(4)	8681(9)	6778(8)	45(4)
C(33)	5878(3)	8106(10)	6384(7)	43(4)
C(34)	6502(4)	9220(9)	7624(7)	40(4)
C(35)	5362(4)	1841(9)	4047(7)	40(4)
C(36)	5026(4)	1448(10)	3953(8)	50(4)
C(37)	5014(4)	3298(10)	3986(8)	51(4)
C(38)	4996(4)	3490(10)	3309(7)	51(4)
C(39)	5366(5)	2634(13)	5165(8)	73(7)
C(40)	5674(5)	2307(14)	5593(7)	82(8)
C(41)	6245(5)	1952(10)	4396(10)	66(6)
C(42)	6486(6)	2055(13)	5069(11)	84(7)
C(43)	5920(5)	2589(11)	3220(9)	60(5)
C(44)	5831(6)	3302(15)	2801(8)	82(7)
C(45)	6503(4)	3289(9)	4024(7)	41(4)
C(46)	6741(4)	2814(14)	3785(10)	74(6)
C(47)	6579(6)	10927(15)	9057(10)	85(7)
C(48)	6635(5)	10148(13)	9194(9)	73(6)
C(49)	5974(5)	10852(12)	8066(9)	63(5)
C(50)	5800(4)	11117(13)	7443(10)	72(6)
C(51)	6323(5)	12242(9)	8417(9)	55(4)
C(52)	6076(6)	12416(11)	8782(10)	75(6)
C(53)	7297(5)	11688(13)	7308(11)	73(6)
C(54)	7561(7)	12298(17)	7401(15)	116(9)
C(55)	6783(5)	12741(10)	7373(10)	70(6)
C(56)	6557(7)	12667(14)	6711(11)	93(8)
C(57)	7220(5)	12036(12)	8473(10)	78(6)
C(58)	7424(5)	11348(11)	8772(10)	69(5)
C(63)	5566(5)	9793(10)	5156(11)	100(9)
C(64)	6768(4)	4825(9)	2641(9)	94(9)
C(65)	5000	1060(14)	2500	65(8)
C(66)	4699(7)	589(13)	2383(10)	92(8)
O(67)	5000	1730(9)	2500	80(7)

Table 10. Bond lengths [Å] and angles [º] for **BT2'**.

Pt(1)-O(1)	2.088(9)
Pt(1)-N(3)	2.100(11)

Pt(1)-P(2)	2.247(4)
Pt(1)-P(1)	2.249(4)
Pt(2)-O(3)	2.093(10)
Pt(2)-N(4)	2.101(11)
Pt(2)-P(4)	2.240(4)
Pt(2)-P(3)	2.263(4)
S(1)-O(6)	1.411(11)
S(1)-O(5)	1.429(11)
S(1)-O(7)	1.433(10)
S(1)-C(63)	1.66(3)
S(2)-O(10)	1.388(11)
S(2)-O(8)	1.415(10)
S(2)-O(9)	1.477(11)
S(2)-C(64)	1.77(2)
P(1)-C(37)	1.821(18)
P(1)-C(35)	1.823(15)
P(1)-C(39)	1.835(17)
P(2)-C(41)	1.762(17)
P(2)-C(43)	1.803(18)
P(2)-C(45)	1.812(16)
P(3)-C(49)	1.775(19)
P(3)-C(51)	1.795(16)
P(3)-C(47)	1.82(2)
P(4)-C(57)	1.79(2)
P(4)-C(55)	1.83(2)
P(4)-C(53)	1.83(2)
F(1)-C(63)	1.403(15)
F(2)-C(63)	1.399(15)
F(3)-C(63)	1.381(16)
F(4)-C(64)	1.406(14)
F(5)-C(64)	1.383(14)
F(6)-C(64)	1.388(13)
O(1)-C(21)	1.31(2)
O(2)-C(21)	1.22(2)
O(3)-C(34)	1.336(18)
O(4)-C(34)	1.246(19)
N(1)-C(1)	1.363(16)
N(1)-C(4)	1.381(15)
N(1)-H(1)	0.88
N(2)-C(9)	1.381(15)
N(2)-C(6)	1.392(16)
N(3)-C(14)	1.350(17)
N(3)-C(13)	1.362(17)

N(4)-C(19)	1.338(17)
N(4)-C(18)	1.345(17)
C(1)-C(2)	1.421(18)
C(1)-C(10)#1	1.421(17)
C(2)-C(3)	1.36(2)
C(2)-H(2)	0.95
C(3)-C(4)	1.464(18)
C(3)-H(3)	0.95
C(4)-C(5)	1.394(18)
C(5)-C(6)	1.376(18)
C(5)-C(11)	1.474(17)
C(6)-C(7)	1.444(17)
C(7)-C(8)	1.346(19)
C(7)-H(7)	0.95
C(8)-C(9)	1.454(18)
C(8)-H(8)	0.95
C(9)-C(10)	1.387(18)
C(10)-C(16)	1.479(17)
C(11)-C(15)	1.392(19)
C(11)-C(12)	1.394(19)
C(12)-C(13)	1.368(18)
C(12)-H(12)	0.95
C(13)-H(13)	0.95
C(14)-C(15)	1.361(18)
C(14)-H(14)	0.95
C(15)-H(15)	0.95
C(16)-C(20)	1.379(17)
C(16)-C(17)	1.389(17)
C(17)-C(18)	1.352(18)
C(17)-H(17)	0.95
C(18)-H(18)	0.95
C(19)-C(20)	1.362(18)
C(19)-H(19)	0.95
C(20)-H(20)	0.95
C(21)-C(22)	1.50(2)
C(22)-C(27)	1.39(2)
C(22)-C(23)	1.41(2)
C(23)-C(24)	1.39(2)
C(23)-H(23)	0.95
C(24)-C(25)	1.40(2)
C(24)-H(24)	0.95
C(25)-C(26)	1.36(2)
C(25)-C(28)	1.465(19)

C(26)-C(27)	1.40(2)
C(26)-H(26)	0.95
C(27)-H(27)	0.95
C(28)-C(33)	1.36(2)
C(28)-C(29)	1.41(2)
C(29)-C(30)	1.39(2)
C(29)-H(29)	0.95
C(30)-C(31)	1.32(2)
C(30)-H(30)	0.95
C(31)-C(32)	1.37(2)
C(31)-C(34)	1.53(2)
C(32)-C(33)	1.37(2)
C(32)-H(32)	0.95
C(33)-H(33)	0.95
C(35)-C(36)	1.541(19)
C(35)-H(35A)	0.99
C(35)-H(35B)	0.99
C(36)-H(36A)	0.98
C(36)-H(36B)	0.98
C(36)-H(36C)	0.98
C(37)-C(38)	1.56(2)
C(37)-H(37A)	0.99
C(37)-H(37B)	0.99
C(38)-H(38A)	0.98
C(38)-H(38B)	0.98
C(38)-H(38C)	0.98
C(39)-C(40)	1.50(3)
C(39)-H(39A)	0.99
C(39)-H(39B)	0.99
C(40)-H(40A)	0.98
C(40)-H(40B)	0.98
C(40)-H(40C)	0.98
C(41)-C(42)	1.58(3)
C(41)-H(41A)	0.99
C(41)-H(41B)	0.99
C(42)-H(42A)	0.98
C(42)-H(42B)	0.98
C(42)-H(42C)	0.98
C(43)-C(44)	1.55(3)
C(43)-H(43A)	0.99
C(43)-H(43B)	0.99
C(44)-H(44A)	0.98
C(44)-H(44B)	0.98

C(44)-H(44C)	0.98
C(45)-C(46)	1.53(2)
C(45)-H(45A)	0.99
C(45)-H(45B)	0.99
C(46)-H(46A)	0.98
C(46)-H(46B)	0.98
C(46)-H(46C)	0.98
C(47)-C(48)	1.41(3)
C(47)-H(47A)	0.99
C(47)-H(47B)	0.99
C(48)-H(48A)	0.98
C(48)-H(48B)	0.98
C(48)-H(48C)	0.98
C(49)-C(50)	1.47(3)
C(49)-H(49A)	0.99
C(49)-H(49B)	0.99
C(50)-H(50A)	0.98
C(50)-H(50B)	0.98
C(50)-H(50C)	0.98
C(51)-C(52)	1.55(3)
C(51)-H(51A)	0.99
C(51)-H(51B)	0.99
C(52)-H(52A)	0.98
C(52)-H(52B)	0.98
C(52)-H(52C)	0.98
C(53)-C(54)	1.52(3)
C(53)-H(53A)	0.99
C(53)-H(53B)	0.99
C(54)-H(54A)	0.98
C(54)-H(54B)	0.98
C(54)-H(54C)	0.98
C(55)-C(56)	1.53(3)
C(55)-H(55A)	0.99
C(55)-H(55B)	0.99
C(56)-H(56A)	0.98
C(56)-H(56B)	0.98
C(56)-H(56C)	0.98
C(57)-C(58)	1.52(3)
C(57)-H(57A)	0.99
C(57)-H(57B)	0.99
C(58)-H(58A)	0.98
C(58)-H(58B)	0.98
C(58)-H(58C)	0.98

C(65)-O(67)	1.17(3)
C(65)-C(66)#2	1.48(3)
C(65)-C(66)	1.48(3)
C(66)-H(66A)	0.98
C(66)-H(66B)	0.98
C(66)-H(66C)	0.98

O(1)-Pt(1)-N(3)	82.7(4)
O(1)-Pt(1)-P(2)	172.6(3)
N(3)-Pt(1)-P(2)	92.9(3)
O(1)-Pt(1)-P(1)	84.5(3)
N(3)-Pt(1)-P(1)	166.9(3)
P(2)-Pt(1)-P(1)	100.16(14)
O(3)-Pt(2)-N(4)	82.2(4)
O(3)-Pt(2)-P(4)	175.6(3)
N(4)-Pt(2)-P(4)	93.7(3)
O(3)-Pt(2)-P(3)	86.0(3)
N(4)-Pt(2)-P(3)	168.2(3)
P(4)-Pt(2)-P(3)	98.10(15)
O(6)-S(1)-O(5)	115.9(11)
O(6)-S(1)-O(7)	116.5(10)
O(5)-S(1)-O(7)	113.5(9)
O(6)-S(1)-C(63)	104.8(11)
O(5)-S(1)-C(63)	100.5(11)
O(7)-S(1)-C(63)	102.7(9)
O(10)-S(2)-O(8)	122.1(10)
O(10)-S(2)-O(9)	110.9(10)
O(8)-S(2)-O(9)	111.7(9)
O(10)-S(2)-C(64)	105.0(8)
O(8)-S(2)-C(64)	101.9(8)
O(9)-S(2)-C(64)	102.7(8)
C(37)-P(1)-C(35)	107.2(8)
C(37)-P(1)-C(39)	105.2(10)
C(35)-P(1)-C(39)	105.0(9)
C(37)-P(1)-Pt(1)	107.3(6)
C(35)-P(1)-Pt(1)	122.0(5)
C(39)-P(1)-Pt(1)	109.0(6)
C(41)-P(2)-C(43)	106.3(10)
C(41)-P(2)-C(45)	104.4(8)
C(43)-P(2)-C(45)	105.6(8)
C(41)-P(2)-Pt(1)	115.2(7)
C(43)-P(2)-Pt(1)	113.6(7)
C(45)-P(2)-Pt(1)	110.9(5)

C(49)-P(3)-C(51)	105.5(9)
C(49)-P(3)-C(47)	106.5(11)
C(51)-P(3)-C(47)	100.3(11)
C(49)-P(3)-Pt(2)	109.6(6)
C(51)-P(3)-Pt(2)	122.4(7)
C(47)-P(3)-Pt(2)	111.2(7)
C(57)-P(4)-C(55)	107.3(10)
C(57)-P(4)-C(53)	103.4(10)
C(55)-P(4)-C(53)	104.6(10)
C(57)-P(4)-Pt(2)	112.1(8)
C(55)-P(4)-Pt(2)	115.8(7)
C(53)-P(4)-Pt(2)	112.5(7)
C(21)-O(1)-Pt(1)	115.7(10)
C(34)-O(3)-Pt(2)	114.3(10)
C(1)-N(1)-C(4)	105.8(10)
C(1)-N(1)-H(1)	127.1
C(4)-N(1)-H(1)	127.1
C(9)-N(2)-C(6)	109.9(10)
C(14)-N(3)-C(13)	118.4(11)
C(14)-N(3)-Pt(1)	119.1(9)
C(13)-N(3)-Pt(1)	122.2(8)
C(19)-N(4)-C(18)	115.7(11)
C(19)-N(4)-Pt(2)	122.5(8)
C(18)-N(4)-Pt(2)	120.1(9)
N(1)-C(1)-C(2)	111.5(11)
N(1)-C(1)-C(10)#1	125.6(11)
C(2)-C(1)-C(10)#1	122.8(12)
C(3)-C(2)-C(1)	107.0(12)
C(3)-C(2)-H(2)	126.5
C(1)-C(2)-H(2)	126.5
C(2)-C(3)-C(4)	106.5(12)
C(2)-C(3)-H(3)	126.7
C(4)-C(3)-H(3)	126.7
N(1)-C(4)-C(5)	127.6(11)
N(1)-C(4)-C(3)	109.0(11)
C(5)-C(4)-C(3)	123.3(11)
C(6)-C(5)-C(4)	127.0(11)
C(6)-C(5)-C(11)	118.2(12)
C(4)-C(5)-C(11)	114.8(11)
C(5)-C(6)-N(2)	125.3(11)
C(5)-C(6)-C(7)	128.4(12)
N(2)-C(6)-C(7)	106.3(11)
C(8)-C(7)-C(6)	108.8(11)

C(8)-C(7)-H(7)	125.6
C(6)-C(7)-H(7)	125.6
C(7)-C(8)-C(9)	108.3(11)
C(7)-C(8)-H(8)	125.8
C(9)-C(8)-H(8)	125.8
N(2)-C(9)-C(10)	126.6(11)
N(2)-C(9)-C(8)	106.5(11)
C(10)-C(9)-C(8)	126.8(11)
C(9)-C(10)-C(1)#1	123.7(11)
C(9)-C(10)-C(16)	120.2(11)
C(1)#1-C(10)-C(16)	115.9(11)
C(15)-C(11)-C(12)	117.1(12)
C(15)-C(11)-C(5)	121.9(12)
C(12)-C(11)-C(5)	120.8(12)
C(13)-C(12)-C(11)	120.3(12)
C(13)-C(12)-H(12)	119.9
C(11)-C(12)-H(12)	119.9
N(3)-C(13)-C(12)	121.5(12)
N(3)-C(13)-H(13)	119.3
C(12)-C(13)-H(13)	119.3
N(3)-C(14)-C(15)	121.8(13)
N(3)-C(14)-H(14)	119.1
C(15)-C(14)-H(14)	119.1
C(14)-C(15)-C(11)	120.7(13)
C(14)-C(15)-H(15)	119.7
C(11)-C(15)-H(15)	119.7
C(20)-C(16)-C(17)	117.3(12)
C(20)-C(16)-C(10)	118.4(11)
C(17)-C(16)-C(10)	124.2(11)
C(18)-C(17)-C(16)	119.1(12)
C(18)-C(17)-H(17)	120.4
C(16)-C(17)-H(17)	120.4
N(4)-C(18)-C(17)	124.4(13)
N(4)-C(18)-H(18)	117.8
C(17)-C(18)-H(18)	117.8
N(4)-C(19)-C(20)	123.7(12)
N(4)-C(19)-H(19)	118.1
C(20)-C(19)-H(19)	118.1
C(19)-C(20)-C(16)	119.6(12)
C(19)-C(20)-H(20)	120.2
C(16)-C(20)-H(20)	120.2
O(2)-C(21)-O(1)	126.2(15)
O(2)-C(21)-C(22)	119.9(17)

O(1)-C(21)-C(22)	113.8(15)
C(27)-C(22)-C(23)	118.6(14)
C(27)-C(22)-C(21)	121.1(15)
C(23)-C(22)-C(21)	119.9(14)
C(24)-C(23)-C(22)	120.1(15)
C(24)-C(23)-H(23)	119.9
C(22)-C(23)-H(23)	119.9
C(23)-C(24)-C(25)	120.3(17)
C(23)-C(24)-H(24)	119.9
C(25)-C(24)-H(24)	119.9
C(26)-C(25)-C(24)	119.3(15)
C(26)-C(25)-C(28)	122.6(14)
C(24)-C(25)-C(28)	118.0(14)
C(25)-C(26)-C(27)	121.3(15)
C(25)-C(26)-H(26)	119.4
C(27)-C(26)-H(26)	119.4
C(22)-C(27)-C(26)	120.3(14)
C(22)-C(27)-H(27)	119.9
C(26)-C(27)-H(27)	119.9
C(33)-C(28)-C(29)	115.3(13)
C(33)-C(28)-C(25)	122.2(14)
C(29)-C(28)-C(25)	122.4(12)
C(30)-C(29)-C(28)	121.2(13)
C(30)-C(29)-H(29)	119.4
C(28)-C(29)-H(29)	119.4
C(31)-C(30)-C(29)	120.8(15)
C(31)-C(30)-H(30)	119.6
C(29)-C(30)-H(30)	119.6
C(30)-C(31)-C(32)	119.6(14)
C(30)-C(31)-C(34)	119.3(14)
C(32)-C(31)-C(34)	121.2(13)
C(33)-C(32)-C(31)	120.2(14)
C(33)-C(32)-H(32)	119.9
C(31)-C(32)-H(32)	119.9
C(28)-C(33)-C(32)	122.8(14)
C(28)-C(33)-H(33)	118.6
C(32)-C(33)-H(33)	118.6
O(4)-C(34)-O(3)	127.3(14)
O(4)-C(34)-C(31)	120.1(13)
O(3)-C(34)-C(31)	112.1(14)
C(36)-C(35)-P(1)	114.2(11)
C(36)-C(35)-H(35A)	108.7
P(1)-C(35)-H(35A)	108.7

C(36)-C(35)-H(35B)	108.7
P(1)-C(35)-H(35B)	108.7
H(35A)-C(35)-H(35B)	107.6
C(35)-C(36)-H(36A)	109.5
C(35)-C(36)-H(36B)	109.5
H(36A)-C(36)-H(36B)	109.5
C(35)-C(36)-H(36C)	109.5
H(36A)-C(36)-H(36C)	109.5
H(36B)-C(36)-H(36C)	109.5
C(38)-C(37)-P(1)	112.2(12)
C(38)-C(37)-H(37A)	109.2
P(1)-C(37)-H(37A)	109.2
C(38)-C(37)-H(37B)	109.2
P(1)-C(37)-H(37B)	109.2
H(37A)-C(37)-H(37B)	107.9
C(37)-C(38)-H(38A)	109.5
C(37)-C(38)-H(38B)	109.5
H(38A)-C(38)-H(38B)	109.5
C(37)-C(38)-H(38C)	109.5
H(38A)-C(38)-H(38C)	109.5
H(38B)-C(38)-H(38C)	109.5
C(40)-C(39)-P(1)	113.5(14)
C(40)-C(39)-H(39A)	108.9
P(1)-C(39)-H(39A)	108.9
C(40)-C(39)-H(39B)	108.9
P(1)-C(39)-H(39B)	108.9
H(39A)-C(39)-H(39B)	107.7
C(39)-C(40)-H(40A)	109.5
C(39)-C(40)-H(40B)	109.5
H(40A)-C(40)-H(40B)	109.5
C(39)-C(40)-H(40C)	109.5
H(40A)-C(40)-H(40C)	109.5
H(40B)-C(40)-H(40C)	109.5
C(42)-C(41)-P(2)	113.2(15)
C(42)-C(41)-H(41A)	108.9
P(2)-C(41)-H(41A)	108.9
C(42)-C(41)-H(41B)	108.9
P(2)-C(41)-H(41B)	108.9
H(41A)-C(41)-H(41B)	107.8
C(41)-C(42)-H(42A)	109.5
C(41)-C(42)-H(42B)	109.5
H(42A)-C(42)-H(42B)	109.5
C(41)-C(42)-H(42C)	109.5

H(42A)-C(42)-H(42C)	109.5
H(42B)-C(42)-H(42C)	109.5
C(44)-C(43)-P(2)	113.0(13)
C(44)-C(43)-H(43A)	109
P(2)-C(43)-H(43A)	109
C(44)-C(43)-H(43B)	109
P(2)-C(43)-H(43B)	109
H(43A)-C(43)-H(43B)	107.8
C(43)-C(44)-H(44A)	109.5
C(43)-C(44)-H(44B)	109.5
H(44A)-C(44)-H(44B)	109.5
C(43)-C(44)-H(44C)	109.5
H(44A)-C(44)-H(44C)	109.5
H(44B)-C(44)-H(44C)	109.5
C(46)-C(45)-P(2)	115.9(12)
C(46)-C(45)-H(45A)	108.3
P(2)-C(45)-H(45A)	108.3
C(46)-C(45)-H(45B)	108.3
P(2)-C(45)-H(45B)	108.3
H(45A)-C(45)-H(45B)	107.4
C(45)-C(46)-H(46A)	109.5
C(45)-C(46)-H(46B)	109.5
H(46A)-C(46)-H(46B)	109.5
C(45)-C(46)-H(46C)	109.5
H(46A)-C(46)-H(46C)	109.5
H(46B)-C(46)-H(46C)	109.5
C(48)-C(47)-P(3)	121.2(19)
C(48)-C(47)-H(47A)	107
P(3)-C(47)-H(47A)	107
C(48)-C(47)-H(47B)	107
P(3)-C(47)-H(47B)	107
H(47A)-C(47)-H(47B)	106.8
C(47)-C(48)-H(48A)	109.5
C(47)-C(48)-H(48B)	109.5
H(48A)-C(48)-H(48B)	109.5
C(47)-C(48)-H(48C)	109.5
H(48A)-C(48)-H(48C)	109.5
H(48B)-C(48)-H(48C)	109.5
C(50)-C(49)-P(3)	107.9(15)
C(50)-C(49)-H(49A)	110.1
P(3)-C(49)-H(49A)	110.1
C(50)-C(49)-H(49B)	110.1
P(3)-C(49)-H(49B)	110.1

H(49A)-C(49)-H(49B)	108.4
C(49)-C(50)-H(50A)	109.5
C(49)-C(50)-H(50B)	109.5
H(50A)-C(50)-H(50B)	109.5
C(49)-C(50)-H(50C)	109.5
H(50A)-C(50)-H(50C)	109.5
H(50B)-C(50)-H(50C)	109.5
C(52)-C(51)-P(3)	115.1(14)
C(52)-C(51)-H(51A)	108.5
P(3)-C(51)-H(51A)	108.5
C(52)-C(51)-H(51B)	108.5
P(3)-C(51)-H(51B)	108.5
H(51A)-C(51)-H(51B)	107.5
C(51)-C(52)-H(52A)	109.5
C(51)-C(52)-H(52B)	109.5
H(52A)-C(52)-H(52B)	109.5
C(51)-C(52)-H(52C)	109.5
H(52A)-C(52)-H(52C)	109.5
H(52B)-C(52)-H(52C)	109.5
C(54)-C(53)-P(4)	116.1(16)
C(54)-C(53)-H(53A)	108.3
P(4)-C(53)-H(53A)	108.3
C(54)-C(53)-H(53B)	108.3
P(4)-C(53)-H(53B)	108.3
H(53A)-C(53)-H(53B)	107.4
C(53)-C(54)-H(54A)	109.5
C(53)-C(54)-H(54B)	109.5
H(54A)-C(54)-H(54B)	109.5
C(53)-C(54)-H(54C)	109.5
H(54A)-C(54)-H(54C)	109.5
H(54B)-C(54)-H(54C)	109.5
C(56)-C(55)-P(4)	113.8(15)
C(56)-C(55)-H(55A)	108.8
P(4)-C(55)-H(55A)	108.8
C(56)-C(55)-H(55B)	108.8
P(4)-C(55)-H(55B)	108.8
H(55A)-C(55)-H(55B)	107.7
C(55)-C(56)-H(56A)	109.5
C(55)-C(56)-H(56B)	109.5
H(56A)-C(56)-H(56B)	109.5
C(55)-C(56)-H(56C)	109.5
H(56A)-C(56)-H(56C)	109.5
H(56B)-C(56)-H(56C)	109.5

C(58)-C(57)-P(4)	112.0(12)
C(58)-C(57)-H(57A)	109.2
P(4)-C(57)-H(57A)	109.2
C(58)-C(57)-H(57B)	109.2
P(4)-C(57)-H(57B)	109.2
H(57A)-C(57)-H(57B)	107.9
C(57)-C(58)-H(58A)	109.5
C(57)-C(58)-H(58B)	109.5
H(58A)-C(58)-H(58B)	109.5
C(57)-C(58)-H(58C)	109.5
H(58A)-C(58)-H(58C)	109.5
H(58B)-C(58)-H(58C)	109.5
F(3)-C(63)-F(2)	98.8(19)
F(3)-C(63)-F(1)	107(3)
F(2)-C(63)-F(1)	105.1(19)
F(3)-C(63)-S(1)	116.3(17)
F(2)-C(63)-S(1)	114.6(16)
F(1)-C(63)-S(1)	113.8(16)
F(5)-C(64)-F(6)	101.1(13)
F(5)-C(64)-F(4)	112.6(16)
F(6)-C(64)-F(4)	112.1(15)
F(5)-C(64)-S(2)	115.5(12)
F(6)-C(64)-S(2)	112.0(12)
F(4)-C(64)-S(2)	103.9(12)
O(67)-C(65)-C(66)#2	124.0(14)
O(67)-C(65)-C(66)	124.0(14)
C(66)#2-C(65)-C(66)	112(3)
C(65)-C(66)-H(66A)	109.5
C(65)-C(66)-H(66B)	109.5
H(66A)-C(66)-H(66B)	109.5
C(65)-C(66)-H(66C)	109.5
H(66A)-C(66)-H(66C)	109.5
H(66B)-C(66)-H(66C)	109.5

Symmetry transformations used to generate equivalent atoms:

#1 -x+3/2,-y+3/2,-z+1 #2 -x+1,y,-z+1/2

Table 11. Atomic coordinates (x 10^4) and equivalent isotropic displacement parameters (Å^{2}x 10^3) for **BT3'**. U(eq) is defined as one third of the trace of the orthogonalized U^{ij} tensor.

	x	y	z	U(eq)
Pt(1)	4111(1)	3450(1)	5479(1)	128(1)

Pt(2)	3825(1)	4802(1)	1183(1)	108(1)
P(1)	3645(5)	4940(5)	319(8)	152(5)
P(2)	4263(5)	5280(4)	1279(8)	140(5)
P(3)	4548(4)	3879(4)	5824(7)	125(5)
P(4)	4116(10)	3020(9)	6198(13)	311(18)
O(1)	4167(10)	3740(9)	4713(16)	140(10)
O(51)	3881(10)	4670(8)	1981(13)	141(9)
C(17)	1964(8)	1988(8)	1729(11)	94(10)
C(8)	1732(8)	1645(9)	1756(13)	117(11)
C(9)	1765(8)	1490(7)	2304(15)	111(11)
C(10)	2017(8)	1737(9)	2615(10)	97(9)
N(3)	2140(7)	2044(7)	2259(12)	98(9)
C(11)	2113(11)	1678(11)	3180(20)	88(9)
C(12)	2350(7)	1931(7)	3466(12)	95(9)
C(13)	2435(8)	1882(7)	4042(12)	99(9)
C(14)	2696(8)	2183(8)	4204(10)	104(10)
C(15)	2771(7)	2419(6)	3728(13)	91(9)
N(4)	2558(7)	2263(7)	3272(10)	89(8)
C(16)	2979(11)	2748(11)	3670(20)	87(9)
C(18)	3867(7)	2913(9)	4577(15)	128(11)
C(19)	3619(9)	2784(8)	4156(12)	108(10)
C(20)	3220(8)	2851(8)	4195(12)	101(10)
C(21)	3069(7)	3047(9)	4654(15)	127(11)
C(22)	3317(10)	3177(9)	5075(12)	140(12)
N(2)	3716(10)	3110(9)	5036(12)	141(11)
C(23)	3610(40)	3460(30)	6730(50)	420(40)
C(24)	4643(15)	3925(17)	6530(20)	149(12)
C(25)	4925(18)	4214(18)	6700(30)	180(20)
C(26)	4443(12)	4363(13)	5550(20)	121(11)
C(27)	4059(16)	4499(17)	5910(30)	170(19)
C(40)	4263(15)	5484(17)	1890(30)	183(14)
C(41)	3900(20)	5700(20)	2140(30)	240(30)
C(43)	3262(19)	4591(18)	40(30)	181(15)
C(45)	4090(20)	4880(20)	-230(30)	200(20)
C(46)	4956(19)	5310(20)	1920(40)	290(30)
C(50)	4065(14)	4382(13)	2158(13)	143(12)
C(56)	3938(11)	4047(11)	3889(10)	143(11)
C(57)	4203(9)	3866(8)	3534(16)	135(11)
C(58)	4221(8)	3972(9)	2975(15)	134(11)
C(59)	3974(10)	4260(10)	2770(11)	125(10)
C(60)	3709(8)	4441(7)	3124(16)	124(11)
C(61)	3691(9)	4335(9)	3684(15)	126(10)
C(62)	3900(15)	3955(16)	4520(14)	154(13)

O(63)	3567(15)	4032(15)	4770(20)	213(17)
O(65)	4248(15)	4151(12)	1837(19)	211(17)
C(67)	3097(7)	4368(6)	1536(12)	89(9)
C(68)	2900(6)	4032(7)	1695(12)	92(10)
C(69)	3049(7)	3668(6)	1556(12)	90(10)
C(70)	3396(8)	3640(5)	1257(12)	100(11)
C(71)	3593(6)	3977(7)	1099(11)	102(11)
N(1)	3444(7)	4341(6)	1238(11)	103(8)
C(74)	4639(11)	2850(20)	6330(30)	350(20)
C(73)	4250(20)	4540(20)	-70(30)	230(30)
C(108)	5218(19)	3473(19)	5190(30)	220(30)
C(109)	5034(14)	3785(17)	5550(30)	159(13)
C(110)	3030(20)	4800(30)	-490(30)	230(30)
C(112)	3430(20)	5397(17)	120(30)	180(14)
C(113)	3100(20)	5470(20)	590(30)	240(30)
C(114)	4370(20)	5666(17)	650(20)	240(30)
C(115)	4759(16)	5018(18)	1520(30)	193(15)
C(116)	4720(20)	5910(18)	860(30)	240(30)
C(117)	3810(20)	3080(30)	6940(30)	420(40)
C(118)	3727(17)	2629(17)	6070(40)	340(30)
C(119)	3860(30)	2220(16)	6260(50)	410(40)
C(120)	4680(30)	2700(40)	6940(30)	440(40)
S(1S)	4404(11)	1684(9)	7280(20)	390(20)
O(1S)	4598(16)	1360(14)	7460(30)	450(30)
O(2S)	4021(16)	1610(20)	7170(30)	450(30)
O(3S)	4600(20)	1894(18)	6900(30)	440(30)
C(1S)	4375(14)	1943(13)	7830(20)	420(30)
F(1S)	4688(18)	2050(20)	8040(30)	470(30)
F(2S)	4180(20)	2250(15)	7780(30)	450(30)
F(3S)	4210(20)	1783(19)	8240(20)	470(30)
S(2S)	5941(11)	5422(12)	2096(16)	359(19)
O(4S)	6030(15)	5130(14)	1730(20)	290(20)
O(5S)	5640(20)	5340(20)	2440(30)	410(30)
O(6S)	6260(19)	5560(20)	2370(30)	430(30)
C(2S)	5798(13)	5783(14)	1734(19)	370(20)
F(4S)	5518(18)	5730(18)	1410(30)	400(20)
F(5S)	5680(20)	6075(14)	2000(30)	410(20)
F(6S)	6040(19)	5947(16)	1420(30)	380(20)

Table 12. Bond lengths [Å] and angles [º] for **BT3'**.

Pt(1)-N(2)	2.08(2)

Pt(1)-O(1)	2.10(4)
Pt(1)-P(3)	2.255(13)
Pt(1)-P(4)	2.27(2)
Pt(2)-O(51)	1.97(3)
Pt(2)-N(1)	2.057(19)
Pt(2)-P(1)	2.210(19)
Pt(2)-P(2)	2.236(13)
P(1)-C(112)	1.80(6)
P(1)-C(43)	1.89(6)
P(1)-C(45)	2.02(7)
P(2)-C(40)	1.61(6)
P(2)-C(115)	2.00(6)
P(2)-C(114)	2.04(2)
P(3)-C(24)	1.72(6)
P(3)-C(109)	1.82(5)
P(3)-C(26)	1.81(5)
P(4)-C(74)	1.91(2)
P(4)-C(118)	1.91(2)
P(4)-C(117)	2.07(2)
O(1)-C(62)	1.26(2)
O(51)-C(50)	1.25(2)
C(17)-C(16)#1	1.33(4)
C(17)-C(8)	1.42
C(17)-N(3)	1.42
C(8)-C(9)	1.42
C(8)-H(8)	0.95
C(9)-C(10)	1.42
C(9)-H(9)	0.95
C(10)-N(3)	1.42
C(10)-C(11)	1.42(5)
C(11)-C(12)	1.36(4)
C(11)-C(69)#1	1.45(4)
C(12)-C(13)	1.42
C(12)-N(4)	1.42
C(13)-C(14)	1.42
C(13)-H(13)	0.95
C(14)-C(15)	1.42
C(14)-H(14)	0.95
C(15)-C(16)	1.34(4)
C(15)-N(4)	1.42
N(4)-H(4)	0.88
C(16)-C(20)	1.55(5)
C(18)-C(19)	1.39

C(18)-N(2)	1.39
C(18)-H(18)	0.95
C(19)-C(20)	1.39
C(19)-H(19)	0.95
C(20)-C(21)	1.39
C(21)-C(22)	1.39
C(21)-H(21)	0.95
C(22)-N(2)	1.39
C(22)-H(22)	0.95
C(23)-C(117)	1.54(2)
C(23)-H(23A)	0.9972
C(23)-H(23B)	0.9995
C(23)-H(23C)	0.9981
C(24)-C(25)	1.45(6)
C(24)-H(24A)	0.99
C(24)-H(24B)	0.99
C(25)-H(25A)	0.98
C(25)-H(25B)	0.98
C(25)-H(25C)	0.98
C(26)-C(27)	1.63(7)
C(26)-H(26A)	0.99
C(26)-H(26B)	0.99
C(27)-H(27A)	1.0126
C(27)-H(27B)	1.014
C(27)-H(27C)	1.0134
C(40)-C(41)	1.56(2)
C(40)-H(40A)	0.99
C(40)-H(40B)	0.99
C(41)-H(41A)	0.9939
C(41)-H(41B)	0.9946
C(41)-H(41C)	0.994
C(43)-C(110)	1.67(9)
C(43)-H(43A)	0.99
C(43)-H(43B)	0.99
C(45)-C(73)	1.34(8)
C(45)-H(45A)	0.99
C(45)-H(45B)	0.99
C(46)-C(115)	1.55(2)
C(46)-H(46A)	0.9838
C(46)-H(46B)	0.9838
C(46)-H(46C)	0.9839
C(50)-O(65)	1.27(2)
C(50)-C(59)	1.56(2)

C(56)-C(57)	1.39
C(56)-C(61)	1.39
C(56)-C(62)	1.55(2)
C(57)-C(58)	1.39
C(57)-H(57)	0.95
C(58)-C(59)	1.39
C(58)-H(58)	0.95
C(59)-C(60)	1.39
C(60)-C(61)	1.39
C(60)-H(60)	0.95
C(61)-H(61)	0.95
C(62)-O(63)	1.32(6)
C(67)-C(68)	1.39
C(67)-N(1)	1.39
C(67)-H(67)	0.95
C(68)-C(69)	1.39
C(68)-H(68)	0.95
C(69)-C(70)	1.39
C(70)-C(71)	1.39
C(70)-H(70)	0.95
C(71)-N(1)	1.39
C(71)-H(71)	0.95
C(74)-C(120)	1.55(2)
C(74)-H(74A)	0.99
C(74)-H(74B)	0.99
C(73)-H(73A)	0.95
C(73)-H(73B)	0.95
C(108)-C(109)	1.52(2)
C(108)-H(10A)	0.9872
C(108)-H(10B)	0.9868
C(108)-H(10C)	0.9866
C(109)-H(10D)	0.99
C(109)-H(10E)	0.99
C(110)-H(11A)	1.0093
C(110)-H(11B)	1.0096
C(110)-H(11C)	1.0102
C(112)-C(113)	1.61(9)
C(112)-H(11D)	0.99
C(112)-H(11E)	0.99
C(113)-H(11F)	1.0391
C(113)-H(11G)	1.0376
C(113)-H(11H)	1.036
C(114)-C(116)	1.55(2)

C(114)-H(11I)	0.99
C(114)-H(11J)	0.99
C(115)-H(11K)	0.99
C(115)-H(11L)	0.99
C(116)-H(11M)	0.9903
C(116)-H(11N)	0.9903
C(116)-H(11O)	0.99
C(117)-H(11P)	0.99
C(117)-H(11Q)	0.99
C(118)-C(119)	1.55(2)
C(118)-H(11R)	0.99
C(118)-H(11S)	0.99
C(119)-H(11T)	0.9946
C(119)-H(11U)	0.9952
C(119)-H(11V)	0.9948
C(120)-H(12A)	1.113
C(120)-H(12B)	1.1285
C(120)-H(12C)	1.1366
S(1S)-O(3S)	1.34(4)
S(1S)-O(2S)	1.36(3)
S(1S)-O(1S)	1.37(3)
S(1S)-C(1S)	1.59(2)
C(1S)-F(1S)	1.24(3)
C(1S)-F(2S)	1.25(3)
C(1S)-F(3S)	1.25(3)
S(2S)-O(4S)	1.36(3)
S(2S)-O(5S)	1.36(3)
S(2S)-O(6S)	1.37(4)
S(2S)-C(2S)	1.59(3)
C(2S)-F(4S)	1.25(3)
C(2S)-F(6S)	1.25(3)
C(2S)-F(5S)	1.26(3)

N(2)-Pt(1)-O(1)	83.1(11)
N(2)-Pt(1)-P(3)	170.2(9)
O(1)-Pt(1)-P(3)	87.1(9)
N(2)-Pt(1)-P(4)	91.5(10)
O(1)-Pt(1)-P(4)	166.6(16)
P(3)-Pt(1)-P(4)	98.2(7)
O(51)-Pt(2)-N(1)	79.8(11)
O(51)-Pt(2)-P(1)	169.2(11)
N(1)-Pt(2)-P(1)	92.7(9)
O(51)-Pt(2)-P(2)	90.1(10)

N(1)-Pt(2)-P(2)	169.9(9)
P(1)-Pt(2)-P(2)	97.4(6)
C(112)-P(1)-C(43)	100(3)
C(112)-P(1)-C(45)	102(3)
C(43)-P(1)-C(45)	103(3)
C(112)-P(1)-Pt(2)	124(3)
C(43)-P(1)-Pt(2)	113(2)
C(45)-P(1)-Pt(2)	112(2)
C(40)-P(2)-C(115)	87(3)
C(40)-P(2)-C(114)	113(3)
C(115)-P(2)-C(114)	111(3)
C(40)-P(2)-Pt(2)	114(2)
C(115)-P(2)-Pt(2)	105.6(17)
C(114)-P(2)-Pt(2)	121.1(16)
C(24)-P(3)-C(109)	101(3)
C(24)-P(3)-C(26)	107(3)
C(109)-P(3)-C(26)	103(3)
C(24)-P(3)-Pt(1)	123.0(19)
C(109)-P(3)-Pt(1)	111.2(19)
C(26)-P(3)-Pt(1)	109.6(14)
C(74)-P(4)-C(118)	118.1(18)
C(74)-P(4)-C(117)	111.0(15)
C(118)-P(4)-C(117)	82(4)
C(74)-P(4)-Pt(1)	109(2)
C(118)-P(4)-Pt(1)	109(2)
C(117)-P(4)-Pt(1)	126(3)
C(62)-O(1)-Pt(1)	122(3)
C(50)-O(51)-Pt(2)	124(2)
C(16)#1-C(17)-C(8)	133(3)
C(16)#1-C(17)-N(3)	119(3)
C(8)-C(17)-N(3)	108
C(17)-C(8)-C(9)	108
C(17)-C(8)-H(8)	126
C(9)-C(8)-H(8)	126
C(10)-C(9)-C(8)	108
C(10)-C(9)-H(9)	126
C(8)-C(9)-H(9)	126
N(3)-C(10)-C(9)	108
N(3)-C(10)-C(11)	128(3)
C(9)-C(10)-C(11)	124(3)
C(10)-N(3)-C(17)	108
C(12)-C(11)-C(10)	121(3)
C(12)-C(11)-C(69)#1	123(9)

C(10)-C(11)-C(69)#1	116(8)
C(11)-C(12)-C(13)	122(3)
C(11)-C(12)-N(4)	130(3)
C(13)-C(12)-N(4)	108
C(14)-C(13)-C(12)	108
C(14)-C(13)-H(13)	126
C(12)-C(13)-H(13)	126
C(13)-C(14)-C(15)	108
C(13)-C(14)-H(14)	126
C(15)-C(14)-H(14)	126
C(16)-C(15)-N(4)	121(3)
C(16)-C(15)-C(14)	131(3)
N(4)-C(15)-C(14)	108
C(15)-N(4)-C(12)	108
C(15)-N(4)-H(4)	126
C(12)-N(4)-H(4)	126
C(17)#1-C(16)-C(15)	137(4)
C(17)#1-C(16)-C(20)	110(3)
C(15)-C(16)-C(20)	113(3)
C(19)-C(18)-N(2)	120
C(19)-C(18)-H(18)	120
N(2)-C(18)-H(18)	120
C(20)-C(19)-C(18)	120
C(20)-C(19)-H(19)	120
C(18)-C(19)-H(19)	120
C(21)-C(20)-C(19)	120
C(21)-C(20)-C(16)	124(3)
C(19)-C(20)-C(16)	116(3)
C(22)-C(21)-C(20)	120
C(22)-C(21)-H(21)	120
C(20)-C(21)-H(21)	120
C(21)-C(22)-N(2)	120
C(21)-C(22)-H(22)	120
N(2)-C(22)-H(22)	120
C(22)-N(2)-C(18)	120
C(22)-N(2)-Pt(1)	121(2)
C(18)-N(2)-Pt(1)	116(2)
C(117)-C(23)-H(23A)	110.6
C(117)-C(23)-H(23B)	111.9
H(23A)-C(23)-H(23B)	107.8
C(117)-C(23)-H(23C)	111.2
H(23A)-C(23)-H(23C)	107.6
H(23B)-C(23)-H(23C)	107.5

C(25)-C(24)-P(3)	118(4)
C(25)-C(24)-H(24A)	107.8
P(3)-C(24)-H(24A)	107.8
C(25)-C(24)-H(24B)	107.6
P(3)-C(24)-H(24B)	107.7
H(24A)-C(24)-H(24B)	107.1
C(24)-C(25)-H(25A)	109.6
C(24)-C(25)-H(25B)	109.4
H(25A)-C(25)-H(25B)	109.5
C(24)-C(25)-H(25C)	109.4
H(25A)-C(25)-H(25C)	109.5
H(25B)-C(25)-H(25C)	109.5
C(27)-C(26)-P(3)	104(4)
C(27)-C(26)-H(26A)	110.9
P(3)-C(26)-H(26A)	111.1
C(27)-C(26)-H(26B)	111
P(3)-C(26)-H(26B)	111.1
H(26A)-C(26)-H(26B)	109.1
C(26)-C(27)-H(27A)	112.3
C(26)-C(27)-H(27B)	112.7
H(27A)-C(27)-H(27B)	106.4
C(26)-C(27)-H(27C)	112.5
H(27A)-C(27)-H(27C)	106.3
H(27B)-C(27)-H(27C)	106.2
C(41)-C(40)-P(2)	123(4)
C(41)-C(40)-H(40A)	106.4
P(2)-C(40)-H(40A)	106.4
C(41)-C(40)-H(40B)	106.6
P(2)-C(40)-H(40B)	106.7
H(40A)-C(40)-H(40B)	106.6
C(40)-C(41)-H(41A)	110.6
C(40)-C(41)-H(41B)	111.1
H(41A)-C(41)-H(41B)	108
C(40)-C(41)-H(41C)	110.7
H(41A)-C(41)-H(41C)	108.1
H(41B)-C(41)-H(41C)	108.1
C(110)-C(43)-P(1)	109(4)
C(110)-C(43)-H(43A)	110
P(1)-C(43)-H(43A)	109.9
C(110)-C(43)-H(43B)	109.9
P(1)-C(43)-H(43B)	109.7
H(43A)-C(43)-H(43B)	108.3
C(73)-C(45)-P(1)	102(5)

C(73)-C(45)-H(45A)	111.3
P(1)-C(45)-H(45A)	111.4
C(73)-C(45)-H(45B)	111.4
P(1)-C(45)-H(45B)	111.4
H(45A)-C(45)-H(45B)	109.3
C(115)-C(46)-H(46A)	109.6
C(115)-C(46)-H(46B)	109.9
H(46A)-C(46)-H(46B)	109.1
C(115)-C(46)-H(46C)	110
H(46A)-C(46)-H(46C)	109.1
H(46B)-C(46)-H(46C)	109.1
O(51)-C(50)-O(65)	123(3)
O(51)-C(50)-C(59)	116(3)
O(65)-C(50)-C(59)	120(4)
C(57)-C(56)-C(61)	120
C(57)-C(56)-C(62)	124(3)
C(61)-C(56)-C(62)	116(3)
C(58)-C(57)-C(56)	120
C(58)-C(57)-H(57)	120
C(56)-C(57)-H(57)	120
C(59)-C(58)-C(57)	120
C(59)-C(58)-H(58)	120
C(57)-C(58)-H(58)	120
C(58)-C(59)-C(60)	120
C(58)-C(59)-C(50)	114(3)
C(60)-C(59)-C(50)	126(3)
C(61)-C(60)-C(59)	120
C(61)-C(60)-H(60)	120
C(59)-C(60)-H(60)	120
C(60)-C(61)-C(56)	120
C(60)-C(61)-H(61)	120
C(56)-C(61)-H(61)	120
O(1)-C(62)-O(63)	125(4)
O(1)-C(62)-C(56)	115(4)
O(63)-C(62)-C(56)	118(4)
C(68)-C(67)-N(1)	120
C(68)-C(67)-H(67)	120
N(1)-C(67)-H(67)	120
C(67)-C(68)-C(69)	120
C(67)-C(68)-H(68)	120
C(69)-C(68)-H(68)	120
C(70)-C(69)-C(68)	120
C(70)-C(69)-C(11)#1	120(2)

C(68)-C(69)-C(11)#1	119(2)
C(69)-C(70)-C(71)	120
C(69)-C(70)-H(70)	120
C(71)-C(70)-H(70)	120
N(1)-C(71)-C(70)	120
N(1)-C(71)-H(71)	120
C(70)-C(71)-H(71)	120
C(71)-N(1)-C(67)	120
C(71)-N(1)-Pt(2)	116.1(13)
C(67)-N(1)-Pt(2)	121.7(14)
C(120)-C(74)-P(4)	110(3)
C(120)-C(74)-H(74A)	108.8
P(4)-C(74)-H(74A)	109.7
C(120)-C(74)-H(74B)	110.4
P(4)-C(74)-H(74B)	109.9
H(74A)-C(74)-H(74B)	108.3
C(45)-C(73)-H(73A)	120
C(45)-C(73)-H(73B)	120
H(73A)-C(73)-H(73B)	120
C(109)-C(108)-H(10A)	110.7
C(109)-C(108)-H(10B)	110
H(10A)-C(108)-H(10B)	108.8
C(109)-C(108)-H(10C)	109.8
H(10A)-C(108)-H(10C)	108.7
H(10B)-C(108)-H(10C)	108.8
C(108)-C(109)-P(3)	135(4)
C(108)-C(109)-H(10D)	103.6
P(3)-C(109)-H(10D)	103.4
C(108)-C(109)-H(10E)	102.8
P(3)-C(109)-H(10E)	103.4
H(10D)-C(109)-H(10E)	105.2
C(43)-C(110)-H(11A)	112
C(43)-C(110)-H(11B)	112.1
H(11A)-C(110)-H(11B)	106.7
C(43)-C(110)-H(11C)	112.3
H(11A)-C(110)-H(11C)	106.8
H(11B)-C(110)-H(11C)	106.7
C(113)-C(112)-P(1)	103(4)
C(113)-C(112)-H(11D)	111.3
P(1)-C(112)-H(11D)	111.2
C(113)-C(112)-H(11E)	110.8
P(1)-C(112)-H(11E)	111.1
H(11D)-C(112)-H(11E)	109.1

C(112)-C(113)-H(11F)	115.1
C(112)-C(113)-H(11G)	114.8
H(11F)-C(113)-H(11G)	103.7
C(112)-C(113)-H(11H)	114.4
H(11F)-C(113)-H(11H)	103.6
H(11G)-C(113)-H(11H)	103.8
C(116)-C(114)-P(2)	104(2)
C(116)-C(114)-H(11I)	111
P(2)-C(114)-H(11I)	110.9
C(116)-C(114)-H(11J)	110.9
P(2)-C(114)-H(11J)	110.8
H(11I)-C(114)-H(11J)	108.9
C(46)-C(115)-P(2)	105(4)
C(46)-C(115)-H(11K)	110.7
P(2)-C(115)-H(11K)	110.7
C(46)-C(115)-H(11L)	111
P(2)-C(115)-H(11L)	111
H(11K)-C(115)-H(11L)	108.9
C(114)-C(116)-H(11M)	110.6
C(114)-C(116)-H(11N)	110.5
H(11M)-C(116)-H(11N)	108.5
C(114)-C(116)-H(11O)	110.3
H(11M)-C(116)-H(11O)	108.4
H(11N)-C(116)-H(11O)	108.5
C(23)-C(117)-P(4)	92(6)
C(23)-C(117)-H(11P)	113.4
P(4)-C(117)-H(11P)	113.3
C(23)-C(117)-H(11Q)	112.9
P(4)-C(117)-H(11Q)	113.3
H(11P)-C(117)-H(11Q)	110.7
C(119)-C(118)-P(4)	112(3)
C(119)-C(118)-H(11R)	109
P(4)-C(118)-H(11R)	109.1
C(119)-C(118)-H(11S)	109.4
P(4)-C(118)-H(11S)	109.2
H(11R)-C(118)-H(11S)	107.9
C(118)-C(119)-H(11T)	110.7
C(118)-C(119)-H(11U)	111.1
H(11T)-C(119)-H(11U)	107.9
C(118)-C(119)-H(11V)	110.9
H(11T)-C(119)-H(11V)	108
H(11U)-C(119)-H(11V)	108
C(74)-C(120)-H(12A)	122.2

C(74)-C(120)-H(12B)	123.9
H(12A)-C(120)-H(12B)	92.5
C(74)-C(120)-H(12C)	124.8
H(12A)-C(120)-H(12C)	92.8
H(12B)-C(120)-H(12C)	91.5
O(3S)-S(1S)-O(2S)	116(3)
O(3S)-S(1S)-O(1S)	114(3)
O(2S)-S(1S)-O(1S)	113(3)
O(3S)-S(1S)-C(1S)	107(3)
O(2S)-S(1S)-C(1S)	102(3)
O(1S)-S(1S)-C(1S)	103(3)
F(1S)-C(1S)-F(2S)	104(4)
F(1S)-C(1S)-F(3S)	103(4)
F(2S)-C(1S)-F(3S)	102(4)
F(1S)-C(1S)-S(1S)	117(3)
F(2S)-C(1S)-S(1S)	115(3)
F(3S)-C(1S)-S(1S)	115(3)
O(4S)-S(2S)-O(5S)	115(3)
O(4S)-S(2S)-O(6S)	113(3)
O(5S)-S(2S)-O(6S)	113(3)
O(4S)-S(2S)-C(2S)	107(3)
O(5S)-S(2S)-C(2S)	105(3)
O(6S)-S(2S)-C(2S)	103(3)
F(4S)-C(2S)-F(6S)	101(4)
F(4S)-C(2S)-F(5S)	101(4)
F(6S)-C(2S)-F(5S)	100(4)
F(4S)-C(2S)-S(2S)	118(3)
F(6S)-C(2S)-S(2S)	118(3)
F(5S)-C(2S)-S(2S)	116(3)

Symmetry transformations used to generate equivalent atoms:

#1 -x+1/2,-y+1/2,-z+1/2

References

S1. Muratsugu, S.; Yamaguchi, A.; Yokota, G. I.; Maeno, T.; Tada, M. Tuning the Structure and Catalytic Activity of Ru Nanoparticle Catalysts by Single 3d Transition-Metal Atoms in Ru12-Metalloporphyrin Precursors. *Chem. Commun.* **2018**, *54*, 4842–4845.

S2. Stang, P. J.; Cao, D. H.; Saito, S.; Arif, A. M. Self-Assembly of Cationic, Tetranuclear, Pt (II) and Pd (II) Macrocyclic Squares. X-Ray Crystal Structure of $[Pt^{2+}(Dppp)(4,4'\text{-Bipyridyl})_2 \bullet OSO_2CF_3]_4$. *J. Am. Chem. Soc.* **1995,** *117*, 6273–6283.